Changes in extreme and mean-state precipitation across scales in a warming climate

Dissertation zur Erlangung des Doktorgrades an der Fakultät für Geowissenschaften der Ludwig-Maximilians Universität München

vorgelegt von

Raul R. Wood

Eingereicht am

14.02.2023, München

Supervisor: Prof. Ralf Ludwig
Department für Geographie, Ludwig-Maximilians Universität München, Bavaria, Germany

Co-Supervisor: Prof. Flavio Lehner
Earth and Atmospheric Sciences, Cornell University, NY, USA

Date of disputation: 05.05.2023

“We stand now where two roads diverge. But unlike the roads in Robert Frost‘s familiar poem, they are not equally fair. The road we have long been traveling is deceptively easy, a smooth superhighway on which we progress with great speed, but at its end lies disaster. The other fork of the road — the one less traveled by — offers our last, our only chance to reach a destination that assures the preservation of the earth.”

Rachel Carson

Executive summary

The climate system, governed by the energy budget of the Earth, is complex, highly interconnected, and influenced by the nonlinear interactions between the atmosphere, ocean, cryosphere, land and biosphere. This system directly reacts to alterations in the Earth's energy budget, triggered by changes in the external forcing, either by natural (i.e., solar cycles, volcanic eruptions) or anthropogenic origin (i.e., greenhouse gases, aerosols, land use change). The continued change in external forcing through anthropogenic origin leads to an increase in the radiative forcing, triggering a warming climate. The thermodynamic consequence of a warming climate is the increased water holding capacity of a warmer atmosphere, which will influence the moisture flux from the surface to the atmosphere and vice versa. Since the energy budget is a closed system, the atmospheric water budget needs to be balanced by an increased horizontal moisture flux which will influence atmospheric circulation. These planetary changes in the climate system will drive a divers regional and local precipitation response. Our society and the environment are impacted by both extremes and variations in the mean-state of precipitation. Thereby the current states of society and the environment are adapted to extremes and levels of variability of the past and are likely not sufficiently resilient to changes in the future. Hence, in Geography and related fields (i.e., Climate Sciences) the robust understanding of the global to local precipitation response to a warming climate is of key interest for the communication of mitigation needs and the development of adaptation strategies.

The scope of this cumulative dissertation is therefore the *detection of robust patterns of global and regional precipitation change in response to a warming climate*. Ensembles of climate model simulations under past and future climate conditions are the foundation for this analysis. However, transient changes in any realization of the climate system, such as observations or any climate model simulation, are the combination of the forced signal and internal climate variability. The internal climate variability, or natural variability, is caused by the chaotic and nonlinear nature of the climate system and is present at any given time. It is therefore often described as an irreducible uncertainty.

To enable the robust quantification of changes in the climate system, including the forced climate response and internal climate variability, the *Single Model Initial-Condition Large Ensemble (SMILE)* framework is used. SMILEs are a state-of-the-art experimental setup in climate modeling. In this setup, a SMILE consists of a single climate model which is run multiple times while keeping the external forcing identical in each run, only changing the initial states at the start of the simulation. The difference in initialization among the different simulation runs samples the uncertainty based on different atmospheric and ocean states as

well as due to the nonlinear nature of the climate system. Each realization of the climate model is equally likely and will result in different trajectories of weather and climate events.

Within all three publications the SMILE framework is used to implicitly account for the intrinsic uncertainty of internal variability in the climate system. Multiple global SMILEs and one regional SMILE have been used to analyze *precipitation in past, current and future climate* conditions regarding *changes in the mean, the variability, and the upper tail (i.e., extremes)* of its distribution. Within the three publications the changes to the above are analyzed on spatial scales from global to local, as well as on temporal scales from three hours to decades.

In the *first publication (Wood et al. 2021),* multiple global SMILEs have been used to detect robust changes in *global and regional precipitation variability on interannual to decadal timescales*. Changes in precipitation variability stand to impact both natural and human systems in profound ways. Precipitation variability encompasses not only extremes like droughts and floods, but also the spectrum of precipitation which populates the times between these extremes. An increase in precipitation variability can for example enhance the volatility of crop yields and dryland productivity as well as impact other natural and human systems. The results in *Wood et al. (2021)* show implicit evidence that precipitation variability is non-stationary and is increasing in response to rising global mean surface temperatures. Thereby, the changes on interannual to decadal timescales are markedly similar. Precipitation variability increases globally at rates of ~4 % per one degree of global surface temperature warming showing a high model agreement over up-to 75 % of the global surface area. The rate exceeds the change in mean precipitation (2.5 % K^{-1}) which implies that the driving mechanisms of the change in mean and variability are different.

In the *second publication (Wood and Ludwig 2020)*, a single regional SMILE, the Canadian Regional Climate Model version 5 large ensemble, was used to analyze future changes in the magnitude of *seasonal and annual maximum precipitation over Europe*. The knowledge on how and why the intensity of extremes changes is critical to becoming a resilient society. The current infrastructure and environment are adapted to observed extremes of the past and might not be sufficiently resilient against the extremes of the future. In this study, the forced change in the magnitude of maximum precipitation was analyzed alongside the change in the internal variability to determine the time-of-emergence when the forced signal robustly emerges from the uncertainty of internal climate variability. The results in *Wood and Ludwig (2020)* show a widespread increase in the annual maximum precipitation on timesteps of three hours to five days. Thereby, the increase in subdaily maximum precipitation is larger than on daily scales. On seasonal scales there is a clear difference between widespread increases in the winter (DJF) compared to widespread decreases in maximum precipitation in summer (JJA) in

the south, west, and east of Europe. The north of Europe continues to show increasing trends even in summer. Areas with low or negative scaling rates in summer indicate that changes are partly or mainly driven by other components than thermodynamics (i.e., dynamic changes). An increase in the Bowen Ratio indicates that dry local moisture conditions might be limiting the thermodynamic component in these regions. Generally, forced signals emerge from internal variability by midcentury.

In the *third publication (Wood 2023)*, the regional SMILE CRCM5-LE, is used to analyze changes in the *probability of extreme precipitation events* in Europe. The upper tail of the precipitation distribution (i.e., extremes) is thereby influenced by both the mean and variability. This means that any change to either of these properties will determine the probability of extremes in the distribution. However, the level of contribution from mean and variability are largely unknown. This could however help in narrowing down the drivers of an increase (decrease) in the number of extreme precipitation events. *Wood (2023)* is the first publication to *attribute these changes to the individual contributions from changes in the mean and variability* in regional to local scales over Europe. The risk of extreme precipitation events increases in a +2 °C warmer world, with roughly 29 percent of all land area in Europe showing a doubling in the number extreme events. With continued warming the probability risk ratio will further increase and by +4 °C of warming already 69 percent of land grid cells are likely to show at least a doubling in extremes. The individual contributions from either the mean or variability can thereby jointly contribute to an amplification of event probability or counteract each other. On annual timescales the contributions are near equal, while in winter the mean contributes more and in summer the contribution from changes in the variability are larger. Thereby, in summer the change in variability can counteract the strong decrease in the mean and can be the sole driver of an increase in event probability. This can locally be observed over France, the Mediterranean Region, and Southeast Europe.

Zusammenfassung

Das Klimasystem, das vom Energiehaushalt der Erde bestimmt wird, ist komplex, stark vernetzt und wird durch die nichtlinearen Wechselwirkungen zwischen Atmosphäre, Ozean, Kryosphäre, Land und Biosphäre beeinflusst. Dieses System reagiert direkt auf Veränderungen im Energiehaushalt der Erde, ausgelöst durch Veränderungen des externen Antriebs, entweder durch natürliche (d.h. Sonnenzyklen, Vulkanausbrüche) oder anthropogene Einflüsse (d.h. Treibhausgase, Aerosole, Landnutzungsänderungen). Die anhaltende Veränderung des externen Antriebs durch anthropogene Einflüsse führt zu einer Zunahme des Strahlungsantriebs, welches eine Erwärmung des Klimas bewirkt. Die Klimaerwärmung führt dabei aufgrund der Thermodynamik zu einer erhöhten Wasserspeicherkapazität der Atmosphäre und damit einhergehend wird der Feuchtetransport von der Landoberfläche zur Atmosphäre und umgekehrt beeinflusst. Da die Energiebilanz ein geschlossenes System ist, muss die atmosphärische Wasserbilanz durch einen größeren horizontalen Feuchtetransport ausgeglichen werden, der die atmosphärische Zirkulation beeinflusst. Diese planetaren Veränderungen des Klimasystem lösen eine vielfältige regionale und lokale Niederschlagsreaktion aus. Unsere Gesellschaft und die Umwelt werden sowohl von Extremen als auch von Schwankungen des mittleren Niederschlags beeinflusst. Dabei ist der aktuelle Systemzustand der Gesellschaft und der Umwelt an die derzeitigen bzw. vergangenen Extremereignisse und Niederschlagsvariabilität angepasst und wahrscheinlich nicht ausreichend widerstandsfähig gegenüber Veränderungen in der Zukunft. Daher ist in der Geographie und benachbarten Forschungsfeldern (z.B. Klimawissenschaften) das robuste Verständnis der durch den Klimawandel hervorgerufenen Veränderungen des globalen und lokalen Niederschlags von zentralem Interesse für die Kommunikation von Mitigationszielen und der Entwicklung von Anpassungsstrategien.

Gegenstand dieser kumulativen Dissertation ist daher die *Erkennung robuster Muster globaler und regionaler Niederschlagsänderungen als Reaktion auf ein sich erwärmendes Klima*. Die Grundlage der Auswertungen bilden Ensembles von Klimamodellsimulationen unter vergangenen und zukünftigen Klimabedingungen. Dabei sind jedoch die transienten Veränderungen einzelner Klimarealisationen, z.B. Beobachtungsdaten oder einzelne Klimasimulationen, das Produkt von Klimasignal und interner Klimavariabilität. Die interne Klimavariabilität oder natürliche Variabilität wird durch das Chaos und die nicht Linearität des Klimasystems verursacht und ist zu jeder Zeit vorhanden. Sie wird daher auch oft als nicht reduzierbare Unsicherheit bezeichnet.

Um eine robuste Abschätzung der Klimaveränderungen, einschließlich des Klimasignals und der internen Klimavariabilität, zu ermöglichen, wird das Single Model Initial-Condition Large

Ensemble (SMILE) Framework verwendet. SMILEs bestehen aus mehreren Modellsimulationen desselben Klimamodels, wobei der externe Antrieb (d.h. Treibhausgaskonzentrationsszenario) in jeder Modellsimulation identisch bleibt und nur die Anfangszustände zu Beginn der Simulation geändert werden. Die Unterschiede in den Startbedingungen zwischen den verschiedenen Modellläufen führt aufgrund der nicht Linearität des Klimasystems zu unterschiedlichen Ausprägungen von Wetter- und Klimaereignissen. Dabei ist jede einzelne Klimasimulation gleich wahrscheinlich und das Ensemble aus den einzelnen Klimasimulationen ermöglicht somit die Quantifizierung der internen Klimavariabilität, welche durch unterschiedliche Zustände der Atmosphäre und Ozeane hervorgerufen wird.

In allen drei Publikationen wird der SMILE Ansatz verwendet, um implizit die intrinsische Unsicherheit der internen Klimavariabilität zu berücksichtigen. Mehrere globale und ein regionales SMILE wurden verwendet um die Veränderungen des mittleren Niederschlags, der Niederschlagsvariabilität und der (feuchten) Extrema in vergangenen, aktuellen und zukünftigen Klimabedingungen zu untersuchen. Dabei wurden die Veränderungen auf räumlichen Skalen von global bis lokal sowie auf den zeitlichen Skalen von dreistündig bis dekadisch analysiert.

In der *ersten Publikation (Wood et al. 2021)* wurden mehrere globale SMILEs verwendet, um *robuste Veränderungen der jährlichen bis dekadischen Niederschlagsvariabilität* auf der *globalen und regionalen Skala* zu erkennen. Veränderungen der Niederschlagsvariabilität werden natürliche und menschliche Systeme tiefgreifend beeinflussen. Die Niederschlagsvariabilität umfasst nicht nur Extreme wie Dürren und Überschwemmungen, sondern auch das Niederschlagsspektrum dazwischen. Eine Zunahme der Niederschlagsvariabilität kann beispielsweise die Volatilität von Ernteerträgen und Trockenlandproduktivität erhöhen und sich auf andere natürliche und menschliche Systeme auswirken. Die Ergebnisse in *Wood et al. (2021)* zeigen eindeutig, dass die Niederschlagsvariabilität nicht stationär ist und mit steigender Globaltemperatur ansteigen wird. Dabei ist die Zunahme der jährlichen bis dekadischen Variabilität sehr ähnlich. Die Niederschlagsvariabilität steigt mit jedem Grad der Erderwärmung um ~4 % an und zeigt dabei eine hohe Übereinstimmung der Modelle über ~75 % der Erdoberfläche. Die Zunahme übersteigt dabei den Anstieg des mittleren Niederschlags (2.5 % K^{-1}) was bedeutet, dass die Treiber der Änderung des Mittelwerts und der Variabilität unterschiedlich sind.

In der *zweiten Publikation (Wood and Ludwig 2020)*, wurde unter der Verwendung eines regionalen SMILEs, das Canadian Regional Climate Model version 5 large ensemble, die zukünftige *Veränderung der saisonalen und jährlichen maximalen Niederschlagsmengen über*

Europa untersucht. Das Wissen darüber, wie und warum sich die Intensität von Extremen ändert, ist entscheidend, um eine widerstandsfähige Gesellschaft zu werden. Die derzeitige Infrastruktur und Umwelt sind auf beobachtete Extremereignisse der Gegenwart und Vergangenheit angepasst und diese Systeme sind womöglich nicht widerstandsfähig gegen zukünftige Extremereignisse. In dieser Studie wurde das Klimasignal der maximalen Niederschlagsmenge gemeinsam mit der Veränderung der internen Klimavariabilität bestimmt, um den Zeitpunkt in der Zukunft zu ermitteln (time-of-emergence) an dem das Klimasignal den Schwankungsbereich der internen Klimavariabilität verlässt. Die Ergebnisse in *Wood and Ludwig (2020)* zeigen einen weiträumigen Anstieg des jährlichen Niederschlagsmaximum für Zeitschritte von drei Stunden bis fünf Tagen. Dabei ist die Zunahme der stündlichen Maximalwerte größer als auf der täglichen Zeitskala. Auf der saisonalen Ebene ist ein klarer Unterschied zwischen einer weiträumigen Zunahme im Winter (DJF) im gesamten Europa und einer weiträumigen Abnahme im Sommer (JJA) im Westen, Süden und Osten Europas zu erkennen. Nordeuropa zeigt auch im Sommer eine weitere Zunahme. Gebiete mit niedrigen oder negativen Skalierungsraten im Sommer weisen darauf hin, dass Veränderungen teilweise oder hauptsächlich durch andere Komponenten als die Thermodynamik (d.h. dynamische Veränderungen) getrieben werden. Eine Zunahme des Bowen Ratios deutet darauf hin, dass trockene Feuchtebedingungen möglicherweise die thermodynamische Komponente in diesen Gebieten limitiert. Generell verlässt das Klimasignal den Schwankungsbereich der internen Klimavariabilität bis zur Mitte des 21.Jahrhunderts.

In der *dritten Publikation (Wood 2023)* wird unter der Verwendung des regionalen SMILE CRCM5-LE die *Veränderung der Wahrscheinlichkeit von extremen Niederschlagsereignissen in Europa* untersucht. Das obere Ende der Niederschlagsverteilung (d.h. Extreme) ist dabei von Mittelwert und Variabilität beeinflusst. Dies bedeutet, dass jegliche Änderung des Mittelwerts oder der Variabilität die Wahrscheinlichkeit von Extremen in der Verteilung bestimmt. Jedoch ist der Anteil von Mittelwert und Variabilität weitgehend unbekannt. Dieses Wissen könnte jedoch dazu beitragen, die möglichen Treiber der Zunahme (Abnahme) der Häufigkeit von Extremereignissen einzugrenzen. *Wood (2023)* ist eine der ersten Publikationen, die die *Veränderung der Häufigkeit von Extremereignissen den individuellen Beiträgen von Veränderungen des Mittelwerts und der Variabilität* auf regionaler und lokaler Skala in Europa zuschreibt. Das Risiko von Extremereignissen steigt in einer +2 °C wärmeren Welt an und zeigt über etwa 29 Prozent der Landoberfläche Europas eine Verdoppelung der Anzahl an Extremereignissen. Bei anhaltender Erwärmung wird die Häufigkeit von Extremereignissen weiter ansteigen und bei einer Erwärmung von +4 °C dürften bereits 69 Prozent der Landoberfläche mindestens eine Verdoppelung aufweisen. Die individuellen Beiträge des

Mittelwerts und der Variabilität können dabei beide zu einer Zunahme der Häufigkeit beitragen oder einander Entgegenwirken. Auf jährlicher Zeitskala sind die Beiträge aus Mittelwert und Variabilität fast ausgeglichen, wohingegen im Winter der Mittelwert einen größeren Einfluss zeigt und im Sommer die Veränderung der Variabilität stärkeren Einfluss hat. Dabei kann im Sommer die Zunahme der Variabilität der starken Abnahme des Mittelwerts entgegenwirken und kann der alleinige Treiber für die Zunahme der Häufigkeit von Extremereignissen sein. Dies kann lokal über Frankreich, dem Mittelmeerraum und Südosteuropa beobachtet werden.

Acronyms

CanESM2	Canadian Earth System Model version 2
CMIP(5)/(6)	Coupled Model Intercomparison Project; version 5 / version 6
CORDEX	Coordinated regional climate downscaling experiment
CPM	Convection permitting model
CRCM5	Canadian Regional Climate Model version 5
ENSO	El-Niño Southern Oscillation
ESM	Earth System Model
GCM	Global Climate Model
GHG	Greenhouse Gas
GMST	Global Mean Surface Temperature
IPCC	Intergovernmental Panel on Climate Change
NAO	North Atlantic Oscillation
NWP	Numerical Weather Prediction
RCM	Regional Climate Model
RCP	Representative Concentration Pathway
SMILE	Single Model Initial-Condition Large Ensemble
SSP	Shared Socio-economic Pathways

List of Figures

List of Tables

Table of Contents

1 Introduction

Our society and the environment are impacted by both extremes and variations in the mean-state. Thereby the current states of society and the environment are adapted to extremes and levels of variability of the past and might not be sufficiently resilient to changes in the future. Recent devastating extreme events throughout the world, such as the July 2021 flooding in Western Germany (Kreienkamp et al. 2021), the heat wave in British Columbia in 2021 (Philip et al. 2021), the 2018-20 drought in Europe (Blauhut et al. 2022; Rakovec et al. 2022), or many more examples show the high vulnerability of our build environment and society against extreme events. It was quantified that climate change has already influenced the severity of these events (Philip et al. 2021; Kreienkamp et al. 2021) and that through continued global warming, droughts (Böhnisch et al. 2021; Aalbers et al. 2022; van der Wiel et al. 2022) and large floods (Brunner et al. 2021) are becoming more severe and frequent. Throughout many iterations of scientific reports by the Intergovernmental Panel on Climate Change (IPCC) and a large body of scientific publications, it is well established that the human influence on the climate system has profound impacts on the mean-state precipitation, precipitation variability, and precipitation extremes.

Precipitation variability is expected to increases under global warming globally at rates larger than the mean climate (Wood et al. 2021; Pendergrass et al. 2017). Also, large scale modes of climate variability, such as the El Nino Southern Oscillation (e.g., Haszpra et al. 2020; Maher et al. 2018) or the North Atlantic Oscillation (e.g., Böhnisch et al. 2020; McKenna and Maycock 2021), which govern the regional or local precipitation response, are expected to change. An increase in precipitation variability can regionally imply a precipitation volatility enhancing the risk of swings between extreme dry and wet conditions (Di Chen et al. 2022; Swain et al. 2018; Madakumbura et al. 2019). Enhancing the volatility of crop yields and ecosystem productivity (Gherardi and Sala 2019; Rowhani et al. 2011; Ritter et al. 2020; Liu et al. 2020) to enhancing flood risk and damage (Nobre et al. 2017). Precipitation variability not only describes the ‘space between’ mean and extreme conditions, but also the time between wet and dry extremes. On the dry side of extremes, droughts are the clearest manifestation of precipitation variability. Drought-related economic losses are directly associated with the agricultural, energy, and public water supply sector (Cammalleri et al. 2020; Freire-González et al. 2017; van Loon 2015) for which losses may be easily quantifiable. However, there are many more impacts that may linger well beyond the drought end and can cause permanent damage to biodiversity and other natural environments (United Nations Office for Disaster Risk Reduction 2021). It is expected that the risk of droughts continues to increase (Aalbers

et al. 2022; Böhnisch et al. 2021; Spinoni et al. 2018) alongside the risk of shorter times between individual drought events and multiyear droughts (van der Wiel et al. 2022).

On the wet side of the extremes, extreme precipitation events are projected to increase globally at rates of 6-7% per 1°C of increased global surface temperature warming (Allen and Ingram 2002; Held and Soden 2006; O'Gorman and Schneider 2009), which follows the rate of atmospheric moisture change. On global and regional scales, the increase in extreme precipitation is robust in observations (Contractor et al. 2021; Fowler et al. 2021; Guerreiro et al. 2018; Westra et al. 2013) and models (Fischer and Knutti 2016; Martel et al. 2021; Myhre et al. 2019; Westra et al. 2014; Fischer et al. 2013). Locally, these scaling rates can be exceeded substantially (Lenderink and van Meijgaard 2008; Lenderink et al. 2017; Fowler et al. 2021; Wood and Ludwig 2020). Thereby, global warming levels above 2°C significantly increase the risk of more severe extreme precipitation events (Kharin et al. 2018). Also, the nature of the weather systems producing extreme precipitation events are subject to change (Kahraman et al. 2021; Prein et al. 2017; Chan et al. 2023; Wasko et al. 2016). These changes to the magnitude and frequency of extremes, as well as the changing characteristic of the driving weather system, is leading to more severe and more frequent flood events (Hattermann et al. 2018; Brunner et al. 2021; van der Wiel et al. 2019).

However, future projections and the quantification of anthropogenic changes in the distribution of precipitation is challenged by the ever-present influence of internal climate variability. Internal variability in the climate system is an irreducible and important source of uncertainty (Hawkins and Sutton 2009; Lehner et al. 2020; Deser et al. 2012). On a year-to-year basis everyone can observe the manifestation of internal climate variability in the form of a hot-dry summer followed by a cold-wet summer. These variations in weather and climate are induced by the complex interplay of natural processes in the atmosphere-ocean-land-biosphere-cryosphere system.

If we imagine a world with a minimal imprint of humans on the natural system (e.g., at pre-industrial times) with centuries to millennia of uninfluenced observed weather and climate records (no volcanic eruptions and identical year-to-year solar radiation), we could imagine internal variability as fluctuations or wiggles around a well-defined stationary mean climate state. However, through natural (e.g., volcanic eruptions) or human causes (e.g., emitting of aerosols and greenhouse-gases) the earth system is undergoing a constant change of its external forcing that influences all components of the system. This means that we rather have a non-stationary climate system in which we have an evolving mean climate with wiggles around the mean where both the mean and the wiggles are influenced by external forcings.

Therefore, any climate realization, such as observations or climate model simulations, are the combination of a forced signal and internal variability.

In this dissertation, *Single Model Initial-condition Large Ensembles (SMILEs)* are used to quantify *changes in extreme and mean-state precipitation across scales in a warming climate*. SMILEs are a state-of-the-art experimental setup in climate modeling which enables the robust quantification of changes in the climate system, including the forced climate response and internal climate variability. In this setup, a single climate model is run multiple times while keeping the external forcing identical in each run, only changing the initial states at the start of the simulation. The difference in initialization among the different simulation runs samples the uncertainty based on different atmospheric and ocean states as well as due to the non-linear nature of the climate system. Each realization of the climate model is equally likely and will result in different trajectories of weather and climate events.

By using multiple SMILEs, the *projected changes in precipitation and its variability across annual to decadal time scales* are analyzed on a global scale (**Publication 1, chapter 4**). On regional scales, *changes in annual and seasonal maximum precipitation* are analyzed in a single regional 50-member SMILE over Europe (**Publication 2, chapter 5**). The same regional SMILE was used to *partition the individual contributions from changes in the mean and variability to explain changes in the probability of annual and seasonal extreme precipitation events* over Europe (**Publication 3, chapter 6**). The key findings from the three publications are discussed in **chapter 7**.

2 Scientific basis

This chapter will give a brief introduction into the scientific basis needed to understand the global and regional precipitation response to a warming climate and why natural climate variability is an important factor contributing to the changes but also contributing to the uncertainties. First, the role of natural climate variability (**section 2.1**) and the common tools to quantify natural climate variability (**section 2.2**) are discussed. The SMILE framework, which is the central tool used within this dissertation, is described (**section 2.3**) alongside the basics of climate modeling (**section 2.4**). Lastly, a brief overview of the theoretical understanding of the global and regional precipitation response to a warming climate is given (**section 2.5**).

2.1 The role of natural climate variability

In climate science and related impact studies, understanding the response of the climate system to external forcings, particularly from anthropogenic origin (i.e., greenhouse gases, aerosols, land use change), are of key interest. However, these transient changes in any realization of the climate system, such as observations or any climate model simulation, are the combination of the forced signal and internal climate variability. The internal climate variability, or natural variability, is caused by the chaotic and nonlinear nature of the climate system and is present at any given time. It is therefore often described as an irreducible uncertainty. On interannual timescales every one of us can observe natural variability. As one summer might be hot and dry, the following might be cold and wet. These interannual fluctuations are caused by different modes of variability, such as the El-Niño Southern Oscillation (ENSO), which can cause anomalous temperature and rainfall patterns over various regions on the globe. Regionally, different modes of variability are of importance, such as the North Atlantic Oscillation (NAO) for European weather and climate, which causes in its positive phase warmer and wetter winters in northern Europe, while cooler and drier conditions in the south, and vice versa for its negative phase (e.g., Hurrell and Deser 2010; Pokorná and Huth 2015; Woollings et al. 2015). From a local perspective these teleconnections might not be apparent at first, since the source region can be located far away (e.g., in the North Atlantic), however they are causally connected by for example shifting storm tracks further north or south, which then locally can determine the magnitude and frequency of extreme events. Extreme events are therefore the most discernible manifestation of internal variability.

On longer time scales (years to decades), internal variability can modulate decadal trends (Maher et al. 2020; Marotzke and Forster 2015), which can lead to misconceptions of the forced signals, as prominently highlighted by the discussion on the global warming hiatus

(Hedemann et al. 2017). Therefore, it is important to analyze the internal variability alongside the forced signal to better quantify the underlying forced change in the presence of large internal climate variability. Over time the forced signal might become large enough to clearly emerge from the noise (i.e., introduced by the natural variability), however on regional scales the internal variability can remain a large uncertainty even far into the future (e.g., Lehner et al. 2020; Wood and Ludwig 2020).

2.2 Tools to quantify natural climate variability

The key to quantifying internal climate variability is a large sample size to capture a wide variety of different atmospheric and ocean states, as well as different modes of climate variability (e.g., ENSO, NAO). The large sample size can either be long observational records or climate model data.

Long observational records can be used to quantify internal climate variability. However, any observational record spanning a long period (e.g., the last 100 years) will be influenced by a forced signal and internal variability, which makes it difficult to disentangle the two components. Any forced trend can be removed by statistical methods (e.g., linear detrending) from the observations (i.e., a single realization) and the residuals can be interpreted as internal variability (e.g., Frankcombe et al. 2018). However, detrending (e.g., removing a linear trend) can introduce large biases in the amplitude and phase of internal variability (Frankcombe et al. 2015; Frankcombe et al. 2018). The imprint of the external forcing might not be adequately removed from the observational record, and instead internal variability and the forced response are mixed (England 2021). Further, throughout the observational period the equipment as well as the location of retrieval will likely have changed, which can introduce artefacts which itself can be misinterpreted as either a forced change or a change in internal variability. This highlights the difficulties of estimating the internal variability along the time dimension under constantly changing external factors. Another caveat is the lack of high quality and long observational records which are sparse and unequally distributed across the globe.

Using climate model data can be a valuable tool to quantify internal climate variability across the entire globe. A way to estimate internal variability in the absence of any changes in external forcing, is the use of long equilibrium climate model simulations (e.g., Thompson et al. 2015; Wittenberg et al. 2014). For these idealized simulations, a climate model is forced by preindustrial external forcings, where the seasonal cycle of incoming solar radiation is repeated every year. In this setup, all concentrations of greenhouse gases, such as CO_2, are kept constant at preindustrial levels. Thus, the external forcing from year-to-year is identical. These simulations are therefore commonly named preindustrial control simulations (or

PiControl). The climate model is run for an extensive period, generating hundreds to thousands of simulation years. Although the external forcing is identical for each of the simulated years, the state of the Earth System is not the same in each year, due to internal climate variability, leading to considerable deviations from year-to-year in the simulation. By removing the influence of a forced signal, caused by a change in external forcing, the entire timeseries from the PiControl simulations can be used to quantify internal variability. In contrast to the observations the internal variability in the PiControl simulations is well defined along the time dimension. A common way to estimate the internal variability is by removing the mean from the simulation and calculating the standard-deviation over the entire length of the simulation. This can be a robust and simple estimate of internal climate variability. However, the estimate from the PiControl simulation is bound to the assumption that internal variability is stationary (i.e., remaining constant at preindustrial levels) and therefore being independent from a change in external forcing. However, Pendergrass et al. (2017) and Wood et al. (2021) show implicit evidence that precipitation variability is changing globally and regionally, implying that internal variability is non-stationary and itself is likely to change under climate change. Other studies show this for Arctic precipitation variability (Bintanja et al. 2020) or changes in ENSO variability (Haszpra et al. 2020; Maher et al. 2018). This implies that the internal climate variability itself is influenced by the change in external forcing. Thus, the hypothesis of the PiControl simulation of a constant magnitude of internal variability is false and the internal variability from the PiControl simulations is bound to a stationary climate. Therefore, another tool besides observations and the PiControl simulations is needed to quantify internal variability in a non-stationary climate.

The current best practice to determine internal variability in a non-stationary climate is the Single Model Initial-Condition Large Ensemble (SMILE) framework. A SMILE is a single climate model which has been run for multiple times (e.g., 50 times) with each single realization following the same external forcing but with different initial conditions at the start of the simulation. The small differences at the start of the simulation lead to different trajectories of weather and climate events due to the chaotic climate system. The differences among the individual realizations can be interpreted as internal variability. With SMILEs it is possible to determine both, the change in the mean-state as well as the change in internal variability under a changing external forcing. By utilizing the ensemble member space, the sample size can be increased for any point in time, for example sampling all 50 members for the 30-year period 1981-2010 will yield a sample size of 1500 equally likely years under the same external forcing. For any such 30-year period in the past, current, or future climate the mean, extremes, and the internal climate variability can be robustly quantified. This allows for the analyze of changes to any of these quantities under a constantly changing external

forcing. The SMILE framework is used as the key tool in this work and will be discussed in more detail in the next section.

Observations should however not be ruled out as an essential tool to quantifying internal climate variability, especially not when the observations can be placed in the context of large ensemble climate model simulations, where they are essential for evaluating the modelled internal variability (Suarez-Gutierrez et al. 2021; Wood et al. 2021) as well as vice versa by utilizing the climate model simulations to evaluate the observational record (Rodgers et al. 2015). Recent and ongoing progress in isolating internal variability from single climate model realizations or observations is being made by using statistical methods (e.g., Wills et al. 2020; Smoliak et al. 2015; Sippel et al. 2019; Deser et al. 2016).

2.3 The large ensemble (SMILE) framework

The basic description of a SMILE setup is the use of a single climate model with multiple realizations for the same scenario. Thereby, the choice of the climate model as well as the choice of the scenario is not relevant. Figure 1 shows the schematic framework for a representative SMILE. The idealized SMILE in Figure 1(a) starts with five different realizations from different start dates in the long PiControl simulation (Figure 1, b), with ten additional small perturbations per initial run introduced in the year 1950, before the now 50 different realizations running freely until the end of the 21st century. In this framework, the two different main types of initialization schemes (macro and micro) are used to create the different realizations. The macro initialization samples initial states from well separated start dates within a long control simulation (Figure 1, b), it therefore samples uncertainty based on different atmospheric and ocean states as well as due to the non-linear nature of the climate system (Hawkins et al. 2016). The micro initialization adds random perturbations (e.g. cloud parameterization) to single macro states (Figure 1, c) sampling the uncertainty based on the non-linear response of the climate system (Hawkins et al. 2016). The macro initialization has the advantage that the inter-member spread (differences among the individual members) is already large from the start of the initialization, while member from micro initializations are very similar at the start and need time to result in the same inter-member spread as the macro counterparts. Leduc et al. (2019) show that it takes up to two years for temperature to evolve to the same magnitude of inter-member spread as from macro initialized members. This can be explained by the fact that the micro initialized members start with same ocean conditions, while macro members normally start with mixed ocean conditions, and it will take the micro members sometime to develop different ocean states. In this study, the differences between

the different initialization schemes are not of relevance for the analysis since the periods of interest are well separated from the initialization time.

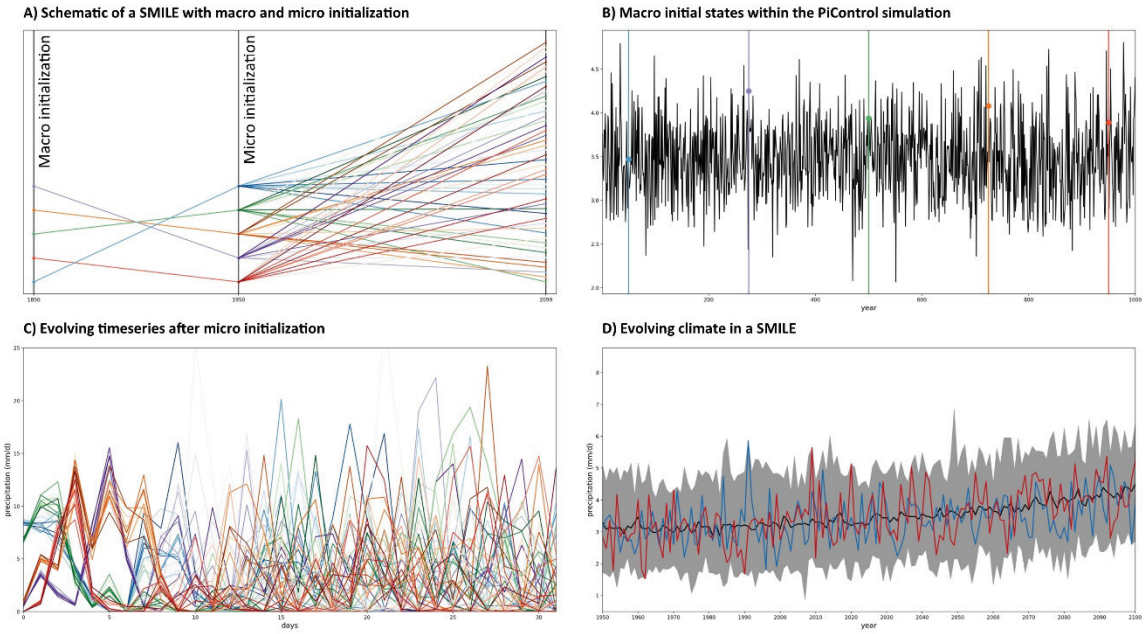

Figure 1 | SMILE Framework. (a) Schematic depiction of a SMILE with macro and micro initialization. (b) Macro initial states (colored dots with vertical lines) sampled from within the PiControl simulation (black line). (c) Evolving weather trajectories within the first 31 days after micro initialization. Same color family (blue, purple, green, orange, red) indicate the origin from the same macro initialization. The color intensity shows different micro initialized simulations. (d) Evolving ensemble mean (black line), ensemble spread (min/max, grey shading), and two individual ensemble members (blue and red line). Data for panels (b)-(d) from the CanESM2 model extracted for the grid cell covering the city of Munich. Data in (b) from the CanESM2 PiControl simulation. Data in (c) and (d) from the 50-member CanESM2 large ensemble simulations.

The required ensemble size for a SMILE is dependent on the research question, target variable, the acceptable error suitable for the application, and the region (Tebaldi et al. 2021; Milinski et al. 2020; Wood et al. 2021). For the determination of the forced response smaller ensemble sizes are suitable for changes on global scales (Maher et al. 2021a; Milinski et al. 2020), but on regional scales it is possible that the sign of the forced trend can be misidentified by smaller ensembles depending on its location (Maher et al. 2019). In contrast, for the question on how internal variability itself is changing larger ensemble sizes are required. Maher et al. (2018) have revealed that for detecting changes in ENSO variability, ensemble sizes beyond 30 member are needed, because ENSO itself is strongly influenced by internal variability. For the question on changing interannual precipitation variability, Wood et al. (2021) show that more members are advisable and are dependent on the geographic region. In the study it is suggest that for higher latitudes at least 30 members are needed, but also in other regions smaller ensembles might not be as reliable. The common ensemble size of the CMIP5 era SMILEs range from 16 (EC-Earth; Hazeleger et al. (2010)) to 100 members (MPI-GE; Maher et al. (2019)). Most SMILEs from this model era were not part of the initial CMIP5 modelling activity and most were ensembles of opportunity. Hence, most SMILEs were limited to the RCP8.5

scenario due to a tradeoff between ensemble size and number of scenarios. In CMIP6, SMILEs are commonly produced with multiple large ensembles from different models and for multiple scenarios.

The main benefit of the SMILE framework is the provisioning of physically consistent large sample sizes of past and future climate events. Many studies have used SMILEs for a better estimation of the models forced response, enabling the clean separation of the forced response (i.e. climate change signal) and internal variability (e.g., Wood and Ludwig 2020; Kay et al. 2015; Maher et al. 2019) including partitioning of uncertainties (e.g., Lehner et al. 2020; Maher et al. 2021b). Other studies used SMILEs to analyze whether climate change influences internal climate variability itself, such as different modes of climate variability (e.g., Böhnisch et al. 2020; McKenna and Maycock 2021; Maher et al. 2018), or more general if interannual to decadal variability is changing (e.g., Wood et al. 2021; Bintanja et al. 2020; Maher et al. 2021b). The large sample size has also been used to study changes in extreme events (e.g., Aalbers et al. 2018; Poschlod and Ludwig 2021; Wood and Ludwig 2020; Bevacqua et al. 2022; Kirchmeier-Young et al. 2017) especially looking at extremes with low probabilities (i.e., long return periods) (e.g., van der Wiel et al. 2019; Martel et al. 2020; Brunner et al. 2021). SMILEs are also utilized as a testbed for new statistical methods including machine learning applications (e.g., Mittermeier et al. 2019; Mittermeier et al. 2022; McKinnon et al. 2017; Heinze-Deml et al. 2021; Lehner et al. 2017). Since observational reference datasets are uncertain (e.g., Alexander et al. 2020; Gampe et al. 2019) and can only represent a single realization of the climate system, model evaluation can also benefit from SMILEs by placing observations within the spread of the ensemble (e.g., Suarez-Gutierrez et al. 2021; Wood et al. 2021; Maher et al. 2019). This is not a complete list of applications and new innovative ways of using SMILEs are constantly being developed. For further examples of the use of SMILEs see Maher et al. (2021a) and Deser et al. (2020).

Since the term large ensemble is not trademarked or defined it is also used for suites of multiple climate models with single realizations (e.g., CMIP, or CORDEX). These multi-model ensembles can also be termed large ensembles, however they do not offer the same clean separation between internal variability and forced signal. However, when comparing large multi-model ensembles (i.e., CMIP5, Euro-CORDEX) with SMILEs, there seems to be considerable internal variability included in multi-model large ensembles (Wood et al. 2021; Maher et al. 2021b; von Trentini et al. 2019). By clustering the CMIP5 multi-model ensemble into sub ensembles with similar or same atmospheric or ocean model components, the artificial ensembles can produce similar magnitudes of internal variability as an ensemble of SMILEs (Maher et al. 2021b). In this dissertation the terminology *large ensemble* is used in the context of SMILEs.

2.4 Basics of climate modeling

Climate models have already been mentioned several times, so what is a climate model and why is it a great tool to study the response of the Earth System to a changing climate? The main purpose of a climate model is to have a digital representation of the Earth system that can be used to run different versions (i.e., scenarios) of past and future climates to better understand the response of the Earth System to changing external forcings. The foundation of climate models are physical equations describing the interactions between the cryosphere, ocean, atmosphere, and biosphere with all important lateral and vertical fluxes of energy and mass compiled in a computer code. Technically this is achieved by dividing the Earth into a three-dimensional grid space of horizontal (representing geographic regions) and vertical (representing different atmospheric and sub-surface levels) grid cells, solving partial differential equations within each grid cell and moving mass and energy between them, while conserving mass, movement, and energy. This process is repeated for each timestep of the simulation which explains the high computational cost of running such models.

If the three-dimensional network of grids circumvents the entire globe, then these models are considered Global Climate Models (GCM). The current generation of GCMs have a spatial resolution of approximately 1°-2.8°, which translates to roughly 100-300km. Compared to current versions, early GCMs had a simple representation of the atmosphere and ocean, and with each new version the components of the Earth system have been updated and extended. One of the latest advancements has been the addition of biogeochemical interactions in the Biosphere and Ocean component. This addition has allowed for a direct computation of biogeochemical cycles, such as the carbon cycle, which play an important role in the climate system. Hence, these models are called Earth System Models (ESM). For simplicity and because a distinction between GCM and ESM is not relevant in this work, both models will be related to as GCMs.

2.4.1 Scenarios

To study the long-term climate change, climate models need to be linked to defined scenarios or pathways of future emissions/concentrations of GHGs and aerosols, as well as land use change, and possible changes in the natural forcing (i.e., solar cycle, volcanic eruptions). All climate model simulations used within the scope of this dissertation are based on the Coupled Model Intercomparison Project 5 (CMIP5) protocols (Taylor et al. 2012). The scenarios for the CMIP5 generation of simulations have been developed for the fifth assessment report (AR5) of the IPCC and are referred to as Representative Concentration Pathways (RCP). The RCP scenarios are representative GHG pathways which will result in a specific additional net radiative forcing (Meinshausen et al. 2011; Moss et al. 2010; van Vuuren et al. 2011). Representative in this context means, that the pathway is only one of many possible

trajectories of GHG concentrations towards the specified radiative forcing. These representative pathways are the result of Integrated Assessment Tools and further post-processing. In contrast to the previous SRES scenarios (Special Report on Emission Scenarios; Nakicenovic, N. and Swart, R. 2000), the RCP scenarios are not directly based on socio-economic pathways (SSP). In the development of the different RCPs socio-economic assumptions (e.g., population and socioeconomic development) have been made, but they rather represent internally consistent sets of time-dependent forcing projections which could potentially be realized by more than one SSP (Collins et al. 2013). In CMIP5 and respectively for the AR5 the four main RCP scenarios RCP2.6, RCP4.5, RCP6.0 and RCP8.5 have been selected (Figure 2, a). Thereby, the numbering of the RCP scenarios represents the approximate net added radiative forcing at their 21st century stabilization or peak radiative forcing value (i.e., RCP**8.5** -> additional **8.5** W/m^2). The highest emission scenario RCP8.5 is often described as a pathway of little climate mitigation and therefore with a high demand for climate adaptation. The CMIP5 multi-model mean response for the RCP8.5 scenario is approx. an increase of +4.61 °C in global mean surface temperature above the pre-industrial period 1850-1900 (Figure 2, b). In contrast, the lowest scenario RCP2.6 represents a pathway with high levels of climate mitigation and respectively a smaller need for climate adaptation. The RCP2.6 scenario projects a GMST warming of +1.61°C above pre-industrial times. In this dissertation only the RCP8.5 scenario is considered.

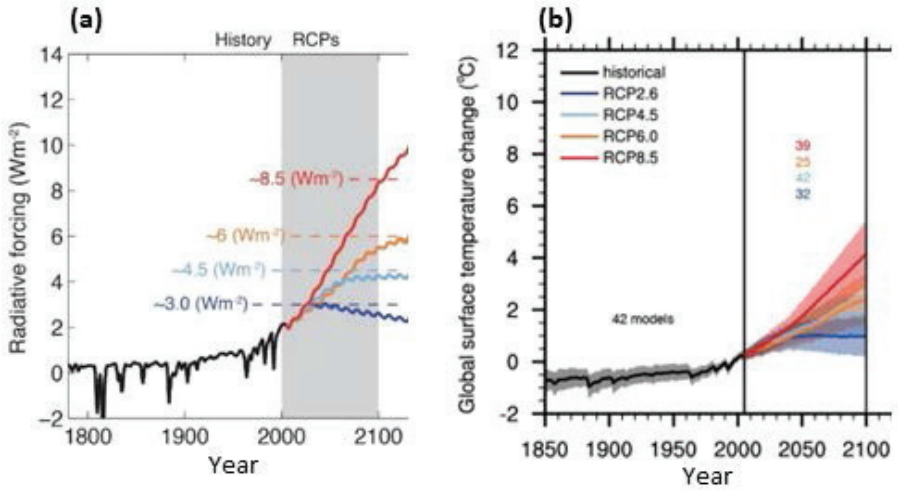

Figure 2 | Different Representative concentration pathway (RCP) scenarios and associated global mean surface temperature change. (a) Additional radiative forcing (Wm^{-2}) in the four CMIP5 RCP scenarios (adapted from: Cubasch et al. 2013); (b) CMIP5 multi-model mean and model spread of global surface temperature change (°C) in response to the different RCP scenarios compared to the reference period 1986-2005. To translate the GMST change into warming above pre-industrial 1850-1900 an additional 0.61°C should be added. This is the assumed observed warming since 1850-1900 until 1986-2005. (adapted from: Collins et al. 2013)

2.4.2 Projection Uncertainties

All climate model simulations are subject to projection uncertainties which can be the result of different scenarios which entail different trajectories of global warming (scenario uncertainty), different models projecting low/high levels of change under the same forcing scenario (model uncertainty), and from the chaotic nature of the earth system (uncertainty from internal climate variability). A comprehensive overview of the three types of projection uncertainties and the fractional partitioning is given in (Hawkins and Sutton 2009; Lehner et al. 2020), and are briefly described here.

The projection uncertainty from ***internal climate variability*** has already been discussed in some detail. The uncertainty originates from the chaotic nature of the earth system induced by natural processes in the atmosphere-ocean-land-biosphere-cryosphere system and can be considered an irreducible source of uncertainty which is present at any given point in the future or past. The current best practices to quantify internal climate variability are discussed in section 2.2.

The ***scenario uncertainty***, or radiative forcing uncertainty, describes the uncertainty related to the unknown future levels of greenhouse gas concentrations. Since these scenarios are socioeconomic what-if scenarios, they can be considered, from a climate science perspective, as an irreducible source of uncertainty. The scenario uncertainty can be quantified by using a multi-model ensemble (i.e., CORDEX, CMIP5/6) run under different emission scenarios (i.e., RCP or SSP-RCP).

Model uncertainty, or climate response uncertainty, are determined by structural differences between the climate models, leading to differences in the model's response to external forcing. The differences between the models arise from differences in model components and the setup/tuning of the model. Some of these model uncertainties can be traced back to differences in the implementation of the associated forcing agents from the RCP scenarios, which can lead to variations to the respective levels of radiative forcing (Collins et al. 2013). Most of the model uncertainty can be boiled down to model imperfections, they can be considered as a reducible uncertainty under constant improvements of the models. The model uncertainty can only be addressed with multi-model ensembles. However, separating the model uncertainty from the uncertainty of internal climate variability remains challenging in traditional multi-model ensembles (Maher et al. 2021b) where individual models only have a single or only a small number of realizations (i.e., CMIP5 or EURO-CORDEX). von Trentini et al. (2019) for example show that the spread of internal climate variability within a single SMILE can cover large parts of the spread in a multi-model ensemble (i.e., EURO-CORDEX). A more robust way in separating model uncertainty from internal climate variability is the use

of a multi-model ensemble consisting of multiple SMILEs (Maher et al. 2021b; Lehner et al. 2020; Wood et al. 2021).

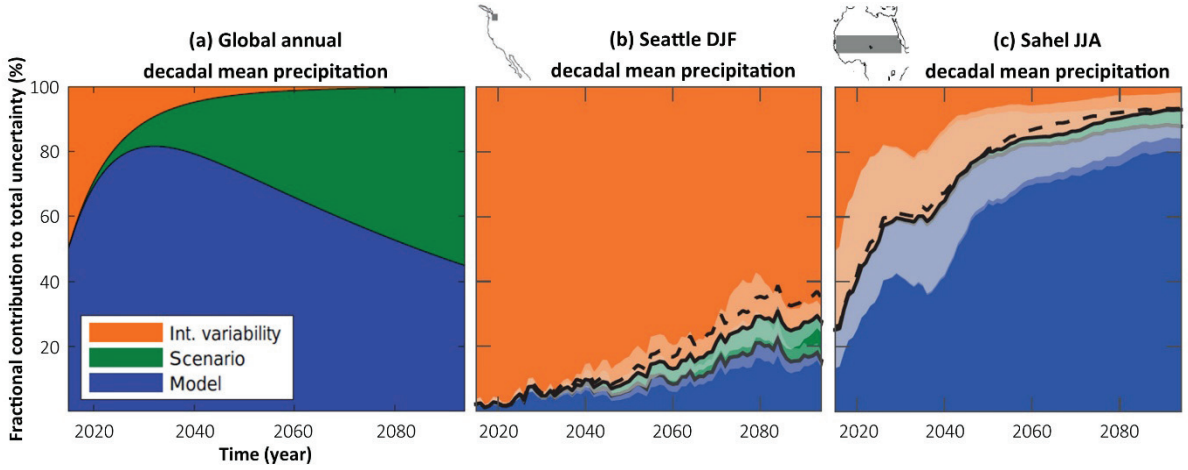

Figure 3 | Fractional contribution to total uncertainty from the three main sources of climate projection uncertainty (internal variability, scenario, and model) for decadal mean precipitation. (a) Global annual decadal mean precipitation, (b) Local uncertainties for Seattle DJF decadal mean precipitation, (c) Regional uncertainty for the Sahel JJA decadal mean precipitation. (adapted from figures 2, 7 in Lehner et al. (2020))

The fractional contribution from all three sources of uncertainty is dependent on the projected time horizon (i.e., short-term (<30 years), mid-term (30-50 years), and long-term (>50 years)), as well as geographic region, regional extent (global vs. local), season, and target variables among others. Figure 3 showcases the fractional contribution of each uncertainty source to decadal projections of precipitation on global, regional and local scales (adapted from Lehner et al. 2020). On longer projection time scales the contribution from scenario uncertainty emerges to be the largest contribution, then model uncertainty and finally with lesser importance internal variability. However, on local scales the influence of internal climate variability grows in importance compared to the global scales and remains important throughout the mid-term and even the long-term perspective (Wood and Ludwig 2020; Lehner et al. 2020). For short-term projections, internal climate variability is the dominant source of uncertainty (Maher et al. 2020; Lehner et al. 2020).

2.4.3 Regional Climate Models

Many local applications require climate information at higher spatial resolutions that current GCM simulations cannot commonly deliver. Although the current generation of GCMs can run on very high resolutions globally, computational limitations have so far hindered large scale applications. Current efforts within the High Resolution Model Intercomparison Project (HighResMIP) for CMIP6 are ongoing to deliver a multi-model ensemble of global simulations on spatial scales of 25-50km (Haarsma et al. 2016). The computational limitations have certainly been a larger issue in the past. Therefore, Regional Climate Models (RCM) or Limited Area models have been developed to bridge the resolution gap. The first models have been

developed in the late 1980s (Dickinson et al. 1989; Giorgi and Bates 1989). These models are run over smaller domains, such as Europe or North America, in a tradeoff between higher spatial resolution and computational cost. The RCMs are generally run on a spatial resolution of 0.11° or 0.44° (~12km or ~50km). The higher resolution allows for the representation of physical processes (e.g., convection, clouds) and geophysical features (e.g., topography, landuse, coastlines) at the subgrid-scale of a GCM, which should further enable better representation of mesoscale systems (i.e., storms and extreme events) (Giorgi and Gutowski 2015). An RCM is normally not run independently and is rather dependent on the information of the GCM. Since, the RCM is simulating a limited area of the globe it requires lateral boundary conditions, which are provided through the driving GCM. This feeding of information from the GCM to the RCM is commonly done in a one-way-nesting setup. One-way-nesting means that information is only shared from the GCM to the RCM without any feedbacks returning to the GCM (Giorgi and Gutowski 2015). While the RCM is able to develop its own weather and climate within its own RCM modeling domain, some information on large-scale circulation from the GCM should be retained (Laprise 2008). This can be achieved through techniques of spectral nudging (von Storch et al. 2000). Especially large-scale features such as the NAO, which is very relevant for the European weather and climate, should be maintained throughout the downscaling process. Böhnisch et al. (2020) show that the large-scale teleconnections, connected to the NAO, are properly propagated from the GCM to the finer RCM scale, for the GCM-RCM pair (CanESM2-CRCM5) that is of relevance for this study.

The added-value of RCM over GCM simulations has been shown in many studies (e.g., Di Luca et al. 2016; Di Virgilio et al. 2020; Giorgi et al. 2016; Rummukainen 2016; Torma et al. 2015). Nonetheless, RCMs can show considerable biases when compared to observational datasets (e.g., Berg et al. 2019; Kotlarski et al. 2014), which is also true for GCM simulations.

Any RCM will add another dimension of model uncertainty in addition to uncertainties already coming from the GCM. Choosing a single RCM to downscale all available GCM simulations would be a great start and would result in a better understanding of the uncertainties coming from the GCM on local scales. However, different RCMs will deliver different results for the same GCM (e.g., Rummukainen 2016). Therefore, the regional climate modelling community has consolidated its efforts, within the Coordinated Regional Climate Downscaling Experiment (CORDEX), in creating regional multi-model ensembles for 14 core regions across the globe (e.g., Endris et al. 2013; Giorgi and Gutowski 2015; Jacob et al. 2014; Mearns et al. 2012; Ruti et al. 2016). The joint goal is to maximize the matrix of GCM-RCM combination for multiple scenarios to address the complex uncertainty quantification.

In addition to these regional multi-model ensembles, some modeling groups have used funding opportunities to dynamically downscale global SMILEs to the RCM resolution to create regional SMILEs (e.g., Addor and Fischer 2015; Leduc et al. 2019; Aalbers et al. 2018; Fyfe et al. 2017). Thereby, each GCM-SMILE member is dynamically downscaled by the same RCM. Differences between the RCM member are due to the initial conditions in the driving GCM with no further perturbations added within the downscaling process, which means that these differences can be interpreted as internal climate variability. One of these regional SMILEs, the CRCM5-LE, is used within this dissertation.

2.5 Theoretical understanding of global and regional precipitation change

The change in precipitation can generally be divided into the two main drivers thermodynamics and dynamical changes, whereby these components can amplify each other or contrast each other (Figure 4, c-d). The change in the global water cycle in a warming climate is partly determined by the thermodynamic response leading to an increase of near surface specific humidity and total atmospheric water content by about 7% per 1°C of warming, as defined by the Clausius-Clapeyron scaling (Held and Soden 2006; Douville et al. 2021). However, the change in global mean precipitation and evaporation is rather constrained by the balance of energy fluxes in the atmosphere and at the surface, hence by the Earth's energy budget (Douville et al. 2021). Thereby, latent heat released by precipitation is balanced by the net atmospheric longwave radiative cooling minus the heating from absorbed incoming sunlight and the sensible heat flux from the surface (Allan et al. 2020). It is established that global mean precipitation increases between ~2-3 % K^{-1} (Allen and Ingram 2002; Allan et al. 2020; Collins et al. 2013) which can be confirmed by the ensemble of SMILEs used in this dissertation showing a multi-SMILE average of 2.5 % K^{-1} (Figure 4, a)(Wood et al. 2021). The mean precipitation response is thereby governed by fast (rapid) adjustments that directly respond to changes in forcing agents (i.e., GHGs and aerosols), and slow adjustments (feedback response) through changes in mean surface temperature in response to radiative forcing (Allan et al. 2020; Sillmann et al. 2019). The increase in atmospheric water vapor due to thermodynamics implies an intensification of the horizontal moisture transport which generally leads to an amplification of regional precipitation minus evaporation (P-E) patterns (Douville et al. 2021). In short the areas with negative P-E patterns, mainly over the oceans, will experience an intensification of the moisture flux from the surface to the atmosphere (Allan et al. 2020). As a consequence the atmospheric moisture balance is achieved by a horizontal moisture transport from the evaporative oceans to high precipitation zones of the atmospheric circulation (Douville et al. 2021). This change in the moisture transport and the greater warming over land than oceans will likely alter atmospheric circulations. Regional

water cycle changes are dominated by changes in the large-scale atmospheric circulations, which is however not yet as well understood as the thermodynamic component (Allan et al. 2020).

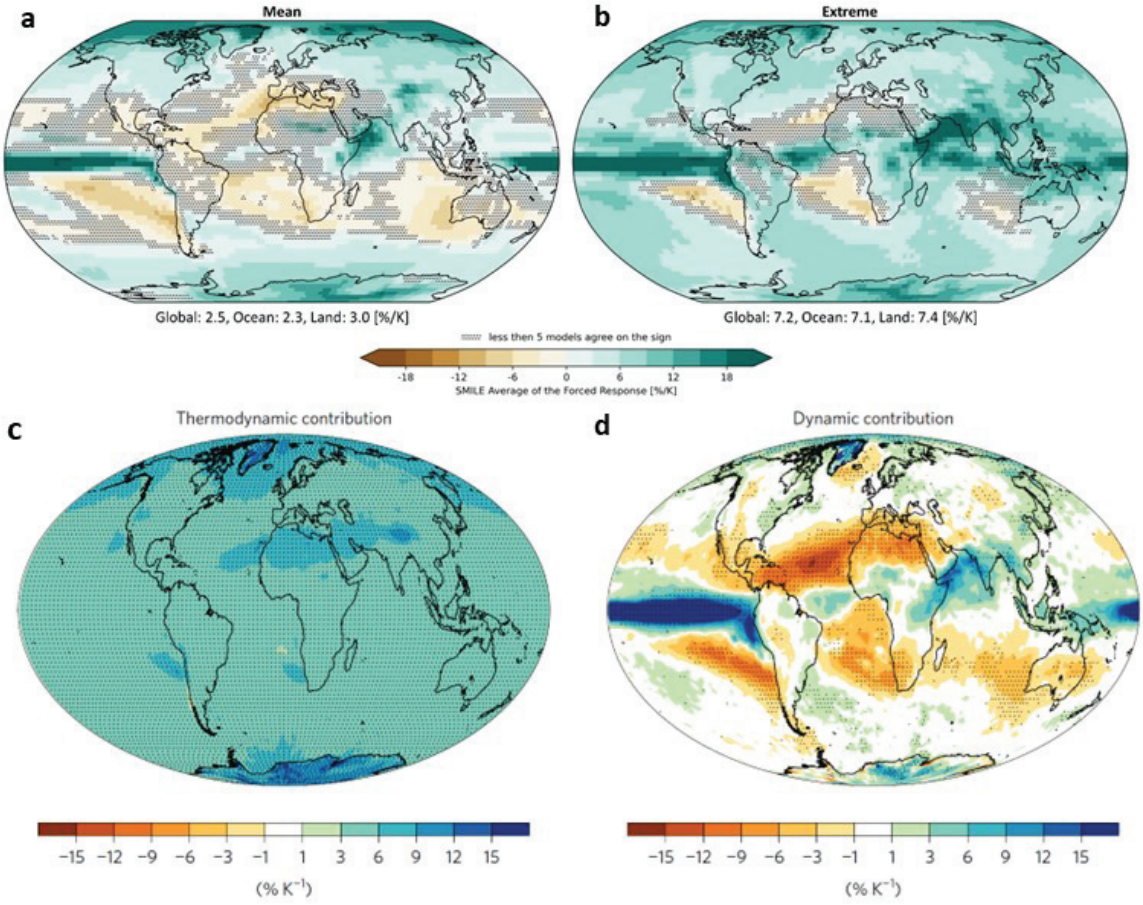

Figure 4 | Global patterns of mean and extreme precipitation change. (a) Multi-SMILE average forced response of mean precipitation at the end of the century. (b) Multi-SMILE average forced response of extreme precipitation (99.9th daily percentile) at the end of the century. (c) Thermodynamic contribution to changes in Rx1d, shown here as the multi-model mean fractional changes in thermodynamic scaling. (d) Dynamic contributions to changes in Rx1d defined as the difference between changes in full scaling and changes in thermodynamic scaling (full minus thermodynamic). (a)-(b) adapted from figure S5 in Wood et al. (2021). (c)-(d) adapted from figure 3 in Pfahl et al. (2017).

In contrast to the changes in mean precipitation, changes in extreme precipitation are not constraint by the Earth's energy budget and are rather constraint by the available atmospheric moisture. Hence, it can be expected that extremes change close to the Clausius-Clapeyron scaling of 7% K^{-1} (O'Gorman and Schneider 2009; Douville et al. 2021) which can be confirmed by the ensemble of SMILEs used in this dissertation showing a multi-SMILE average of 7.2 % K^{-1} (Figure 4, b)(Wood et al. 2021). However, the thermodynamic response which is relatively homogenous across the globe (Figure 4, c) can be modified by dynamical responses by either amplifying the regional thermodynamic response or by counteracting leading to a sign change (Figure 4, d). Thereby the two components (i.e., thermodynamics and dynamical changes) are not independent of each other but rather physically connected (Pfahl et al. 2017). The

mechanisms controlling the dynamical component and the changes thereof are regionally and seasonally divers. The models generally agree well on the thermodynamic response but show large model uncertainties for the changes in dynamic drivers (Zappa et al. 2013; Harvey et al. 2020). Over Europe there are many studies that try to unravel the dynamic component driving the regional and seasonal precipitation response (e.g., Brogli et al. 2019; Kröner et al. 2017; Kjellström et al. 2013; Vries et al. 2022; Coumou et al. 2015; Tang et al. 2018). As an example two possible changes to the dynamic component governing changes in long duration extremes (Bevacqua et al. 2022) and determining convective sub-daily extremes (Chan et al. 2023) are discussed.

Bevacqua et al. (2020) show that in winter the number of cyclone clusters (i.e., consecutive cyclones moving across the same region) could reduce while the mean precipitation intensity of each cyclones increases. Thereby, the increase in mean precipitation intensity per cyclone can be explained by the larger water holding capacity of a warmer atmosphere, i.e. thermodynamics. Over Northern Europe, the number of clusters remains unchanged while experiencing an increase in mean precipitation per cluster which overall increases the accumulated precipitation extremes from cyclones. Over Central Europe, despite a large increase in the mean precipitation per cluster, the accumulated precipitation extremes show only a moderate increase due to an overall reduction in the number of cyclones. Over Southern Europe, the accumulated extreme precipitation decreases due to a decrease in the number of cyclones. Which is generally consistent with the findings in Zappa et al. (2015), that show regionally reduced cyclone activity while mean precipitation intensity increases. In this study, they further show a reduction in the number of weakly precipitating cyclones while the number of strong and extreme precipitating cyclones increases.

Changes to the storm characteristics of mesoscale-convective systems could explain the change in magnitude and frequency of extreme sub-daily precipitation events by changes in the duration and size of storms (Fowler et al. 2021). Mesoscale-convective systems are important contributors to extreme precipitation in Europe. However, there are currently contrasting lines of evidence, and no consensus is established. The study of Chan et al. (2023) has compared two different Pan-European CPM simulations, concluding that both show increases in peak precipitation intensity, total precipitation volume, and temporal clustering of mesoscale-convective storms in response to a warming climate. However, the two models disagree on how storm characteristics change. While the one model projects more frequent, smaller, and slower-moving storms, the other model projects fewer, larger, and faster-moving storms.

Although constant progress is being made, these studies highlight that it is difficult to narrow down the dominant drivers of mean and extreme precipitation change due to model uncertainty and internal climate variability. A first step in understanding the processes involved is the robust quantification of the forced change in mean and extreme precipitation in response to climate change. This dissertation contributes to detecting robust signals in the forced response in the presence of large internal climate variability.

3 Framing of the scientific publications

This cumulative dissertation is based on three peer-reviewed scientific articles of which two have been fully published in the international scientific journals of *Environmental Research Letters* and *Geophysical Research Letters*. The third paper has been submitted to the open-access journal *Earth System Dynamics*.

In Geography and related fields (i.e., Climate Sciences), robust understanding of the response of the climate system to external forcings, particularly from anthropogenic origin (i.e., greenhouse gases, aerosols, land use change), are of key interest for the communication of mitigation targets and the development of adaptation strategies. However, these transient changes in any realization of the climate system, such as observations or any climate model simulation, are the combination of the forced response and internal climate variability. This means that robust patterns of change are, depending on the time horizon, not easy to detect due to the noise from internal climate variability.

The scope of this cumulative dissertation is the *detection of robust patterns of global and regional precipitation change in response to a warming climate*. Within all three publications the SMILE framework is used to implicitly account for the intrinsic uncertainty of internal variability in the climate system. Multiple global SMILEs and one regional SMILE have been used to analyze precipitation in past, current and future climate conditions regarding changes in the mean, the variability, and the upper tail (i.e., extremes) of its distribution. Within the three publications the changes to the above are analyzed on spatial scales from global to local, as well as on temporal scales from three hours to decades. In the following the scope of each publication including the initial hypothesis and posed research questions are discussed, as well as the transition between publications.

The first publication *Wood et al. (2021)* (**chapter 4**) sets the contextual baseline of this work by proving that the climate simulations from the global SMILEs agree with the theoretical understanding of the global and regional precipitation response to a warming climate and are therefore a valid and useful tool for further analysis. In this publication a set of multiple global SMILEs was used to test the hypothesis of *non-stationarity in precipitation variability* and as a response to rising global mean surface temperature an *increase in precipitation variability on interannual to decadal timescales*. Within the scope of this paper the individual global SMILES (see Table 1) were first evaluated for their representation of interannual variability using two different global gridded observational datasets (see Table 2), before analyzing the forced changes and multi-model agreement in future precipitation variability. The following hypothesis and research questions are addressed in the publication:

H1: *Precipitation variability is non-stationary and increases with rising global mean surface temperature on interannual to decadal timescales.*

RQ1.1: (a) *Are SMILEs capable of capturing observed interannual variability? (b) Does the ensemble size influence the representation of variability?*

RQ1.2: *Is precipitation variability increasing with an increase in global surface temperature and are the changes in variability comparable on interannual to decadal timescales?*

RQ1.3: *Are changes in precipitation variability robust across SMILEs and if not where are the areas with high structural uncertainty?*

Table 1 | Overview of the global and regional large ensemble climate simulations used

Global SMILEs							
Modeling Center	**Model Version**	**Spatial Resolution**	**Initialization (methods)**	**Ensemble Size**	**Scenario**	**Reference**	**Paper**
CCCma	CanESM2	~2.8° x 2.8°	Macro and Micro	50	RCP8.5	Kirchmeier-Young et al. (2017)	1
NCAR	CESM1	~1.3° x 0.9°	Micro	40	RCP8.5	Kay et al. (2015)	1
CSIRO	MK3.6	~1.9° x 1.9°	Macro	30	RCP8.5	Jeffrey et al. (2013)	1
SMHI/KNMI	EC-Earth	~1.1° x 1.1°	Micro	16	RCP8.5	Hazeleger et al. (2010)	1
GFDL	CM3	~2.0° x 2.5°	Micro	20	RCP8.5	Sun et al. (2018)	1
GFDL	ESM2M	~2.0° x 2.5°	Macro	30	RCP8.5	Rodgers et al. (2015); Schlunegger et al. (2019)	1
MPI	MPI-ESM-LR	~1.9° x 1.9°	Macro	100	RCP8.5	Maher et al. (2019)	1
Regional SMILEs							
Modeling Center	**Model Version**	**Spatial Resolution**	**Boundary Conditions (GCM)**	**Ensemble Size**	**Scenario**	**Reference**	**Paper**
Ouranos	CRCM5	~0.11°x0.11°	CanESM2	50	RCP8.5	Leduc et al. (2019)	2, 3
Ouranos	CRCM5	~0.11°x0.11°	CanESM2	35	piControl		3

The first publication already delivers valuable information on the changes of mean-state and extreme precipitation as well as of precipitation variability. However, the global SMILEs are too coarse to properly represent the complex regional to local precipitation response over Europe. Especially for precipitation extremes, higher resolution climate models are necessary to adequately represent the complex topography over Europe. Therefore, in the second publication *Wood and Ludwig (2020)* (**chapter 5**) a single regional SMILE (see Table 1) was used to test whether the *magnitude of annual and seasonal maximum precipitation increases* and whether the forced signal *robustly emerges from internal climate variability* over Europe. The

regional SMILE (i.e., CRCM5-LE) is a dynamically downscaled version of one global SMILE (i.e., CanESM2-LE) which has been part of the first publication. The findings from the first publication have proven that the driving CanESM2-LE represents interannual variability well as well as its agreement on changes in precipitation with the other SMILEs over Europe. The following hypothesis and research questions are addressed in the second publication:

> **H2:** *The magnitude of heavy precipitation is increasing over Europe in a warming climate with changes emerging from internal variability.*
>
> **RQ2.1**: *(a) Is seasonal and annual maximum precipitation changing over Europe? (b) Is the magnitude of change dependent on the season and temporal aggregation?*
>
> **RQ2.2:** *Do the changes in seasonal and annual extremes follow the Clausius-Clapeyron scaling?*
>
> **RQ2.3:** *When can we expect changes in extreme precipitation to robustly emerge from internal variability?*

The first two publications show that the mean and variability of precipitation are changing in response to a warming climate, but that these changes are not synchronized, implying that the change in the mean and variability are driven by different mechanisms. The upper tail of the precipitation distribution (i.e., extremes) is thereby influenced by both the mean and variability. This means that any change to either of these properties will determine the probability of extremes in the distribution. The third publication *Wood (2023)* (**chapter 6**) investigates the *importance of changes in both the mean and variability* for the *changes in the probability of extreme precipitation events* in Europe. Climate simulations, from the same regional SMILE as in publication two (see Table 1), at pre-industrial, current and future climate conditions are used. The following hypothesis and research questions are addressed in the second publication:

> **H3:** *Changes in the probability of extreme precipitation events are governed by changes in both the mean and variability.*
>
> **RQ3.1:** *(a) Do current climate projections over Europe already show an increase in the probability of extreme precipitation events? (b) Will the risk of extreme precipitation events continue to increase in future climates?*
>
> **RQ3.2:** *(a) What are the individual contributions from changes in the mean and variability to the total change in probability risk ratio? (b) Are the individual contributions dependent on the season, level of aggregation, or level of extremeness?*

Table 2 | Overview of observational datasets used in evaluation studies

Gridded observational datasets from the FROGS database (Roca et al. 2019)					
Dataset Name	**Spatial Resolution**	**Coverage**	**Period**	**Reference**	**Paper**
REGEN-ALL-v2019	1° x 1°	Global land	1950-2016	Contractor et al. (2020)	1
GPCC-FDD-v2018	1° x 1°	Global land	1982-2016	Ziese et al. (2018)	1
In-situ meteorological station data					
Dataset Provider	**Spatial Resolution**	**Coverage**	**Period**	**Reference**	**Paper**
DWD	Point	Germany	1995-2019	DWD (2020)	2
MeteoSwiss	Point	Switzerland	1995-2019	MeteoSwiss (2020)	2

The following **chapters 4-6** include the three individual publications alongside a plain language summary for each publication and some general information on the respective journal. In **chapter 7** the posed research questions are addressed by discussing the key findings of each publication upon which the initial hypothesis is either accepted or rejected. Further, the broader impact of the findings and work are briefly discussed. In **chapter 8** the perspective on how the SMILE framework can be fused with other novel climate modeling and impact modeling frameworks is discussed. Lastly, **chapter 9** gives a brief overview of other co-authored publications.

4 Changes in precipitation and its variability on a global scale

This work has been published in the Journal *Environmental Research Letters*.

Wood, Raul R.; Lehner, Flavio; Pendergrass, Angeline G.; Schlunegger, Sarah (2021): Changes in precipitation variability across time scales in multiple global climate model large ensembles. In Environ. Res. Lett. 16 (8), p. 84022. DOI: 10.1088/1748-9326/ac10dd.

Plain language Summary:

Anthropogenic changes in the variability of precipitation stand to impact both natural and human systems in profound ways. Precipitation variability encompasses not only extremes like droughts and floods, but also the spectrum of precipitation which populates the times between these extremes. An increase in precipitation variability can enhance the volatility of crop yields and dryland productivity as well as other natural and human systems. Understanding the changes in precipitation variability alongside changes in mean and extreme precipitation is essential in unraveling the hydrological cycle's response to warming. We use a suite of state-of-the-art climate models, with each model consisting of a single-model initial-condition large ensemble (SMILE), yielding at least 16 individual realizations of equally likely evolutions of future climate states for each climate model. The SMILE framework allows for increased precision in estimating the evolving distribution of precipitation, allowing for forced changes in precipitation variability to be compared across climate models. The relation between the rise in global surface temperature and the change in precipitation variability is explored on timescales from annual to decadal. Agreement among the model ensembles is evaluated as a sign of robustness for the projected changes.

Author's Contribution:

RRW designed the concept and methodology of the work and carried out the analysis including figures. RRW wrote the manuscript with contributions from all co-authors.

Journal:

"*Environmental Research Letters* (ERL) is a high-impact, open-access journal intended to be the meeting place of the research and policy communities concerned with environmental change and management. [...] The journal's coverage reflects the increasingly interdisciplinary nature of environmental science, recognizing the wide-ranging contributions to the development of methods, tools and evaluation strategies relevant to the field. Submissions from across all components of the Earth system, i.e. land, atmosphere, cryosphere, biosphere and hydrosphere, and exchanges between these components are

welcome. […] The core of ERL's content draws from observations, numerical modelling, theoretical and experimental approaches to environmental science, and especially science relevant to policy, impacts, and decision-making." (IOP Publishing 2021)

Journal Metrics	
Impact Factor (2-Year)	6.947
Impact Factor (5-Year)	8.414
CiteScore (2021)	9.4
CiteScore Rank (2021)	#20/228
	General Environmental Sciences

ENVIRONMENTAL RESEARCH
LETTERS

LETTER

Changes in precipitation variability across time scales in multiple global climate model large ensembles

Raul R Wood[1,*], Flavio Lehner[2,3,4], Angeline G Pendergrass[2,4] and Sarah Schlunegger[5]

[1] Department of Geography, LMU Munich, Germany
[2] Department of Earth and Atmospheric Sciences, Cornell University, Ithaca, NY, United States of America
[3] Institute for Atmospheric and Climate Science, ETH Zürich, Switzerland
[4] National Center for Atmospheric Research, Boulder, CO, United States of America
[5] Atmospheric and Oceanic Sciences, Princeton University, Princeton, NJ, United States of America
[*] Author to whom any correspondence should be addressed.

E-mail: raul.wood@lmu.de

Keywords: precipitation variability, large ensembles, interannual, decadal, historical, future

Supplementary material for this article is available online

OPEN ACCESS

RECEIVED
1 March 2021

REVISED
23 June 2021

ACCEPTED FOR PUBLICATION
2 July 2021

PUBLISHED
26 July 2021

Abstract

Anthropogenic changes in the variability of precipitation stand to impact both natural and human systems in profound ways. Precipitation variability encompasses not only extremes like droughts and floods, but also the spectrum of precipitation which populates the times between these extremes. Understanding the changes in precipitation variability alongside changes in mean and extreme precipitation is essential in unraveling the hydrological cycle's response to warming. We use a suite of state-of-the-art climate models, with each model consisting of a single-model initial-condition large ensemble (SMILE), yielding at least 15 individual realizations of equally likely evolutions of future climate state for each climate model. The SMILE framework allows for increased precision in estimating the evolving distribution of precipitation, allowing for forced changes in precipitation variability to be compared across climate models. We show that the scaling rates of precipitation variability, the relation between the rise in global temperature and changes in precipitation variability, are markedly robust across timescales from interannual to decadal. Over mid- and high latitudes, it is very likely that precipitation is increasing across the entire spectrum from means to extremes, as is precipitation variability across all timescales, and seasonally these changes can be amplified. Model or structural uncertainty is a prevailing uncertainty especially over the Tropics and Subtropics. We uncover that model-based estimates of historical interannual precipitation variability are sensitive to the number of ensemble members used, with 'small' initial-condition ensembles (of less than 30 members) systematically underestimating precipitation variability, highlighting the utility of the SMILE framework for the representation of the full precipitation distribution.

1. Introduction

Anthropogenic changes in the variability of precipitation stand to impact both natural and human systems in profound ways, from enhancing volatility of crop yields and dryland productivity (Rowhani *et al* 2011, Gherardi and Sala 2019), which renders vulnerable populations and livestock (Shively 2017, Sloat *et al* 2018), to enhancing flood risk and damage (Nobre *et al* 2017). Changes in mean or extreme precipitation alone are not the only drivers of shifts in the distribution of hydrometeorological events. The 'space between' mean and extreme also determines the properties of the distribution. Precipitation variability connects the times between dry and wet periods, between droughts and floods. Scientific understanding and projection of such changes in the hydrological cycle, including understanding of the uncertainties inherent to their manifestation, is therefore critical for informing policy and management decisions aimed at mitigating and/or adaption to imminent hydrometeorological threats.

There is scientific consensus that mean precipitation is changing with warming globally at a rate of about 2% K^{-1} (Allen and Ingram 2002, Allan *et al* 2020), driven by an increase in moisture but constrained by radiation cooling. Heavy precipitation (99.9th all-day percentile of daily precipitation) is increasing at a rate of around 7% K^{-1} globally, mainly driven by the change in near surface moisture (O'Gorman and Schneider 2009). At local scales, these rates can be higher due to changes in dynamics (Lenderink and van Meijgaard 2008, Berg *et al* 2009, Westra *et al* 2014, Lenderink *et al* 2017, Wood and Ludwig 2020). It is however not settled whether the change in precipitation variability with warming follows the change of mean precipitation or the rate of near surface moisture. Pendergrass *et al* (2017) have argued that precipitation variability changes globally above the rate of mean precipitation, but below the rate of heavy precipitation. The physical processes leading to changes in mean and extreme precipitation, as well as variability can thereby be different (Bintanja *et al* 2020, van der Wiel and Bintanja 2021). Changes in variability are commonly studied on regional scales, for example the Asian Monsoon regions (Brown *et al* 2017a), the North American Monsoon (Dong *et al* 2018), or the Arctic (Bintanja *et al* 2020). Earlier studies have shown an increase in interannual variability to be strongest in the tropics and mid-latitudes (Boer 2009, Seager *et al* 2012, He and Li 2019). However, most work has focused on variability changes related to changes in El Nino-Southern Oscillation (ENSO) (Maher *et al* 2018, Haszpra *et al* 2020).

Quantification of anthropogenic changes in the distribution of precipitation is challenged by the ever-present influence of internal climate variability. Internal variability in the climate system is an irreducible and important source of uncertainty induced by natural processes in the atmosphere-ocean-land-biosphere-cryosphere system (Hawkins and Sutton 2009, Deser *et al* 2012, Lehner *et al* 2020). It is difficult to account for internal variability in a single climate model simulation, because it can only show a limited number of possible weather and climate events. This limitation holds true for the observational record as well. The current best-practice to robustly estimate the model's forced response and its internal variability is by using long control simulations or large ensembles (Brown *et al* 2017b, Maher *et al* 2018, Milinski *et al* 2020). Although, progress is being made on isolating internal variability in individual simulations and observations using statistical methods (Smoliak *et al* 2015, Deser *et al* 2016, Sippel *et al* 2019, Wills *et al* 2020). However, long control simulations cannot account for forced changes in internal variability in a changing climate. Large ensembles are multi-member climate simulations using a single climate model under the same external forcing (i.e. radiative forcing), applying perturbations at the initialization of each member, which will create diverging climate trajectories. These ensembles can be described as single-model initial-condition large ensembles (SMILEs, for examples see Kay *et al* 2015, Maher *et al* 2019). While multi-model archives with mainly single or only a limited number of members, such as the Coupled Model Intercomparison Project (CMIP) phase 5, confound structural uncertainty (differences in model formulation) with those from internal variability, archives of multiple SMILEs are well suited to address both sources of uncertainties. Within CMIP, internal variability accounts for roughly half of intermodel spread for projected changes in precipitation over North America and Europe over the next 50 years (Deser *et al* 2020 and references therein). Also, changes in large scale dynamics, such as ENSO, which itself drive interannual variability in surface climate variables, often show a small signal-to-noise ratio, such that large ensembles are needed to robustly compute their variance and its change (Maher *et al* 2018, Milinski *et al* 2020).

Disentangling forced changes in variance from natural variance, particularly at decadal timescales, is statistically untenable with a single climate realization, because of their small sample size, but achievable through using SMILEs, due to their large sample size. Further, SMILEs enable a more robust model evaluation by providing more complete information on biases (Maher *et al* 2019, Suarez-Gutierrez *et al* 2020). There are now a growing number of SMILEs stored in public archives (Deser *et al* 2020), affording more multi-SMILE studies (Maher *et al* 2020, 2021, Schlunegger *et al* 2020).

Here, we use six state-of-the-art fully-coupled global SMILEs with daily data from the Multi-Model Large Ensemble Archive (MMLEA; Deser *et al* 2020) to quantify changes in precipitation (mean and extreme) and its variability on timescales from annual to decadal under the Representative Concentration Pathway 8.5 (RCP8.5) scenario. The usage of multiple SMILEs enables us to answer the question whether and where changes in variability are robust and whether different models agree on these changes. We use a simple evaluation framework for interannual precipitation variability in SMILEs and analyze to what extent ensemble size influences the representation of variability.

2. Data

2.1. Large ensembles

We make use of six publicly available SMILEs with daily precipitation data, and one SMILE with monthly data (MPI). These SMILEs constitute a reliable representation of the CMIP5 ensemble (Lehner

Table 1. Single-model initial-condition large ensembles (SMILEs) used in this study.

Modeling center	Model version	Resolution (atm ocn^{-1})	Initialization (methods)	No. of members	Reference
CCCma	CanESM2[a]	∼2.8° × 2.8°/∼1.4° × 0.9°	Macro and Micro	50	Kirchmeier-Young *et al* (2017)
NCAR	CESM1[a]	∼1.3° × 0.9°/nominal 1.0°	Micro	40	Kay *et al* (2015)
CSIRO	MK3.6[a]	∼1.9° × 1.9°/∼1.9° × 1.0°	Macro	30	Jeffrey *et al* (2013)
SMHI/KNMI	EC-Earth[a]	∼1.1° × 1.1°/nominal 1.0°	Micro	16	Hazeleger *et al* (2010)
GFDL	CM3[a]	2.0° × 2.5°/1.0° × 0.9°	Micro	20	Sun *et al* (2018)
GFDL	ESM2M[b]	2.0° × 2.5°/1.0° × 0.9°	Macro	30	Rodgers *et al* (2015) Schlunegger *et al* (2019)
MPI	MPI-ESM-LR[a,c]	∼1.9° × 1.9°/nominal 1.5°	Macro	100	Maher *et al* (2019)

[a] Daily outputs are available on the Multi-Model Large-Ensemble Archive (MMLEA): www.cesm.ucar.edu/projects/community-projects/MMLEA/.
[b] Daily outputs are available on the Princeton Multi-ESM Large Ensemble Archive: http://poseidon.princeton.edu.
[c] Monthly outputs.

et al 2020, Maher *et al* 2021) and the individual models are largely structural independent (Knutti *et al* 2013, Sanderson *et al* 2015). All SMILEs follow standard CMIP5 'historical' and RCP8.5 forcing protocols. The strong forcing scenario allows for the analysis of changes across a broader range of climate sensitivities, allowing for a more robust separation of internal versus model uncertainty. The models range from ∼2.8° to ∼1.0° horizontal resolution and from 16 to 100 ensemble members. In terms of initialization, the models used either Micro, Macro, or both schemes (Hawkins *et al* 2016). For detailed model specifications and experimental design, the reader is referred to the references in table 1.

2.2. Precipitation observations

Two daily land-based precipitation datasets with a spatial resolution of 1° × 1° from the FROGS database (Roca *et al* 2019) are used. The REGEN-ALL-v2019 (Contractor *et al* 2020) (hereafter REGEN) is used based on the longest time period (1950–2016) and, according to Alexander *et al* (2020), ranks in the center of various datasets based on a comparison of multiple 'ETCCDI' precipitation indices. To check whether the choice of reference dataset influences the results, the GPCC-FDD-v2018 (Ziese *et al* 2018) (hereafter GPCC) was chosen as a second observational dataset. The GPCC timeseries is considerably shorter (1982–2016) and ranks among the wettest datasets (Alexander *et al* 2020).

3. Methods

3.1. Changes in precipitation and its variability

Chen and Knutson (2008) recommend that prior to any comparison of models with distinct resolutions, the models should be conservatively remapped to a common resolution before the calculation of statistics. Following this recommendation, we conservatively remap all data (climate models and observations) to the coarsest model resolution of ∼2.8° × 2.8° (i.e. CanESM2) prior to any calculations. By following this order of processing, we can regard differences as model biases (structural uncertainty) rather than the impact of spatial scales. We look at the pattern of change in mean and extreme precipitation to establish that the six SMILEs are a good representation of the CMIP5 models before analyzing the changes in interannual, multiyear, and decadal variability. Extreme precipitation is defined as the 99.9th percentile of all-day daily precipitation (i.e. all days in the year not excluding dry days) within historical and future 20 year periods. The 99.9th percentile represents the wettest 7.3 d in 20 years which corresponds to 1 in 1000 d or occurring roughly every 3 years. Schär *et al* (2016) have shown that all-day precipitation should be favored over wet-days only.

Standard-deviation of precipitation is used as a metric for precipitation variability. For longer timescales, daily data is aggregated first to annual means and subsequently to five year and decadal means, using a rolling window. The aggregation is done for each 20 year period for each member separately and afterwards data is pooled from all members to calculate the standard-deviation. Changes in variability are calculated as the relative change of future periods versus the historical period scaled by each model's forced global-temperature change (GMST). Seasonal variability is the interannual variability of the respective season. All changes are shown relative to the historical period 1955–1974 (also for the global-temperature change) with maps showing changes by 2080–2099. Standard-deviation might not be the most suitable metric to assess precipitation variability on daily scales, due to the high number of dry days leading to a skewed distribution, however by using annual to decadal means largely alleviates

this issue. Pendergrass *et al* (2017) have shown that standard-deviation is a robust tool for the quantification of variability at annual to decadal timescales.

We consider a change 'robust' when at least 5 out of 6 models agree on the sign of the forced response, following guidance from IPCC (2013). Model uncertainty in the magnitude of change is defined as the standard-deviation of the individual ensemble means forced changes by 2080–2099, which gives a measure for how similar the projected changes in the SMILEs are.

3.2. Evaluating precipitation variability

Observations will match neither the exact evolution of either a single model realization nor the ensemble mean, but observations can be put in the context of the model's ensemble mean and its variability. We have therefore adapted the evaluation framework from Maher *et al* (2019) and Suarez-Gutierrez *et al* (2020) to evaluate precipitation variability.

We compare observed annual anomalies of precipitation to anomalies from the climate models for land-areas only. Anomalies are calculated as the relative differences of the annual means to the climatological baseline (1955–1974 for REGEN and 1985–2004 for GPCC). The climate model anomalies are calculated for each member separately and with respect to the REGEN or GPCC baseline period. The location of each year's observational anomaly within each year's ensemble spread is determined, to see whether the observations fall outside the ensemble spread (0–100th percentile range) or within the central 75th percentile bounds (12.5th–87.5th percentile) of the ensemble. Ideally, the observations should cover the entire spread of the ensemble over time and should not cluster in the center of the ensemble (more than 80% of years within the central 75th percentile range) or be located outside the ensemble spread for more than 10% of years. The clustering of observations in the center of the ensemble indicates an overestimation of the variability by the model. Conversely, many observations outside the ensemble spread indicate an underestimation of variability.

To assess whether the ensemble size influences the over- or underestimation of variability, we sample 100 random combinations (without replacement) of 16 members (corresponding to the smallest ensemble size, i.e. EC-Earth) and 30 members from the MPI ensemble. The 100 member MPI ensemble is used to minimize the resampling bias. A resampling bias occurs when the samples use more than 50% of the full ensemble size to generate the random samples (Milinski *et al* 2020). The random samples are not independent anymore because they share too many of the same members. For the evaluation, each of the 100 random samples (of 16 and 30 members) are compared separately to the REGEN anomalies. We then determine for each grid cell how many of the samples show an over- or underestimation. At least 66% of samples must agree either on an overestimation (at least 80% of observed annual anomalies within the 75th percentile range) or underestimation (at least 10% of anomalies outside the ensemble spread) of variability to be assigned one of the two categories, otherwise they are marked as having no structural bias. The comparison of the two synthetic MPI ensembles (16 and 30 member) with the full MPI ensemble and the other six SMILEs, allows for a separation of ensemble size dependence and model dependence. Thereby, the ensemble size dependence is based on the comparison of the synthetic MPI ensembles with the full MPI ensemble first, before emerging regions are checked for consistency with the other smaller SMILEs (<30 members). Whereas model dependence is based on the comparison of the individual SMILEs and the full MPI ensemble.

4. Evaluating precipitation variability

4.1. Historical precipitation variability in the 6 SMILEs

In figure 1, the results for the gridcell-based evaluation show that interannual variability over North and Central America, Europe and Western Russia is generally well captured by most models. The observational network in these areas is quite dense, which reduces the potential for observational uncertainty associated with this result. Generally, all models show a better representation of variability over the Northern compared to the Southern Hemisphere. Structural differences between models are apparent, in particular in tropical regions: while three SMILEs (CanESM2, CSIRO, and GFDL-ESM2M) show an overestimation of variability over South America, others show good agreement or an underestimation. Similar results are found in India, where CanESM2 and CSIRO overestimate the variability and other models do not (i.e. CESM, GFDL-CM3, GFDL-ESM2M). Overall, the evaluation highlights CESM and MPI (seen in figure 2(a)) as capturing precipitation variability most adequately over most parts of global land area. However, other SMILEs are equally good in some parts of the world and therefore interpretation depends on the region of interest.

We checked whether the climatological baseline period for the anomaly calculation (figure S1 (available online at stacks.iop.org/ERL/16/084022/mmedia)) or the observational dataset (figure S2) itself affects the results. The general patterns seem to be unaffected by both, although individual gridcells might exhibit differences. Further, it was checked whether trends in interannual variability in the observations or SMILEs affects the results. We detrended both the observed and SMILE annual anomalies by applying a linear least-square fit to the data and subtracting it from the data. Over Africa and the northern High Latitudes, the detrended data shows a better representation, which might indicate a mismatch of a

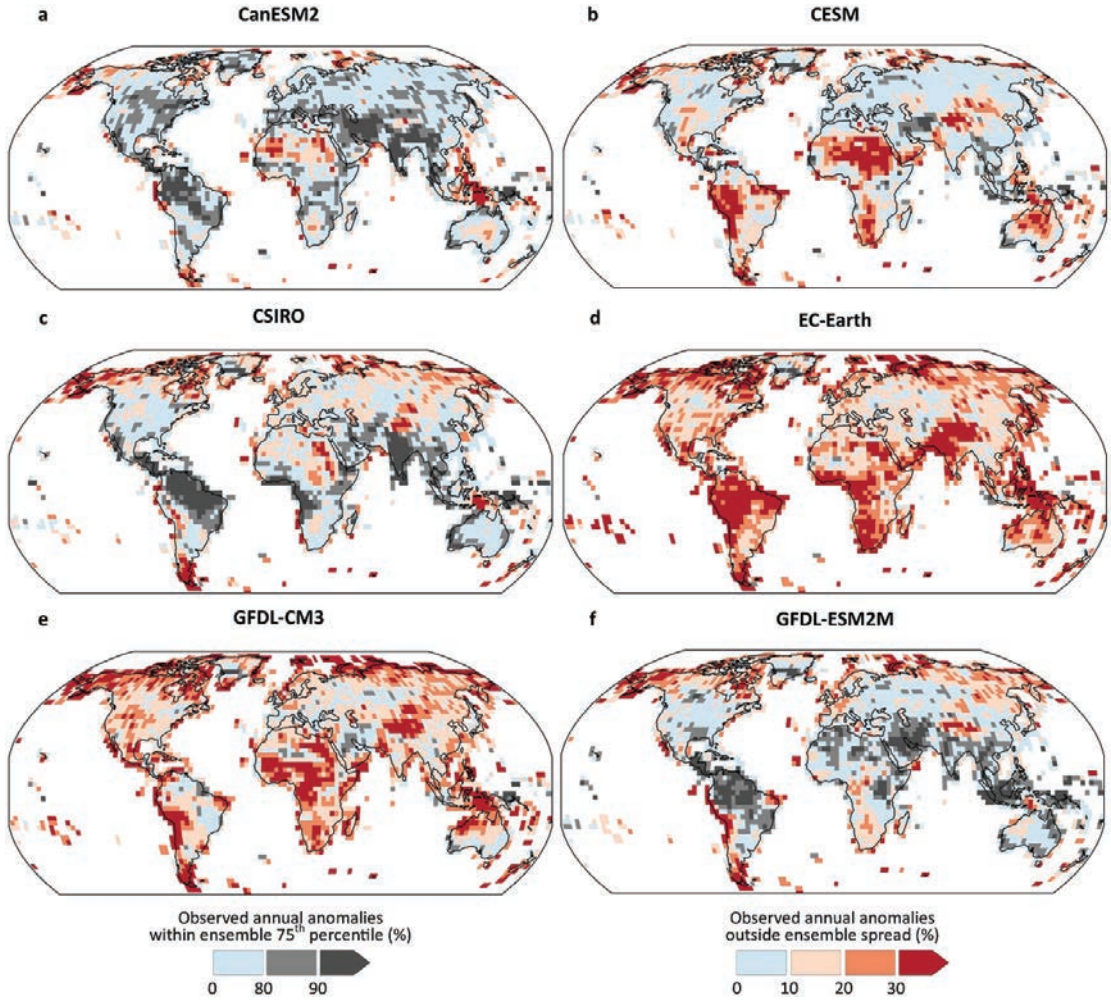

Figure 1. Evaluation of annual precipitation anomalies simulated by six different SMILEs compared to REGEN observed anomalies over land from 1955 until 2016. Light blue shading shows areas with a good representation of interannual precipitation variability. Grey shading suggests an overestimation of variability, red shading an underestimation of variability, and white areas show no-data. The grey shading shows the fraction of observed annual anomalies within the ensemble central 75th percentile range (e.g. for 85% of years the observational anomalies are within the ensemble 75th percentile range (light grey)). Red shading shows the fraction of observed annual anomalies outside the ensemble spread (e.g. for 25% of years the observed anomalies are outside the ensemble spread (above or below) (medium red shading)). Anomalies are relative to the climatological baseline of 1955–1974. Maps are cut to 60°S and 90°N.

forced change in historical variability between some models and observations (figure S3). Although overall the general takeaways remain the same.

4.2. Influence of the ensemble size

The results in figure 1 might reveal an influence of the ensemble size on how adequately models can capture precipitation variability. The SMILEs with a small ensemble size (EC-Earth: 16, GFDL-CM3: 20) both show a tendency to underestimate variability across land, while the larger SMILE CanESM2 (50) tends to show an overestimation of variability. To analyze this further, we use an additional large SMILE, the 100 member MPI ensemble, to quantify the influence of the ensemble size on precipitation variability. We compare the full MPI ensemble (100 members) representing large ensemble sizes, with multiple random combinations of 16 and 30 members from the MPI, representing small and medium ensemble sizes.

An underestimation of precipitation variability over northern hemisphere mid- to high latitudes, as seen in the EC-Earth (figure 1(d)) and the MPI 16 members (figure 2(b)), are likely ensemble size dependent. Over the High Latitudes even ensemble sizes of 30 members might be too small (figures 1(c), (f) and 2(c)) and more members are needed. The SMILEs with at least 40 members (CanESM2, CESM, MPI) all seem to be better at representing High Latitude variability.

The underestimation of variability over South America, East Asia, South-East Asia, and Northern Australia, as seen in the ensembles with <30 members (figures 1(d), (e) and 2(b)), are partly ensemble size dependent. The under- or overestimation over the majority of Africa is rather related to structural uncertainty and not ensemble size, as well as over the Amazon, Northern Africa, the Middle East, and India.

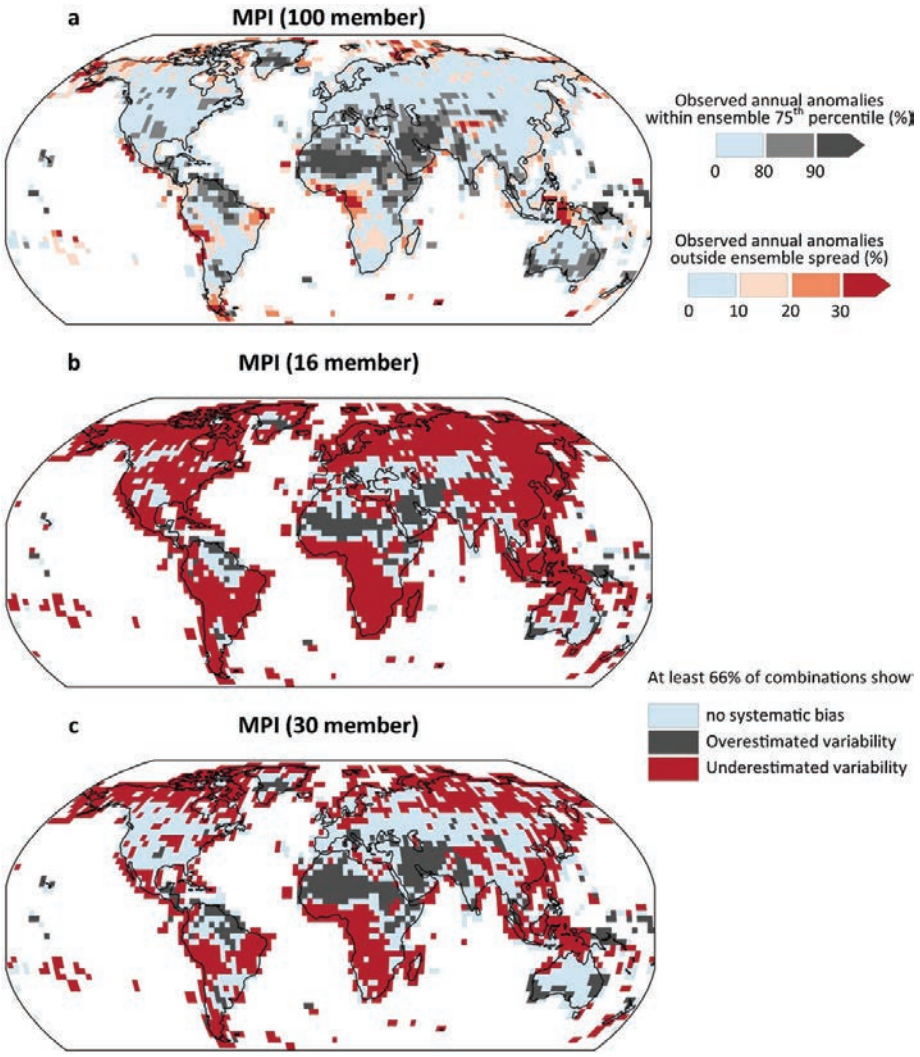

Figure 2. Evaluation of ensemble size dependence in interannual precipitation variability. (a) The evaluation result of the full MPI ensemble (100 member) following methods in figure 1. (b) Shows the result of 100 random combinations of 16 members drawn from the MPI ensemble. At least 66% of combinations show either (light blue) no systematic bias, (grey) overestimation of variability, or (red) underestimation of variability. The grey and red category are the generalization of the colorbars in panel (a). Grey represents at least 80% of observed annual anomalies within the ensemble 75th percentile range. Red represents at least 10% of anomalies outside the ensemble spread. (c) Shows the result of 100 random combinations of 30 members drawn from the MPI ensemble.

5. Future changes in precipitation variability

Prior to the analysis of changes in precipitation variability, we have checked whether the six SMILEs are a good representation of the CMIP5 model suite, on different spectra of the rainfall distribution. For the change in mean precipitation, we can largely agree with previous studies (Lehner *et al* 2020, Maher *et al* 2021) on a good agreement of the SMILEs with CMIP5. The SMILEs project a global average change of 2.5% K^{-1} (figure S5(a)) which follows the early assumptions by Allen and Ingram (2002). Comparing the change in extreme precipitation with results for the CMIP5 ensemble (Pendergrass *et al* 2017), we can in addition assert this for extreme precipitation. The SMILEs project changes at a rate of 7.2% K^{-1} globally (figure S5(b)) in conjunction with the rate of near surface moisture change (O'Gorman and Schneider 2009).

Precipitation variability increases globally by 3.7–4% K^{-1} for timescales of annual to decadal (figures 3(a)–(c)), which is higher than the increase in mean state precipitation (2.5% K^{-1}, figure S5(a)) but lower than the scaling of near surface moisture change. Over land, where changes have the biggest impact on society, variability increases at a higher rate, around 4.5–4.7% K^{-1}. Over oceans the increase is modestly lower, around 3.4–3.7% K^{-1}. These scaling rates already show how remarkably similar the scaling rates are over all timescales. However, changes in interannual variability show higher model agreement over larger parts of the globe than for the longer timescales. Around 75% of gridcells globally show high model agreement for interannual variability changes, while only ∼66% of grid

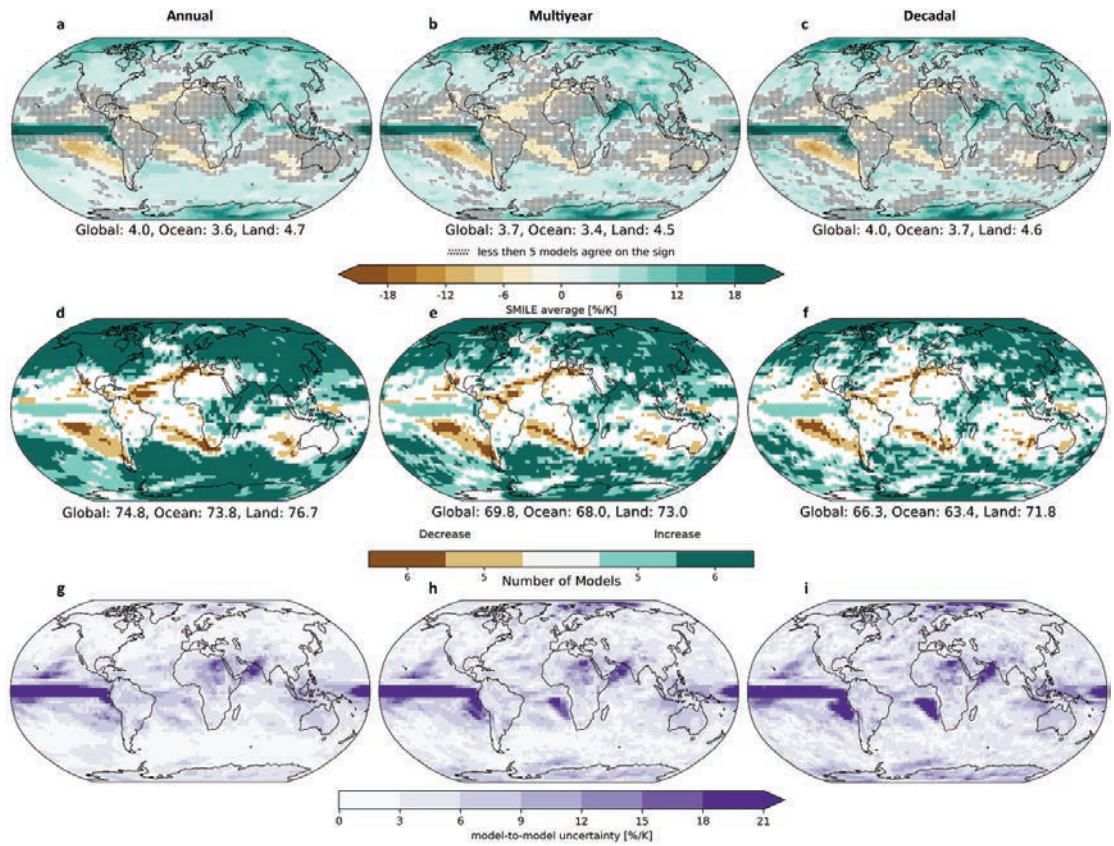

Figure 3. Patterns of variability change by 2080–2099. Left column ((a), (d), (g)) shows maps for annual variability; center column ((b), (e), (f)) for multiyear variability; and right column ((c), (f), (i)) for decadal variability. Upper row (a)–(c) shows the multi SMILE forced response as the relative change scaled by the GMST change w.r.t. 1955–1974. Hatching indicates low model agreement (less than 5 models agree on the sign). Numbers below the panels indicate area weighted averages over the globe, ocean, and land in % K^{-1}. Center row (d)–(f) shows the number of models agreeing on the sign of change (browns: negative/decreasing; greens: positive/increasing). White colors indicate low model agreement with less than 5 models in agreement. Numbers below the panels indicate the percentage of global, ocean, and land gridcells with model agreement. Bottom row (g)–(i) shows the model-to-model uncertainty in the forced response (standard-deviation across the individual SMILE's forced change).

cells show agreement on decadal variability changes (figures 3(d)–(f)). Model agreement over land is slightly higher than over the ocean or globally.

The relatively large number of gridcells with high model agreement indicates that the individual SMILEs generally agree and show similar global rates. However, two distinctive exceptions must be mentioned. First, GFDL-ESM2M shows little to no change (0.1–0.8% K^{-1}) in variability across all timescales (figures S6–S8). This could potentially be linked to a weakening of the ENSO amplitude and less frequent extreme El-Nino events as shown by the GFDL-ESM2M (Kohyama and Hartmann 2017). The GFDL-ESM2M has been shown to have a more realistic ENSO nonlinearity compared to other models from the CMIP5 archive. Kohyama and Hartmann (2017) argue for a La Nina-like warming rather than El Nino-like mean-state warming proposed by most other models. However, the causality of the proposed mechanisms needs to be further investigated as well as the connection to the here shown forced response of precipitation variability (or lack thereof) in the GFDL-ESM2M. Over the mid- and high latitudes, the GFDL-ESM2M is consistent with the other SMILEs, showing an increase in variability.

Secondly, EC-Earth shows globally considerably higher scaling rates for precipitation variability changes across all timescales, between 8.2 and 8.9% K^{-1} (figures S6–S8), which is above the near surface moisture change of 6–7% K^{-1}. As shown in section 4, the EC-Earth shows smaller historical interannual variability, compared to other SMILEs, and generally underestimates historical variability. The small variability might be connected to small ensembles not being able to capture the full variance of modes of variability, as shown by Maher *et al* (2018) for ENSO variance. A smaller variability in the historical period can lead to higher percentage changes compared to a SMILE with a higher variability and the same absolute change. Both examples (GFDL-ESM2M and EC-Earth) show that model-to-model agreement on the sign might be given, but that structural uncertainty is still relevant for model-to-model agreement on the magnitude of change. These differences are highlighted by the model-to-model uncertainty (i.e. standard-deviation of the SMILE's

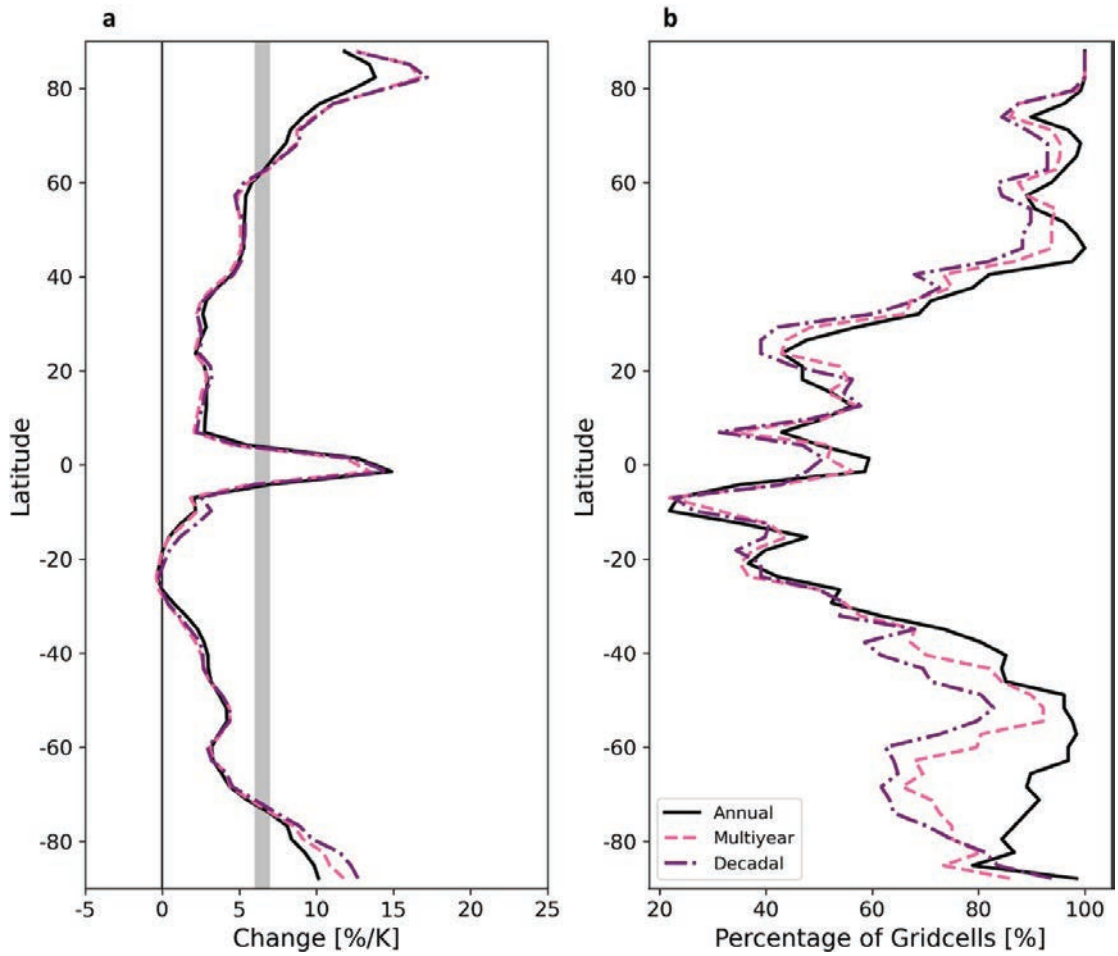

Figure 4. (a) Latitudinal zonal averages of precipitation variability change and (b) percentage of gridcells with high model agreement on the sign of change (at least 5 out 6 models agree) by 2080–2099. In panel (a) the vertical black line marks zero and the grey band indicates the Clausius-Clapeyron relation (6–7% K^{-1}).

forced changes) which are increasing from interannual to decadal timescales (figures 3(g)–(i)).

The areas with low model agreement in interannual variability and longer timescales over land (i.e. South America, Northern Africa, and Middle East) are consistent with the areas of high structural uncertainty shown in the previous section. Regions with low model agreement over the oceans are mainly around subtropical subsidence regions with decreasing precipitation variability (figures 3(a)–(c)) and decreasing mean state precipitation (figure S5(a)). Here, we find high model agreement in the centers, but declining model agreement towards the edges, due to differences in the geographic extent. We note that a point-wise comparison will conceptually underestimate the agreement of the models, as dynamical boundaries and features, such as the jet stream, or divergence and convergence zones are not geographically coincident between models (Madsen *et al* 2017, Brown *et al* 2020, Harvey *et al* 2020), despite possibly showing consistent trends within the features. For the subtropical descending regions, He and Li (2019) show that interannual variability is constrained by mean state precipitation and that the change in interannual variability is almost proportional to the change in mean state precipitation.

Regionally, precipitation variability strongly increases in all SMILEs over the Pacific ITCZ (figures 3(a)–(c)) across all timescales (except for GFDL-ESM2M), as also shown for mean and extreme precipitation (figures S5(a) and (b)). It needs to be noted that the model-to-model uncertainty is substantial over the ITCZ (figures 3(g)–(i)). However, the dynamical changes in the ITCZ are yet not well understood (Allan *et al* 2020). Precipitation variability increases over the South Pacific Convergence Zone (SPCZ) alongside a widespread increase in extreme precipitation. This might indicate that the change in precipitation variability is linked to an increase in severe weather events, which has been shown by Cai *et al* (2012) indicating a near doubling of zonal SPCZ event occurrence, although it needs to be acknowledged that climate-model simulations of the SPCZ still show persistent biases (Brown *et al* 2020 and references therein). In contrast, the south-eastern Pacific dry zone gets drier (figure S5(a)) and precipitation variability decreases, which aligns with the paradigm of wet-gets-wetter and dry-gets-drier found mostly

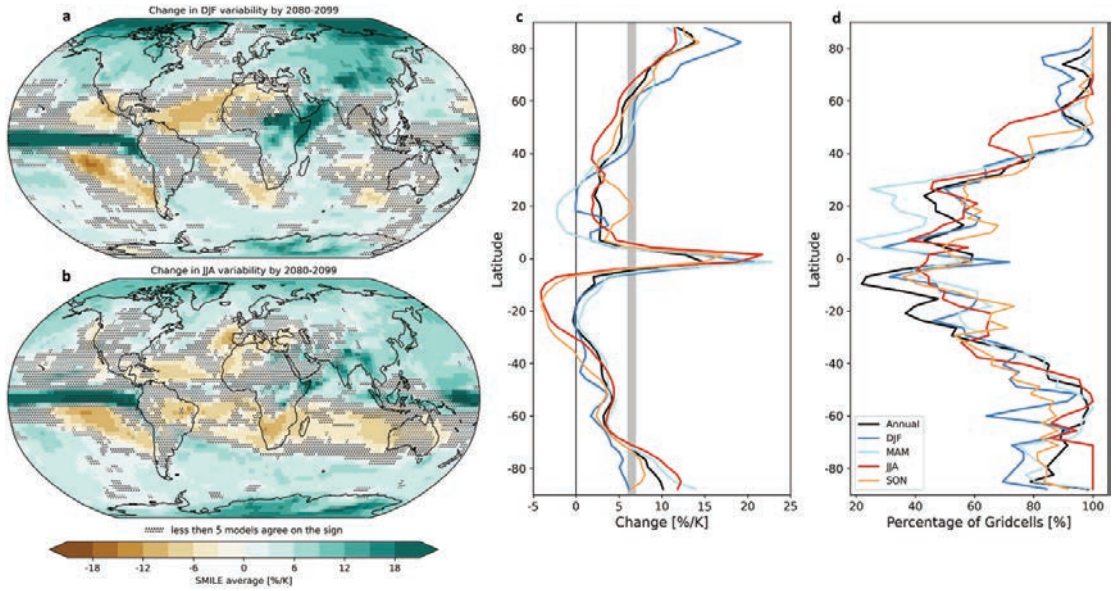

Figure 5. Forced changes in seasonal variability by 2080–2099. (a) Change in winter (DJF) variability; (b) change in summer (JJA) variability; (c) latitudinal zonal averages for annual and seasonal changes; (d) percentage of gridcells with agreement on the sign. In panel (c) the vertical black line marks zero and the grey band indicates the Clausius-Clapeyron relation (6–7% K^{-1}).

over oceans. Generally, in the Tropics and Subtropics model agreement is much lower (<60% of gridcells) than in the mid- and high latitudes for all variability timescales (figure 4(b)).

Over the mid- and high latitudes, it is very likely that the hydrological cycle intensifies, and that variability increases across all timescales at scaling rates around or above the Clausius-Clapeyron (CC) relation of 7% K^{-1} (north of 60°N, figure 4(a)). The scaling rates are even higher for the change in wintertime variability (DJF) with 2xCC in the Arctic (figures 5(a) and (c)). An increase in arctic interannual precipitation variability was also shown by Bintanja *et al* (2020), linking the changes to an increased poleward moisture transport. Over North America, Dong *et al* (2018) link an increase in Mid-latitude wintertime variability to an increase in moisture (thermodynamical component), while the subtropical South is more dominated by a change in circulation variability (dynamical component). Over the northern hemisphere, at least 80% of gridcells show an increase in variability across all timescales. Over the southern hemisphere, interannual variability also shows high model agreement over at least 80% of gridcells, but longer durations show lower agreement over 60% and more of gridcells (figure 4(b)).

The SMILEs agree on an increase in variability across all timescales over the South Asian and East Asian Monsoon region which is consistent with Brown *et al* (2017a) for timescales shorter than decadal. Our results also indicate an increase in decadal variability in these regions. The increase in the South and East Asian Monsoon region is most noticeable in the change of the summertime variability (JJA) at rates above 7% K^{-1} (figure 5(b)).

Generally, the patterns for changes in precipitation variability are quite complex and on seasonal scales these patterns are even more complex, highlighting the importance of local dynamics boosting or attenuating changes.

6. Summary and conclusions

We have used six single-model initial-condition large ensembles (SMILEs) to analyze changes in mean and extreme precipitation, as well as precipitation variability across multiple timescales (annual to decadal) by the end of the century under the RCP8.5 emission scenario.

Mean and extreme precipitation increases in the multi-SMILE average at a rate of 2.5 and 7.2% K^{-1} globally following the theoretical scaling rates. These results indicate that the six SMILEs agree with the results from the CMIP5 models and are therefore a suitable super ensemble for mean state precipitation analysis, which recently has also been shown by Lehner *et al* (2020) and Maher *et al* (2021), and can now also be asserted to extreme precipitation.

We can show implicit evidence for a forced change in internal variability in a warming climate which leads to an increase in precipitation variability from interannual to decadal timescales. We can further show that the scaling rates are markedly stable across all timescales and that they can locally exceed the Clausius-Clapeyron relation (>7% K^{-1}). Interannual precipitation variability increases at rates of 4% K^{-1} (4.7% K^{-1}) globally (over land), multiyear variability increases at rates of 3.7% K^{-1} (4.5% K^{-1}), and decadal variability at rates of 4% K^{-1} (4.6% K^{-1}). Seasonal variability can exceed these rates especially

over land in winter (DJF, 5.8% K^{-1}) as well as locally, highlighting the importance of changes in local processes. These high scaling rates have considerable relevance for local climate adaptation plans.

The increase in precipitation variability implies an increase in precipitation volatility with an enhanced risk of swings between extreme dry and wet periods, as shown by Swain *et al* (2018) for California. This could pose challenges for communities that rely on precipitation as a primary water source. While projections remain uncertain over the majority of Africa, we can show an increase in precipitation variability over Eastern Africa across all timescales.

Over northern hemisphere mid- and high latitudes, model agreement on the sign is very high with at least 80% of gridcells showing an increase in variability across all timescales. Thus, while reducing model-to-model differences will only slightly improve model agreement on the sign, it will still improve agreement on the magnitude of change. Over the Tropics and Subtropics model agreement is considerably lower than elsewhere, which means that reducing structural uncertainty will improve both the agreement on the sign and the magnitude of change.

For interannual variability, the patterns from the SMILEs show considerable resemblance to results from the CMIP5 ensemble (Pendergrass *et al* 2017, He and Li 2019, Maher *et al* 2021), which shows that there is considerable amount of internal variability included in CMIP5. Further, it shows that the multi-SMILE ensemble can be a valuable tool to test the hypothesis derived from the CMIP5 ensemble, and extent our understanding of dynamical changes, such as ENSO, which drive local variability and could explain model differences (e.g. the lack of variability change in the GFDL-ESM2M).

Alongside the changes in precipitation variability, we conducted a first evaluation of historical interannual precipitation variability in the 6 SMILEs. While there are several caveats to consider (e.g. smoothing of precipitation variability during the interpolation and remapping process, temporal artifacts related to changes in the observational system, or varying degrees of quality of the underlying data) we mainly focused on the model-to-model differences rather than absolute biases. Overall, the evaluation highlights CESM and MPI as capturing interannual precipitation variability most adequately over most parts of global land area. The evaluation reveals that especially over the Tropics and Subtropics structural uncertainty remains critical, which is supported by the low model agreement on future forced changes in precipitation variability. Lastly, we show that small ensembles (less than 30 members) tend to underestimate historical annual precipitation variability (e.g. northern hemisphere mid- and high latitudes, Northern Australia, East Asia). This suggests that ensembles with at least 30 members are needed for a robust quantification of interannual variability of precipitation.

Data availability statement

The GFDL-ESM2M daily data are publicly available through the Princeton Multi-ESM Large Ensemble Archive (http://poseidon.princeton.edu). All other SMILEs are available on the Multi-Model Large Ensemble Archive (MMLEA; www.cesm.ucar.edu/projects/community-projects/MMLEA/). The observational datasets are available on the FROGS database (Roca *et al* 2019) and are openly available at: https://doi.org/10.14768/06337394-73A9-407C-9997-0E380DAC5598.

Acknowledgments

We acknowledge US CLIVAR for support of the Multi-Model Large Ensemble Archive (MMLEA). Data was analyzed using the Iris Python library (v2.4; https://scitools.org.uk/iris). R R W was supported by the ClimEx project, funded by the Bavarian Ministry for the Environment and Consumer protection. F L was supported by the Swiss National Science Foundation (Grant No. PZ00P2_174128). This work was partly supported by the Regional and Global Model Analysis (RGMA) component of the Earth and Environmental System Modeling Program of the U.S. Department of Energy's Office of Biological & Environmental Research (BER) via NSF IA 1844590, and by the National Center for Atmospheric Research, which is a major facility sponsored by the National Science Foundation (NSF) under cooperative Agreement No. 1947282. S S was supported by NASA award NNX17AI75G and by NSF's Southern Ocean Carbon and Climate Observations and Modeling (SOCCOM) Project under the NSF Award PLR-1425989, with additional support from NOAA and NASA.

ORCID iDs

Raul R Wood https://orcid.org/0000-0003-4172-7719
Angeline G Pendergrass https://orcid.org/0000-0003-2542-1461

References

Alexander L V, Bador M, Roca R, Contractor S, Donat M G and Nguyen P L 2020 Intercomparison of annual precipitation indices and extremes over global land areas from in situ, space-based and reanalysis products *Environ. Res. Lett.* **15** 055002

Allan R P *et al* 2020 Advances in understanding large-scale responses of the water cycle to climate change *Ann. New York Acad. Sci.* **1472** 49–75

Allen M R and Ingram W J 2002 Constraints on future changes in climate and the hydrologic cycle *Nature* **419** 224–32

Berg P, Haerter J O, Thejll P, Piani C, Hagemann S and Christensen J H 2009 Seasonal characteristics of the relationship between daily precipitation intensity and surface temperature *J. Geophys. Res.* **114** D18102
Bintanja R, van der Wiel K, van der Linden E C, Reusen J, Bogerd L, Krikken F and Selten F M 2020 Strong future increases in Arctic precipitation variability linked to poleward moisture transport *Sci. Adv.* **6** eaax6869
Boer G J 2009 Changes in interannual variability and decadal potential predictability under global warming *J. Clim.* **22** 3098–109
Brown J R, Lengaigne M, Lintner B R, Widlansky M J, van der Wiel K, Dutheil C, Linsley B K, Matthews A J and Renwick J 2020 South Pacific Convergence Zone dynamics, variability and impacts in a changing climate *Nat. Rev. Earth Environ.* **1** 530–43
Brown J R, Moise A F and Colman R A 2017a Projected increases in daily to decadal variability of Asian-Australian monsoon rainfall *Geophys. Res. Lett.* **44** 5683–90
Brown P T, Ming Y, Li W and Hill S A 2017b Change in the magnitude and mechanisms of global temperature variability with warming *Nat. Clim. Change* **7** 743–8
Cai W *et al* 2012 More extreme swings of the South Pacific convergence zone due to greenhouse warming *Nature* **488** 365–9
Chen C-T and Knutson T 2008 On the verification and comparison of extreme rainfall indices from climate models *J. Clim.* **21** 1605–21
Contractor S, Donat M G, Alexander L V, Ziese M, Meyer-Christoffer A, Schneider U, Rustemeier E, Becker A, Durre I and Vose R S 2020 Rainfall estimates on a gridded network (REGEN)—a global land-based gridded dataset of daily precipitation from 1950 to 2016 *Hydrol. Earth Syst. Sci.* **24** 919–43
Deser C *et al* 2020 Insights from Earth system model initial-condition large ensembles and future prospects *Nat. Clim. Change* **10** 277–86
Deser C, Knutti R, Solomon S and Phillips A S 2012 Communication of the role of natural variability in future North American climate *Nat. Clim. Change* **2** 775–9
Deser C, Terray L and Phillips A S 2016 Forced and internal components of winter air temperature trends over North America during the past 50 years: mechanisms and implications *J. Clim.* **29** 2237–58
Dong L, Leung L R and Song F 2018 Future changes of subseasonal precipitation variability in North America during winter under global warming *Geophys. Res. Lett.* **45** 12467–76
Gherardi L A and Sala O E 2019 Effect of interannual precipitation variability on dryland productivity: a global synthesis *Glob. Change Biol.* **25** 269–76
Harvey B J, Cook P, Shaffrey L C and Schiemann R 2020 The response of the Northern Hemisphere storm tracks and jet streams to climate change in the CMIP3, CMIP5, and CMIP6 climate models *J. Geophys. Res. Atmos.* **125** e2020JD032701
Haszpra T, Herein M and Bódai T 2020 Investigating ENSO and its teleconnections under climate change in an ensemble view—a new perspective *Earth Syst. Dyn.* **11** 267–80
Hawkins E, Smith R S, Gregory J M and Stainforth D A 2016 Irreducible uncertainty in near-term climate projections *Clim. Dyn.* **46** 3807–19
Hawkins E and Sutton R 2009 The potential to narrow uncertainty in regional climate predictions *Bull. Am. Meteorol. Soc.* **90** 1095–108
Hazeleger W *et al* 2010 EC-Earth *Bull. Am. Meteorol. Soc.* **91** 1357–64
He C and Li T 2019 Does global warming amplify interannual climate variability? *Clim. Dyn.* **52** 2667–84
IPCC 2013 *Climate Change 2013: The Physical Science Basis. Contribution of Working Group I to the Fifth Assessment Report of the Intergovernmental Panel on Climate Change* ed T F Stocker, D Qin, G-K Plattner, M Tignor, S K Allen, J Boschung, A Nauels, Y Xia, V Bex and P M Midgley (Cambridge: Cambridge University Press)
Jeffrey S, Rotstayn L, Collier M, Dravitzki S, Hamalainen C, Moeseneder C, Wong K and Skytus J 2013 Australia's CMIP5 submission using the CSIRO-Mk3.6 model *Aust. Meteorol. Oceanogr. J.* **63** 1–14
Kay J E *et al* 2015 The community earth system model (CESM) large ensemble project: a community resource for studying climate change in the presence of internal climate variability *Bull. Am. Meteorol. Soc.* **96** 1333–49
Kirchmeier-Young M C, Zwiers F W and Gillett N P 2017 Attribution of extreme events in Arctic Sea ice extent *J. Clim.* **30** 553–71
Knutti R, Masson D and Gettelman A 2013 Climate model genealogy: generation CMIP5 and how we got there *Geophys. Res. Lett.* **40** 1194–9
Kohyama T and Hartmann D L 2017 Nonlinear ENSO warming suppression (NEWS) *J. Clim.* **30** 4227–51
Lehner F, Deser C, Maher N, Marotzke J, Fischer E M, Brunner L, Knutti R and Hawkins E 2020 Partitioning climate projection uncertainty with multiple large ensembles and CMIP5/6 *Earth Syst. Dyn.* **11** 491–508
Lenderink G, Barbero R, Loriaux J M and Fowler H J 2017 Super-clausius–clapeyron scaling of extreme hourly convective precipitation and its relation to large-scale atmospheric conditions *J. Clim.* **30** 6037–52
Lenderink G and van Meijgaard E 2008 Increase in hourly precipitation extremes beyond expectations from temperature changes *Nat. Geosci.* **1** 511–4
Madsen M S, Langen P L, Boberg F and Christensen J H 2017 Inflated uncertainty in multimodel-based regional climate projections *Geophys. Res. Lett.* **44** 11606–13
Maher N *et al* 2019 The Max Planck Institute Grand Ensemble: enabling the exploration of climate system variability *J. Adv. Model. Earth Syst.* **11** 2050–69
Maher N, Lehner F and Marotzke J 2020 Quantifying the role of internal variability in the temperature we expect to observe in the coming decades *Environ. Res. Lett.* **15** 054014
Maher N, Matei D, Milinski S and Marotzke J 2018 enso change in climate projections: forced response or internal variability? *Geophys. Res. Lett.* **45** 11390–8
Maher N, Power S B and Marotzke J 2021 More accurate quantification of model-to-model agreement in externally forced climatic responses over the coming century *Nat. Commun.* **12** 788
Milinski S, Maher N and Olonscheck D 2020 How large does a large ensemble need to be? *Earth Syst. Dyn.* **11** 885–901
Nobre G G, Jongman B, Aerts J and Ward P J 2017 The role of climate variability in extreme floods in Europe *Environ. Res. Lett.* **12** 84012
O'Gorman P A and Schneider T 2009 The physical basis for increases in precipitation extremes in simulations of 21st-century climate change *Proc. Natl Acad. Sci. USA* **106** 14773–7
Pendergrass A G, Knutti R, Lehner F, Deser C and Sanderson B M 2017 Precipitation variability increases in a warmer climate *Sci. Rep.* **7** 17966
Roca R, Alexander L V, Potter G, Bador M, Jucá R, Contractor S, Bosilovich M G and Cloché S 2019 FROGS: a daily $1^\circ \times 1^\circ$ gridded precipitation database of rain gauge, satellite and reanalysis products *Earth Syst. Sci. Data* **11** 1017–35
Rodgers K B, Lin J and Frölicher T L 2015 Emergence of multiple ocean ecosystem drivers in a large ensemble suite with an Earth system model *Biogeosciences* **12** 3301–20
Rowhani P, Lobell D B, Linderman M and Ramankutty N 2011 Climate variability and crop production in Tanzania *Agric. For. Meteorol.* **151** 449–60
Sanderson B M, Knutti R and Caldwell P 2015 Addressing interdependency in a multimodel ensemble by interpolation of model properties *J. Clim.* **28** 5150–70
Schär C *et al* 2016 Percentile indices for assessing changes in heavy precipitation events *Clim. Change* **137** 201–16

Schlunegger S et al 2020 Time of emergence and large ensemble intercomparison for ocean biogeochemical trends *Glob. Biogeochem. Cycles* **34** e2019GB006453

Schlunegger S, Rodgers K B, Sarmiento J L, Frölicher T L, Dunne J P, Ishii M and Slater R 2019 Emergence of anthropogenic signals in the ocean carbon cycle *Nat. Clim. Change* **9** 719–25

Seager R, Naik N and Vogel L 2012 Does global warming cause intensified interannual hydroclimate variability? *J. Clim.* **25** 3355–72

Shively G E 2017 Infrastructure mitigates the sensitivity of child growth to local agriculture and rainfall in Nepal and Uganda *Proc. Natl Acad. Sci. USA* **114** 903–8

Sippel S, Meinshausen N, Merrifield A, Lehner F, Pendergrass A G, Fischer E and Knutti R 2019 Uncovering the forced climate response from a single ensemble member using statistical learning *J. Clim.* **32** 5677–99

Sloat L L, Gerber J S, Samberg L H, Smith W K, Herrero M, Ferreira L G, Godde C M and West P C 2018 Increasing importance of precipitation variability on global livestock grazing lands *Nat. Clim. Change* **8** 214–8

Smoliak B V, Wallace J M, Lin P and Fu Q 2015 Dynamical adjustment of the Northern Hemisphere surface air temperature field: methodology and application to observations *J. Clim.* **28** 1613–29

Suarez-Gutierrez L, Müller W A, Li C and Marotzke J 2020 Hotspots of extreme heat under global warming *Clim. Dyn.* **55** 429–47

Sun L, Alexander M and Deser C 2018 Evolution of the global coupled climate response to Arctic Sea ice loss during 1990–2090 and its contribution to climate change *J. Clim.* **31** 7823–43

Swain D L, Langenbrunner B, Neelin J D and Hall A 2018 Increasing precipitation volatility in twenty-first-century California *Nat. Clim. Change* **8** 427–33

van der Wiel K and Bintanja R 2021 Contribution of climatic changes in mean and variability to monthly temperature and precipitation extremes *Commun. Earth Environ.* **2** 1

Westra S, Fowler H J, Evans J P, Alexander L V, Berg P, Johnson F, Kendon E J, Lenderink G and Roberts N M 2014 Future changes to the intensity and frequency of short-duration extreme rainfall *Rev. Geophys.* **52** 522–55

Wills R C J, Battisti D S, Armour K C, Schneider T and Deser C 2020 Pattern recognition methods to separate forced responses from internal variability in climate model ensembles and observations *J. Clim.* **33** 8693–719

Wood R R and Ludwig R 2020 Analyzing internal variability and forced response of subdaily and daily extreme precipitation over Europe *Geophys. Res. Lett.* **47** e2020GL089300

Ziese M 2018 GPCC Full Data Daily Version 2018 at 1.0°: Daily Land-Surface Precipitation from Rain-Gauges built on GTS-based and Historic Data (https://doi.org/10.5676/DWD_GPCC/FD_D_V2018_100)

5 Changes in extreme precipitation over Europe

This work has been published in the Journal *Geophysical Research Letters*.

Wood, Raul R.; Ludwig, Ralf (2020): Analyzing Internal Variability and Forced Response of Subdaily and Daily Extreme Precipitation Over Europe. In Geophys. Res. Lett. 47 (17). DOI: 10.1029/2020GL089300.

Plain language Summary:

The knowledge on how and why the intensity and frequency of extremes changes is critical to becoming a resilient society. The current infrastructure and environment are adapted to observed extremes of the past and might not be sufficiently resilient against the extremes of the future. Observations are only one possible realization of a chaotic system, and the past and future climate system is altered by natural variations, and anthropogenic contributions. Since we can only measure one realization of the world, we need climate models to investigate the influence of natural variability and anthropogenic factors on the climate system. In this study, the detection of regional patterns of future changes in annual and seasonal maximum precipitation over Europe and the contribution of the uncertainty of natural variability on these changes is analyzed. For the separation of the forced signal and natural variability the regional SMILE CRCM5-LE is used. The time-of-emergence, the time in the future when the signal emerges from the noise of internal variability is determined. The CRCM5-LE is a single regional climate model driven by 50 realizations of a single global climate model (CanESM2-LE) under the same emission scenario (RCP8.5). The differences between the 50 equally probable climate realizations originate from the non-linear response of the climate system and represent natural climate variability.

Author's Contribution:

RRW designed the concept and methodology of the work, carried out the analysis including figures, and wrote the manuscript with contributions from RL.

Journal:

"*Geophysical Research Letters (GRL)* publishes high-impact, innovative, and timely research on major scientific advances in all the major geoscience disciplines. Papers should have broad and immediate implications meriting rapid decisions and high visibility." (Wiley 2021)

Journal Metrics	
Impact Factor	5.58
CiteScore (2021)	8.5
CiteScore Rank (2021)	#13/191
	General Earth and Planetary Sciences

AGU ADVANCING EARTH AND SPACE SCIENCE

Geophysical Research Letters

RESEARCH LETTER
10.1029/2020GL089300

Key Points:
- Subdaily extreme precipitation intensifies faster than daily extremes and mean precipitation
- On regional scales internal variability remains a dominant source of uncertainty until the end of the 21st century
- Widespread scaling rates of subdaily extremes above Clausius-Clapeyron over Northern and Eastern Europe

Supporting Information:
- Supporting Information S1

Correspondence to:
R. R. Wood,
raul.wood@lmu.de

Citation:
Wood, R. R., & Ludwig, R. (2020). Analyzing internal variability and forced response of subdaily and daily extreme precipitation over Europe. *Geophysical Research Letters*, *47*, e2020GL089300. https://doi.org/10.1029/2020GL089300

Received 11 JUN 2020
Accepted 4 AUG 2020
Accepted article online 10 AUG 2020

Analyzing Internal Variability and Forced Response of Subdaily and Daily Extreme Precipitation Over Europe

R. R. Wood[1] and **R. Ludwig**[1]

[1]Department of Geography, LMU, Munich, Germany

Abstract At regional to local scales internal variability is expected to be a dominant source of uncertainty in analyzing precipitation extremes and mean precipitation even far into the 21st century. A debated topic is whether a faster increase in subdaily precipitation extremes can be expected. Here we analyzed seasonal maximum precipitation in various time steps (3 hr, days, and 5 days) from a high-resolution 50-member large-ensemble (CRCM5-LE) and compared them to changes in mean precipitation over Europe. Our results show that the magnitude of change in extreme precipitation varies for season and duration. Subdaily extremes increase at higher rates than daily extremes and show higher scaling with temperature. Northern Europe shows widespread scaling above Clausius-Clapeyron of subdaily extremes in all seasons and for daily extremes in winter/spring. Scaling above Clausius-Clapeyron is also visible over Eastern Europe in winter/spring. For most regions and seasons the forced response emerges from the internal variability by midcentury.

Plain Language Summary The knowledge on how and why the intensity and frequency of extremes changes is critical to a resilient society. Our adaptive measures that are currently in place are based on observed extremes of the past. We know that observations are only one realization of a chaotic system and that the climate system is altered by natural variations, and anthropogenic contributions. Since we can only measure one realization of the world, we need climate models to investigate the influence of natural variability and anthropogenic factors. In this study we focus on the contribution of natural variability and the detection of regional patterns of changes in extreme precipitation. We used regional climate simulations, driven by multiple runs of global climate simulations under the same emission scenario, but with slight changes at the start of the simulation to imitate the butterfly effect of the climate system and simulate natural variability. We have found that natural variability plays a dominant role in the first half of the 21st century. But we have also found that subdaily extreme precipitation is increasing at a higher rate than daily extremes and that some of this change can be attributed to the warming of the atmosphere.

1. Introduction

Extreme precipitation events are becoming more likely under climate change due to atmospheric warming and the inherent alterations of the hydrological cycle (Allen & Ingram, 2002; Held & Soden, 2006; Wentz et al., 2007). Increasing intensities and frequencies of extreme events pose an imminent threat to humans, the economy, and the environment. On continental to global scales, models agree on the forced response (FR) of precipitation extremes (Fischer et al., 2014) and observations show increases in daily extreme precipitation (Alexander, 2016; Asadieh & Krakauer, 2015; Donat et al., 2016; Fischer & Knutti, 2016; Min et al., 2011; Westra et al., 2013) and subdaily extremes (Barbero et al., 2017; Guerreiro et al., 2018; Xiao et al., 2016) on a global scale.

There is currently a debate on whether subdaily precipitation extremes follow the Clausius-Clapeyron (CC) scaling or whether they increase at a higher rate. Based on observations and models, extreme precipitation is expected to increase with the availability of water vapor in the atmosphere, following the CC scaling of 6–7% per degree global warming. Mean precipitation on the other hand scales at a much lower rate of 1–3% per degree warming (Allen & Ingram, 2002; Held & Soden, 2006). Twice the CC scaling in hourly observations was first shown in Lenderink and van Meijgaard (2008) for stations in the Netherlands and was meanwhile shown for stations throughout the world (Westra et al., 2014, and references therein). This shift from CC to super-CC scaling (>7%/K) can be attributed to a shift from stratiform to convective precipitation (Berg

et al., 2013; Haerter & Berg, 2009; Molnar et al., 2015) and may also arise due to the physics of the clouds and the latent heat released during condensation, boosting the convection (Lenderink et al., 2017).

Climate models on global and regional scales project extreme precipitation to increase in the 21st century (Aalbers et al., 2018; Bao et al., 2017; Beniston et al., 2007; Boberg et al., 2010; Fischer et al., 2013; Fischer & Knutti, 2014; Martel et al., 2018, 2019; Pendergrass & Hartmann, 2014; Rajczak et al., 2013; Sillmann et al., 2013), which is attributable to human influences (Fischer & Knutti, 2015). Additionally, precipitation extremes are expected to undergo a shift in seasonality from summer to spring and autumn (Brönnimann et al., 2018; Marelle et al., 2018).

The internal variability (IV) of the climate system is an important source of uncertainty (Deser, Knutti, et al., 2012; Deser, Phillips, et al., 2012; Fischer et al., 2013, 2014; Hawkins & Sutton, 2009; Hegerl et al., 2004; Kendon et al., 2008; Lehner et al., 2020), especially on regional scales (Prein & Pendergrass, 2019). Over the middle and high latitudes IV might be in the same magnitude as the forced anthropogenic response (Deser, Knutti, et al., 2012; Deser, Phillips, et al., 2012). It originates from the coupled interaction of the land, atmosphere, oceans, and cryosphere (Deser et al., 2014), which is always present, even at longer timescales. Isolating the effects of IV from those of anthropogenic climate change requires ensembles of simulations from a given climate model that is subject to the identical external forcing (Deser et al., 2014). Kendon et al. (2008) and Kjellström et al. (2013) state that using large ensembles to Sample IV will lead to benefits in the ability to accurately project future changes in local precipitation extremes.

By using the large-ensemble approach the real FR can be analyzed. When using only one realization of a model the effects of IV are neglected and the analyzed realization only shows one possible change. This can also be true for small ensemble sizes in which the IV might be underrepresented and changes might be misinterpreted as significant (Milinski et al., 2019).

Several single-model initial-condition large ensembles (SMILEs) are now available which allow for the analysis of the IV and the real underlying FR of the model. There are several SMILEs available on the global scale (i.e., Fyfe et al., 2017; Kay et al., 2015; Maher et al., 2019). However, the magnitude, variability, and regional- to local-scale spatial patterns of climate variables are better represented in high-resolution RCMs (Chan et al., 2013; Giorgi et al., 2016; Kotlarski et al., 2014; Maraun et al., 2010; Prein et al., 2016). Several studies have shown that hourly precipitation is better represented in convection-permitting model (CPM) simulations (Kendon et al., 2017; Prein et al., 2015; Westra et al., 2014), and Berg et al. (2019) pointed out model deficiencies at hourly resolution in RCM simulations. However, due to their high computational cost the number of CPM simulations is still limited in time and spatial extent, which makes it difficult to study the effects of IV on local subdaily rainfall. Giorgi (2019) argues that due to the increased noise at CPM resolution we will require an ensemble of simulations. Therefore, large ensembles of RCMs are still the best estimate of IV on local to regional scales. The CRCM5 50-member large-ensemble (CRCM5-LE, Canadian Regional Climate Model Version 5) is the first Pan-European SMILE of high resolution (0.11°) (Leduc et al., 2019). Other regional large ensembles exist for Europe in coarser resolution (Addor & Fischer, 2015) or on a smaller domain (Aalbers et al., 2018).

In this study, the effects of climate change on the intensity change of seasonal and annual maximum 3-hourly (Rx3h), daily (Rx1d), 5-daily (Rx5d), and mean precipitation are analyzed alongside the influence of the IV. For this purpose, the simulations from the CRCM5-LE were analyzed to distinguish between the effect of climate change and natural variability. This study tries to answer these questions:

Is there a strong seasonal variability in the FR of maximum precipitation? When can we expect changes in extreme precipitation to robustly emerge from IV? Is the CC expression constraining scaling rates of precipitation extremes at subdaily and daily resolutions?

2. Data and Methods

2.1. Model Setup

The analysis of this paper is based on hourly precipitation data from the CRCM5-LE. The data originate from the first of its kind pan-European high-resolution initial-condition multimember dynamical downscaling experiment (Leduc et al., 2019) resulting in 50 equally likely transient (1950–2099) climate simulations from the same global climate (GCM) and regional climate model (RCM) combination. The multimember

initial-condition simulations from the Canadian Earth System Model version 2 Large-Ensemble (CanESM2-LE; Fyfe et al., 2017) were dynamically downscaled with the CRCM5 (v.3.3.3.1; Martynov et al., 2013; Šeparović et al., 2013) in a one-way nesting setup over Europe resulting in the 0.11° (approximately 12 km) resolution CRCM5-LE. All 50 CanESM2-LE simulations are driven with observed emissions (in CO_2 and non-CO_2 GHGs, aerosols, and land cover) during the historical period until 2005. For the subsequent period 2006–2099 all simulations were performed using the IPCC RCP8.5 scenario (Meinshausen et al., 2011). The differences among the single CRCM5 members are due to the small initial-condition perturbations in the driving CanESM2-LE and can be interpreted as the natural variability (in the following IV) of the climate system. At 0.11° resolution the CRCM5 model parameterizes deep convection following the approach of Kain and Fritsch (1990) and shallow convection is based on a transient version of Kuo (1965) scheme (Bélair et al., 2005).

2.2. Methods

For each member, season, and year the seasonal and annual maximum 3-hourly (Rx3h), daily (Rx1d), and 5-daily (Rx5d) precipitation was calculated, as well as seasonal (annual) mean precipitation. Seasonal maxima can be lower than annual maxima. The respective seasons are winter (DJF: December, January, and February), spring (MAM: March, April, and May), summer (JJA: June, July, and August), and fall (SON: September, October, and November). Changes in mean and extreme precipitation are differences in 30-year seasonal (annual) means compared to the reference period 1980–2009 calculated first for each member and afterward averaged over all 50 members. Figures 1–3 represent end of the century (2070–2099) changes, while Figure 4 shows transient changes.

The distribution of the 30-year mean values of the 50-members in the future was compared to the distribution in the reference period by applying a two-sided t test with unequal variances (p value: 0.01) to check for a significant change in the mean (Figure 1). The IV is determined as the standard deviation of the 50-member mean values (Figure 2) or relative changes (Figure 4).

There are several different ways to scale extreme precipitation with temperature by using the local or regional (dew point) temperature (Ban et al., 2015; Kendon et al., 2014, 2019) or binning with local temperature variations (X. Zhang, Zwiers, et al., 2017). Here we have scaled precipitation with the CRCM5 domain-averaged mean temperature change rather than using the local (grid cell) changes, because winterly and longer duration extremes can be expected to be influenced by remote moisture sources, which are insufficiently represented by local temperature. In Figure 3, the scaling rates are calculated as $\Delta P/\Delta T$ (%/K), where ΔP is, for example, the relative change in seasonal (annual) Rx3h and ΔT the change in mean seasonal (annual) surface temperature compared to 1980–2009.

Additionally, the time-of-emergence is marked, where the signals are for the first time exceeding the IV and remain above (Figure 4). Five regions of interest were analyzed (NEUR: Northern Europe, WEUR: Western Europe, CEUR: Central Europe, EEUR: Eastern Europe, and SEUR: Southern Europe; see Figure S1 in the supporting information).

For a general evaluation of the CRCM5-LE see Leduc et al. (2019), and for an evaluation of seasonal maximum precipitation and the timing of the annual maximum see the supporting information (Figures S10–S21).

3. Spatial Patterns of FR and IV

Annual maxima of subdaily precipitation are increasing throughout the European domain (EU) (Figure 1j), except for the Iberian Peninsula (IP, no change or decreasing). The FR of seasonal maxima (Figures 1f–1i) however reveals varying trends across seasons. While Rx3h is increasing throughout the EU in winter, and spring/fall showing similarity to the FR of annual maxima, the seasonal changes in summer are remarkably diverse. Over France and the Mediterranean Rx3h is strongly decreasing in summer, while CEUR, British Isles (BI) and NEUR showing prevailing increases.

Comparing these seasonal changes to changes of mean precipitation (Figure S4), then subdaily extremes show increasing trends over CEUR, BI, and southern Scandinavia, despite strong decreasing summerly mean precipitation over the majority of EU. These regional differences in FR can partly be explained by

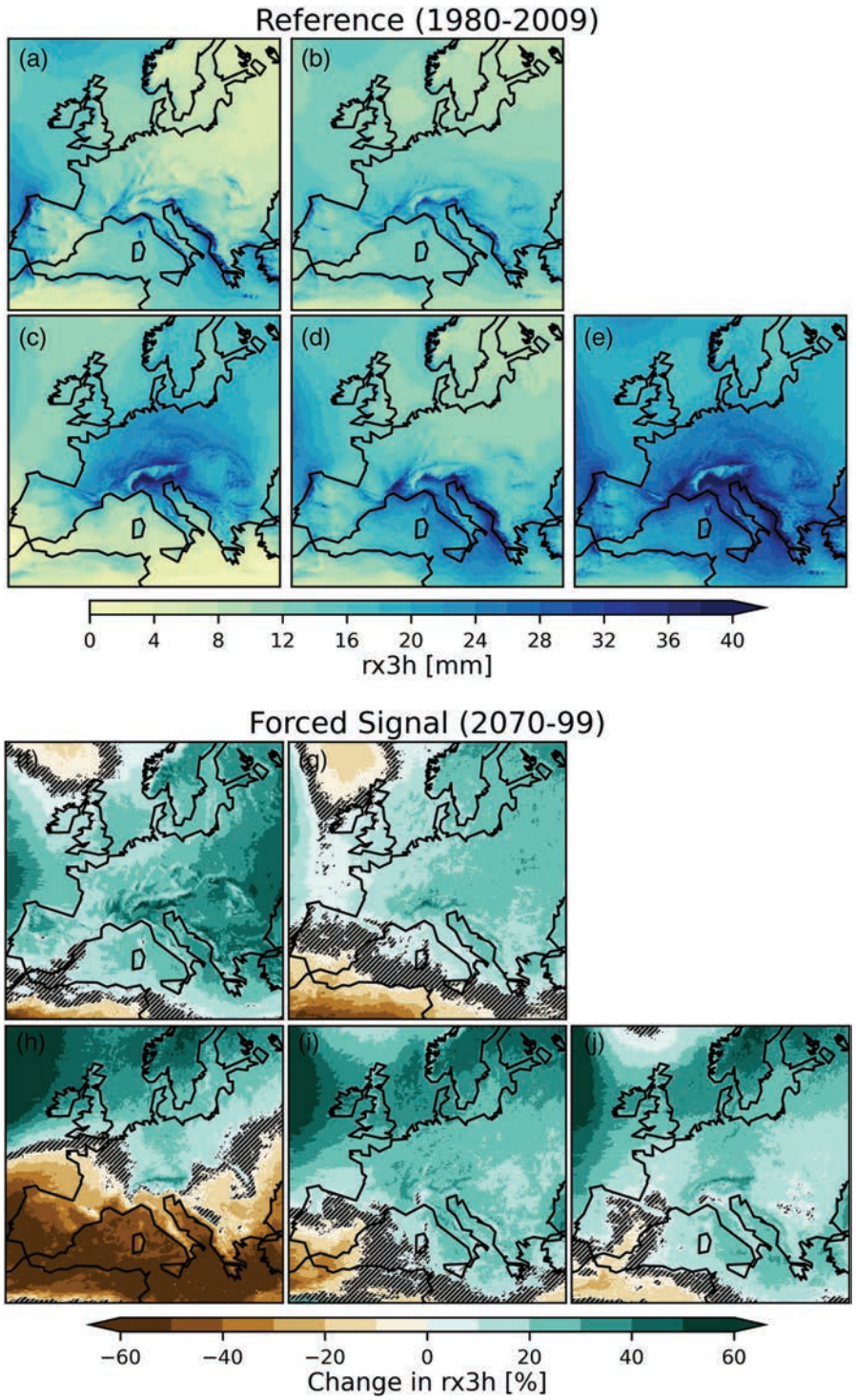

Figure 1. Spatial pattern of mean Rx3h in the reference period (1980–2009, a–e) and the 50-member mean forced signal in percent at the end of the century (2070–2099, f–j) for seasons winter (a, f), spring (b, g), summer (c, h), fall (d, i), and annual (e, j). Hatched areas in (f–j) indicate nonsignificant areas according to a two-sided *t* test with unequal variances (*p* value: 0.01).

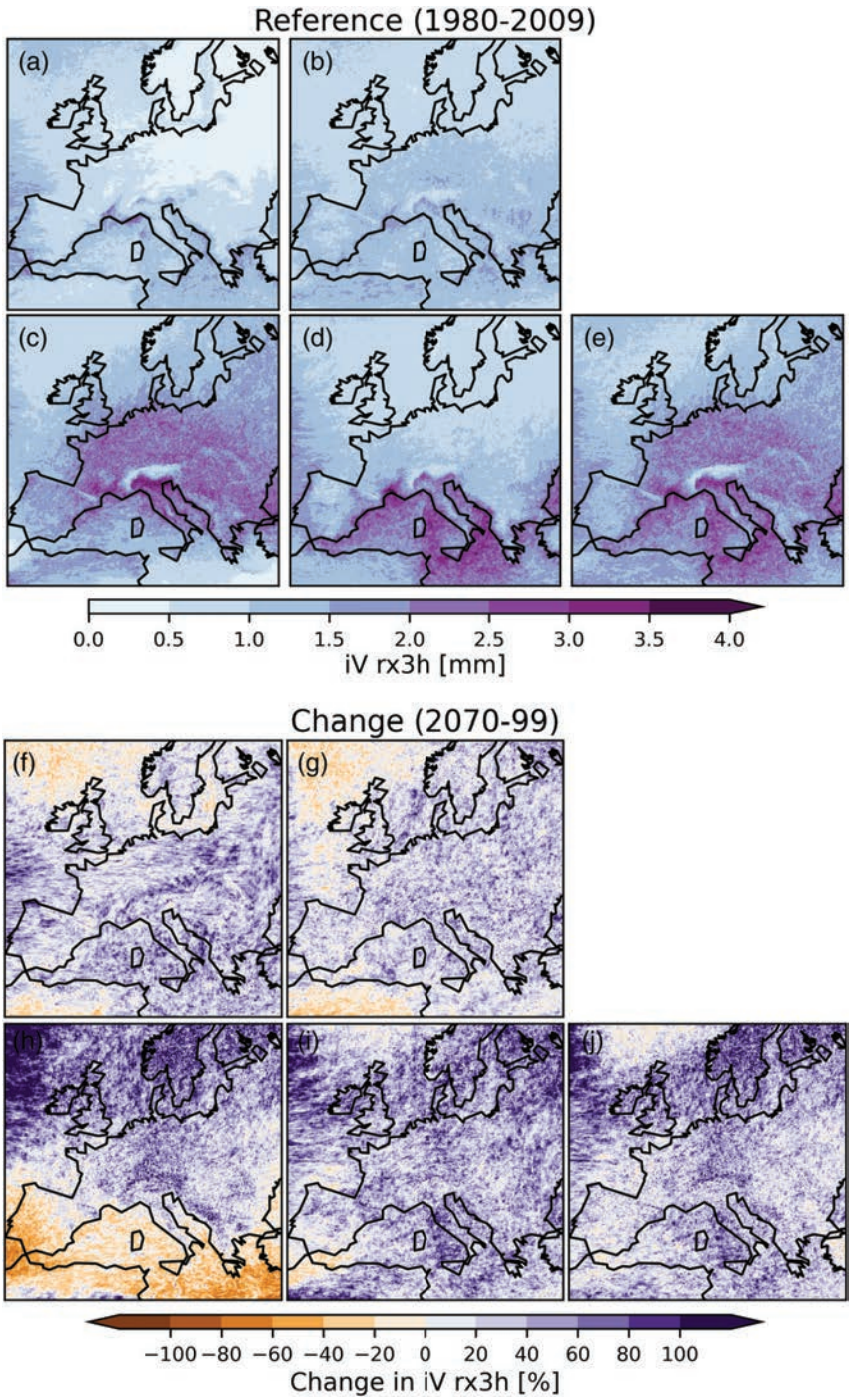

Figure 2. Internal variability of Rx3h in the reference period (1980–2009, a–e) and relative changes by 2070–99 (f–j) for seasons winter (a, f), spring (b, g), summer(c, h), fall (d, i), and annual (e, j).

the continued availability of moisture for the formation of convection. The Bowen Ratio (BR), which is the ratio between sensible and latent heat flux, indicates the continued dominance of latent heat over the regions with increasing Rx3h in summer (Figure S5). The regions with decreasing Rx3h on the other hand show a dramatic increase in BR, indicating an increase in sensible heat. Especially over the Mediterranean, the decreasing mean precipitation in the preceding season amplifies the lack of moisture from surface.

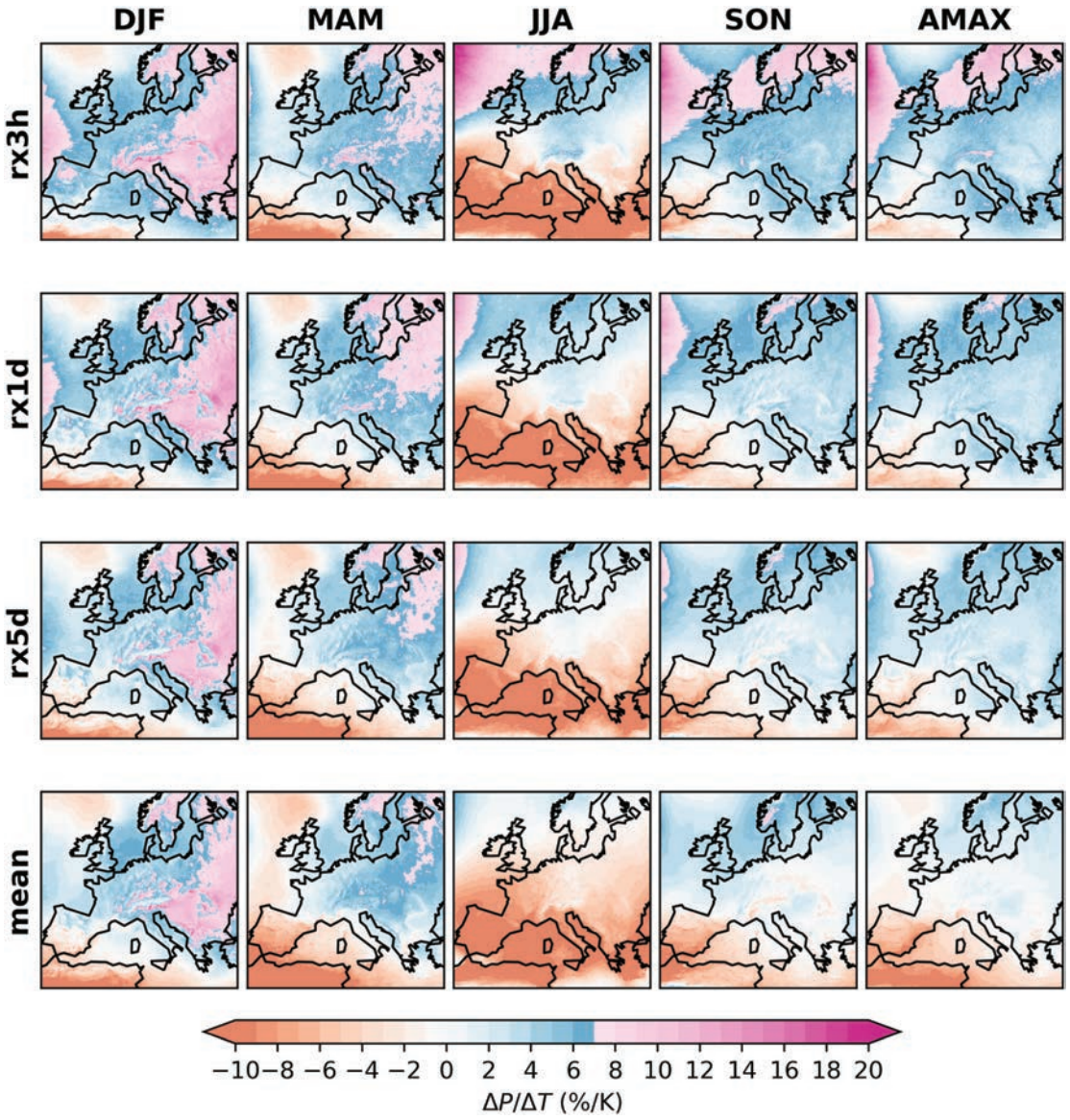

Figure 3. Precipitation scaling with domain-average temperature change by 2070–2099 compared to 1980–2009. Columns indicate seasons/annual; rows indicate extreme indices (Rx3h, Rx1d, and Rx5d) and mean precipitation (mean). Areas with a negative scaling are shown in red colors; scaling above the Clausius-Clapeyron scaling (>7%/K) is shown in magenta colors.

The patterns for the FR of Rx1d (Figures S2f–S2j) are similar to Rx3h, however showing overall lower changes for seasonal as well as annual maxima. Rx1d can originate from shorter duration rainfall bursts, hence the similarity to subdaily maxima. Rx5d originate from stratiform precipitation rather than convective precipitation and therefore show closer resemblance to the FR of mean precipitation (Figures S3f–S3j for Rx5d and Figures S4f–S4j for mean precipitation). In general, longer duration extremes increase at a lower rate than subdaily extremes.

The IV of Rx3h is in general highest in summer and lowest in winter (Figures 2a–2d), which is attributable to the role of convection in summer. However, in high-elevation regions (Alps and Pyrenees) the variability in summer is remarkable lower than their surroundings, which might indicate a lack of convection. In general, the IV of Rx3h is homogeneous over large areas of the domain only showing topographic features in summer. The IV of Rx1d, Rx5d, and mean precipitation show higher values along large topographic features (Figures S6a–S6e, S7a–S7e, and S8a–S8e).

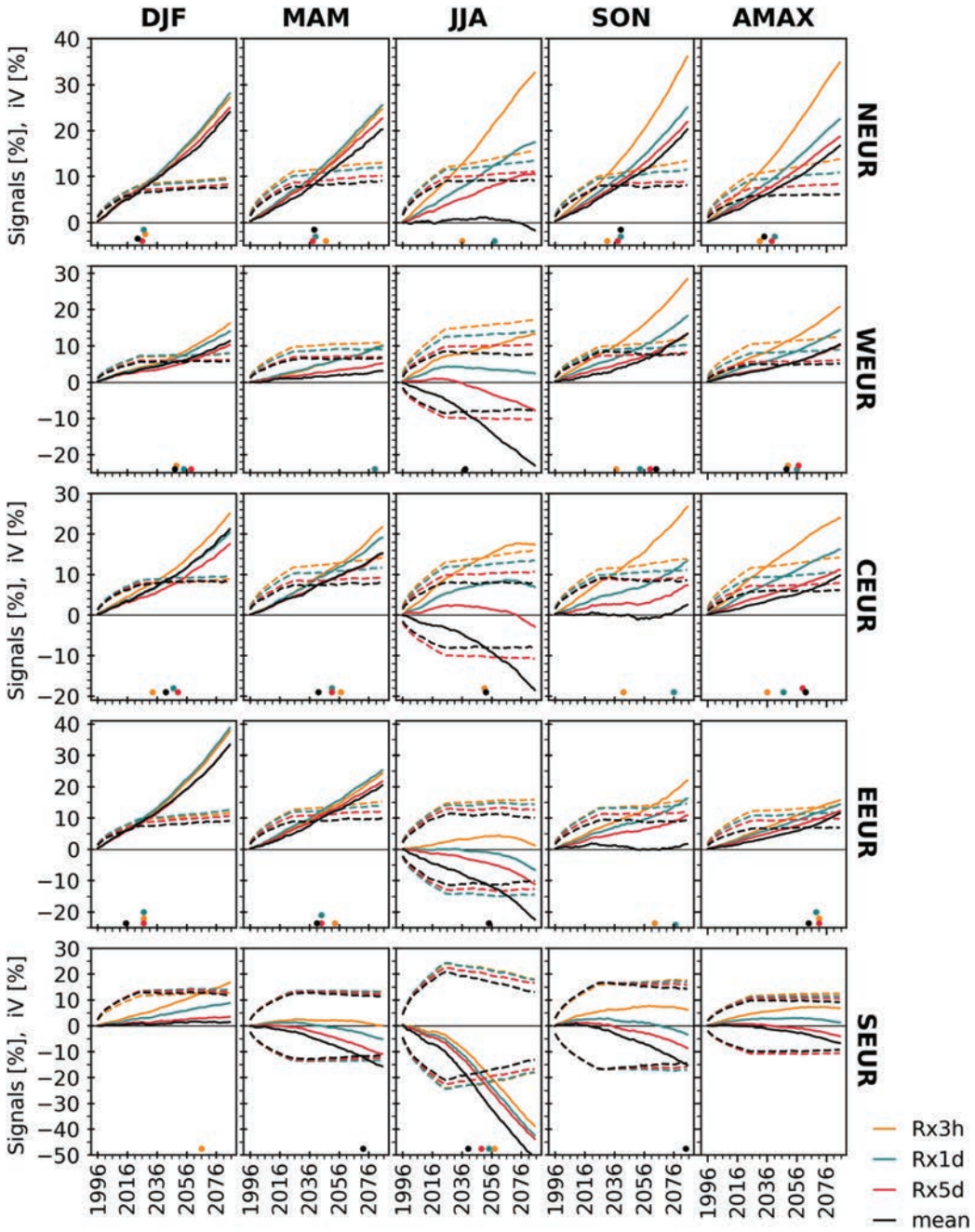

Figure 4. Transient 30-year moving window of forced response and internal variability. Solid lines: ensemble-mean relative changes, dashed lines: internal variability (standard deviation of the 50-member relative changes). If signals show negative values, the internal variability is shown as positive and negative. Columns: seasons and annual; rows: regions. Points indicate the time-of-emergence where signal/noise remains above 1.

The changes of IV by the end of the century reveal an increase in variability for seasonal and annual Rx3h (Figures 2f–2j) throughout the EU. NEUR show strong relative changes in IV in summer, fall, and annual maxima, which indicates the increasing role of convection. In contrast the variability over the IP is decreasing in summer for Rx3h as well as all other indices (Figures S6h, S7h, and S8h), which implies, together with the strong decrease in FR, the increasing lack of precipitation over the IP and Mediterranean Sea.

In general, the changes of IV for Rx1d, Rx5d, and mean precipitation are regionally more diverse than for Rx3h, showing small areas throughout the domain with increases and decreases in all seasons. This emphasizes the role of IV as a source of uncertainty on regional scales.

4. Scaling With Mean Temperature Change

Scaling changes with temperature allows for a first look at whether changes can be attributed to thermodynamics or if it is rather likely to be influenced by dynamic changes. Figure 3 shows CC or super-CC scaling (>7%/K) for Rx3h over NEUR throughout all seasons and for annual maxima, which implies thermodynamics having a dominant role. Other regions also indicate super-CC scaling for Rx3h mainly in winter and partly in spring over EEUR, the Balkan Peninsula, Northern Italy, southern part of CEUR, or Northwestern IP. In summer and in the annual maxima, parts of the Alps show super-CC scaling for Rx3h, which might be connected to an increase of convective events over high alpine elevations as shown in Giorgi et al. (2016). Longer duration extremes show generally considerably less areas with super-CC scaling, and mainly only in winter and partly in spring. This can also be seen in Figure S9.

The large proportion of land areas without CC-scaling or negative scaling indicates that the changes are mainly driven by other effects than thermodynamics. In some recent studies (Kröner et al., 2017; Pfahl et al., 2017) it is shown that other factors may have stronger contributions than thermodynamics. Pfahl et al. (2017) argue that the negative changes in extreme precipitation can be related to decreases in the vertical velocity, which can even offset the influence of thermodynamic change. The changes of regional dynamics might partly be attributed to a northward shift of present day pattern of vertical velocity, which can be related to a general expansion of the Hadley cells (Kröner et al., 2017; Pfahl et al., 2017). As a result of the extension of the Hadley cell, SEUR would become more strongly affected by subsidence, which would lead to reduced convection (Kröner et al., 2017). Brogli et al. (2019) argue that Hadley cells only have a small influence on European climate change and rather propose a change in lapse rates and meridional change as important factors. Also, changes in cyclone intensities can play a role as shown for the Mediterranean (Pfahl et al., 2017; Zappa et al., 2015). Other factors that can contribute to a drying are the land-ocean warming contrast and soil-moisture feedbacks (Kröner et al., 2017).

5. Transient Changes of Extreme Precipitation and Emergence From IV

Looking at the evolution of the FR and IV (Figure 4), there is a clear tendency in all regions and all seasons that shorter extremes show stronger signals for both intensity and IV. In general, the Rx3h is the upper bound of change and mean precipitation the lower bound. The Rx3h and Rx1d show a very similar FR in several regions, mainly in winter or spring. In summer, the Rx3h exceeds by far the other indices showing a large discrepancy between the change in mean precipitation and Rx3h. The change in mean precipitation and Rx3h are counter directional in all regions except NEUR. Thus, this implies that different processes govern the response of the hydrological cycle. Tang et al. (2018) explain the drying of the south and wetting of north, by showing an enhanced sea-level-pressure pattern (similar to NAO-AO), which can divert the jet stream and storm tracks northward reducing precipitation in the Mediterranean and increasing precipitation in NEUR in summer.

Apart from the summer signals, smooth linear trends are visible tending to accelerate toward the end of the century. WEUR shows a strong trend for Rx3h within the first 10 years followed by a period of reduced increase and acceleration toward the end again. This altered near future behavior is also visible for Rx1d, which is followed by a slow decrease in summer; Rx5d in summer shows no trend at first, then decreases. CEUR and EEUR show linear trends for summer until around 2060 with a followed flattening in CEUR and a reversal in EEUR. These hooked shape trends might indicate that land-atmosphere feedbacks undergo a considerable change under global warming. This might indicate that the moisture availability rather than the storage capacity of the atmosphere constrains extreme precipitation (Berg et al., 2009; Drobinski et al., 2016; Hardwick Jones et al., 2010) and therefore only seen in summer, where mean precipitation is largely decreasing.

Madsen et al. (2014) conclude an increase in daily extreme precipitation based on observations for several European areas, confirming the findings of the projected future changes in daily extreme precipitation in

this study: over the United Kingdom in winter, spring, and autumn; over Germany and western Czech Republic in winter; over French Mediterranean regions; Belgium and Northeastern Italy.

In Figure 4, the IV is defined as the standard deviation of the 50-member relative changes. The IV is increasing for about three decades before stabilizing at around 10–20% in SEUR and 5–15% in other regions. It shows the importance of IV on shorter timescales and after stabilizing an emergence of robust signals depends on the intensity of the FR. The uncertainty from IV plays an important role on regional scales until midcentury, as also shown by Lehner et al. (2020). The decrease in IV toward the end of the century over SEUR in summer can be explained by approaching zero precipitation, which leads to a compression of the standard deviation.

The information about the FR and the IV can be used to assess whether a signal is strong and attributable to climate change or whether the change is still clouded by the uncertainty that lies within the range of IV. The time when the signal leaves the band of IV (a signal-to-noise ratio greater than 1) is referred to as time-of-emergence. The Rx3h emerges in almost all seasons and regions from the IV before the middle of the century.

Only where the FR is small emergence is either reached later or no emergence before the end of the century is reached. Where the FR of Rx3h is smaller or like Rx1d, the FR of subdaily extremes emerges later than the daily FR due to smaller IV in Rx1d. Otherwise, subdaily extremes generally emerge before daily extremes. For seasonal maxima in winter as well as for annual maxima all indices show an emergence before the end of the century, except in SEUR. Here, only in summer all indices agree on an emergence before midcentury. In general, the signals of all indices emerge earlier in winter than in summer, which can be attributed to higher values of IV in summer. Indices emerging in the second half of the century or not emerging at all highlight the importance of IV as a dominant source of uncertainty on regional scales late into the 21st century.

6. Conclusion and Discussion

In this study we have analyzed seasonal and annual maximum precipitation for various temporal resolutions (3-hr, days, and 5 days) from the CRCM5-LE under the RCP8.5 scenario.

Is the CC expression constraining scaling rates of precipitation extremes at subdaily and daily resolutions? We show that subdaily extremes (Rx3h) exhibit stronger increases and higher CC-scaling than daily extremes and mean precipitation. These findings are consistent with other studies (e.g., W. Zhang, Villarini, et al., 2017). While regions such as NEUR and EEUR exhibit precipitation extremes with super-CC scaling (>7%/K), which might indicate that changes are mainly driven by thermodynamics, other areas such as France or SEUR seem to be strongly influenced by dynamic changes (e.g., a change in storm tracks or altered latent heat flux induced by reduced soil moisture). In these regions the alterations of the IV could also be triggered by dynamic changes.

Is there a strong seasonal variability in the FR of maximum precipitation? The trends of Rx3h can differ considerably from one season to the other. While NEUR and WEUR show even higher trends for summer, SEUR shows decreasing trends in summer compared to increases (winter) or no change.

When can we expect changes in extreme precipitation to robustly emerge from IV? Despite the dominant source of uncertainty induced by the IV, robust signals can be detected within the 21st century on regional scales. For almost all indices and seasons a time-of-emergence before midcentury can be projected. The Rx3h tends to emerge earlier than daily indices or mean precipitation, as well as an earlier emergence in winter over summer, which is also suggested by Kendon et al. (2018). However, especially in areas with small signals the IV remains a dominant source of uncertainty even until the end of the century. Also, Prein and Pendergrass (2019) and Lehner et al. (2020) argue that on regional scales IV will remain a dominant source of uncertainty.

Since the signals predominantly emerge before 2050, they are likely to be independent of the RCP scenario. The rate of extreme precipitation change scaled with temperature does not substantially vary across RCP scenarios (Berg et al., 2019; Pendergrass et al., 2015) until the midcentury, and even late in the 21st century there is still a considerable overlap for RCP4.5 and RCP8.5 results (Sanderson et al., 2018). Also, Lehner

et al. (2020) show that scenario uncertainty becomes relevant after 2050. Therefore, we can have confidence in the sign of extreme precipitation change, the higher scaling of subdaily extremes versus longer duration extremes, and the evolution of the IV.

Comparing our results with the only other high-resolution large-ensemble study over Western Europe (Aalbers et al., 2018) indicates a strong coherence of the regional pattern of mean and extreme precipitation, which implies that other regional SMILEs agree in the increase in extreme precipitation as well as their spatial patterns. However, as shown by Berg et al. (2019) RCMs show model deficiencies for hourly summer precipitation due the parametrization of convection that may alter the magnitude of change. It would be important to extend this study to CPM simulations to study the impact of convection parametrization on the results shown for subdaily extremes. Innocenti et al. (2019) showed for North America that the CRCM5-LE can reproduce the annual and diurnal cycle of annual maximum daily and subdaily precipitation and that they are comparable to a 4 km WRF simulation. For four smaller European regions Hodnebrog et al. (2019) compared the CRCM5-LE to 3 km WRF simulations and show that the WRF CPM shows smaller increases of summerly Rx1h but that both show a stronger intensification of subdaily extremes compared to daily extremes or mean precipitation and that IV is a dominant source of uncertainty.

On the regional scale more high-resolution large ensembles are needed to comprehensively analyze the robustness of regional patterns and to narrow down the individual sources of uncertainties that arise from model deficiencies, emission scenarios, and IV.

Data Availability Statement

The CRCM5-LE precipitation data are available to the scientific community online (http://www.climex-project.org).

Acknowledgments

The CRCM5-LE was created within the ClimEx project, which was funded by the Bavarian State Ministry for the Environment and Consumer Protection. Computations of the CRCM5-LE were made on the SuperMUC supercomputer at Leibniz Supercomputing Centre of the Bavarian Academy of Sciences and Humanities. We acknowledge Environment and Climate Change Canada for providing the CanESM2-LE driving data.

References

Aalbers, E. E., Lenderink, G., van Meijgaard, E., & van den Hurk, B. J. J. M. (2018). Local-scale changes in mean and heavy precipitation in Western Europe, climate change or internal variability? *Climate Dynamics*, *50*(11–12), 4745–4766. https://doi.org/10.1007/s00382-017-3901-9

Addor, N., & Fischer, E. M. (2015). The influence of natural variability and interpolation errors on bias characterization in RCM simulations. *Journal of Geophysical Research: Atmospheres*, *120*, 10,180–10,195. https://doi.org/10.1002/2014JD022824

Alexander, L. V. (2016). Global observed long-term changes in temperature and precipitation extremes: A review of progress and limitations in IPCC assessments and beyond. *Weather and Climate Extremes*, *11*, 4–16. https://doi.org/10.1016/j.wace.2015.10.007

Allen, M. R., & Ingram, W. J. (2002). Constraints on future changes in climate and the hydrologic cycle. *Nature*, *419*(6903), 228–232. https://doi.org/10.1038/nature01092

Asadieh, B., & Krakauer, N. Y. (2015). Global trends in extreme precipitation: Climate models versus observations. *Hydrology and Earth System Sciences*, *19*(2), 877–891. https://doi.org/10.5194/hess-19-877-2015

Ban, N., Schmidli, J., & Schär, C. (2015). Heavy precipitation in a changing climate: Does short-term summer precipitation increase faster? *Geophysical Research Letters*, *42*, 1165–1172. https://doi.org/10.1002/2014GL062588

Bao, J., Sherwood, S. C., Alexander, L. V., & Evans, J. P. (2017). Future increases in extreme precipitation exceed observed scaling rates. *Nature Climate Change*, *7*(2), 128–132. https://doi.org/10.1038/nclimate3201

Barbero, R., Fowler, H. J., Lenderink, G., & Blenkinsop, S. (2017). Is the intensification of precipitation extremes with global warming better detected at hourly than daily resolutions? *Geophysical Research Letters*, *44*, 974–983. https://doi.org/10.1002/2016GL071917

Bélair, S., Mailhot, J., Girard, C., & Vaillancourt, P. (2005). Boundary layer and shallow cumulus clouds in a medium-range forecast of a large-scale weather system. *Monthly Weather Review*, *133*(7), 1938–1960. https://doi.org/10.1175/MWR2958.1

Beniston, M., Stephenson, D. B., Christensen, O. B., Ferro, C. A. T., Frei, C., Goyette, S., et al. (2007). Future extreme events in European climate: An exploration of regional climate model projections. *Climatic Change*, *81*(S1), 71–95. https://doi.org/10.1007/s10584-006-9226-z

Berg, P., Christensen, O. B., Klehmet, K., Lenderink, G., Olsson, J., Teichmann, C., & Yang, W. (2019). Summertime precipitation extremes in a EURO-CORDEX 0.11° ensemble at an hourly resolution. *Natural Hazards and Earth System Sciences*, *19*(4), 957–971. https://doi.org/10.5194/nhess-19-957-2019

Berg, P., Haerter, J. O., Thejll, P., Piani, C., Hagemann, S., & Christensen, J. H. (2009). Seasonal characteristics of the relationship between daily precipitation intensity and surface temperature. *Journal of Geophysical Research*, *114*, D18102. https://doi.org/10.1029/2009JD012008

Berg, P., Moseley, C.r., & Haerter, J. O. (2013). Strong increase in convective precipitation in response to higher temperatures. *Nature Geoscience*, *6*(3), 181–185. https://doi.org/10.1038/ngeo1731

Boberg, F., Berg, P., Thejll, P., Gutowski, W. J., & Christensen, J. H. (2010). Improved confidence in climate change projections of precipitation further evaluated using daily statistics from ENSEMBLES models. *Climate Dynamics*, *35*(7–8), 1509–1520. https://doi.org/10.1007/s00382-009-0683-8

Brogli, R., Kröner, N., Sørland, S. L., Lüthi, D., & Schär, C. (2019). The role of Hadley circulation and lapse-rate changes for the future European summer climate. *Journal of Climate*, *32*(2), 385–404. https://doi.org/10.1175/JCLI-D-18-0431.1

Brönnimann, S., Rajczak, J., Fischer, E. M., Raible, C. C., Rohrer, M., & Schär, C. (2018). Changing seasonality of moderate and extreme precipitation events in the Alps. *Natural Hazards and Earth System Sciences*, *18*(7), 2047–2056. https://doi.org/10.5194/nhess-18-2047-2018

Chan, S. C., Kendon, E. J., Fowler, H. J., Blenkinsop, S., Ferro, C. A. T., & Stephenson, D. B. (2013). Does increasing the spatial resolution of a regional climate model improve the simulated daily precipitation? *Climate Dynamics*, *41*(5–6), 1475–1495. https://doi.org/10.1007/s00382-012-1568-9

Deser, C., Knutti, R., Solomon, S., & Phillips, A. S. (2012). Communication of the role of natural variability in future North American climate. *Nature Climate Change*, *2*(11), 775–779. https://doi.org/10.1038/nclimate1562

Deser, C., Phillips, A., Bourdette, V., & Teng, H. (2012). Uncertainty in climate change projections: The role of internal variability. *Climate Dynamics*, *38*(3–4), 527–546. https://doi.org/10.1007/s00382-010-0977-x

Deser, C., Phillips, A. S., Alexander, M. A., & Smoliak, B. V. (2014). Projecting North American climate over the next 50 years: Uncertainty due to internal variability. *Journal of Climate*, *27*(6), 2271–2296. https://doi.org/10.1175/JCLI-D-13-00451.1

Donat, M. G., Alexander, L. V., Herold, N., & Dittus, A. J. (2016). Temperature and precipitation extremes in century-long gridded observations, reanalyses, and atmospheric model simulations. *Journal of Geophysical Research: Atmospheres*, *121*, 11,174–11,189. https://doi.org/10.1002/2016JD025480

Drobinski, P., Alonzo, B., Bastin, S., Silva, N. D., & Muller, C. (2016). Scaling of precipitation extremes with temperature in the French Mediterranean region: What explains the hook shape? *Journal of Geophysical Research: Atmospheres*, *121*, 3100–3119. https://doi.org/10.1002/2015JD023497

Fischer, E. M., Beyerle, U., & Knutti, R. (2013). Robust spatially aggregated projections of climate extremes. *Nature Climate Change*, *3*(12), 1033–1038. https://doi.org/10.1038/nclimate2051

Fischer, E. M., & Knutti, R. (2014). Detection of spatially aggregated changes in temperature and precipitation extremes. *Geophysical Research Letters*, *41*, 547–554. https://doi.org/10.1002/2013GL058499

Fischer, E. M., & Knutti, R. (2015). Anthropogenic contribution to global occurrence of heavy-precipitation and high-temperature extremes. *Nature Climate Change*, *5*(6), 560–564. https://doi.org/10.1038/nclimate2617

Fischer, E. M., & Knutti, R. (2016). Observed heavy precipitation increase confirms theory and early models. *Nature Climate Change*, *6*(11), 986–991. https://doi.org/10.1038/nclimate3110

Fischer, E. M., Sedláček, J., Hawkins, E., & Knutti, R. (2014). Models agree on forced response pattern of precipitation and temperature extremes. *Geophysical Research Letters*, *41*, 8554–8562. https://doi.org/10.1002/2014GL062018

Fyfe, J. C., Derksen, C., Mudryk, L., Flato, G. M., Santer, B. D., Swart, N. C., et al. (2017). Large near-term projected snowpack loss over the western United States. *Nature Communications*, *8*, 14,996. https://doi.org/10.1038/ncomms14996

Giorgi, F. (2019). Thirty years of regional climate modeling: Where are we and where are we going next? *Journal of Geophysical Research: Atmospheres*, *124*, 5696–5723. https://doi.org/10.1029/2018JD030094

Giorgi, F., Torma, C., Coppola, E., Ban, N., Schär, C., & Somot, S. (2016). Enhanced summer convective rainfall at Alpine high elevations in response to climate warming. *Nature Geoscience*, *9*(8), 584–589. https://doi.org/10.1038/ngeo2761

Guerreiro, S. B., Fowler, H. J., Barbero, R., Westra, S., Lenderink, G., Blenkinsop, S., et al. (2018). Detection of continental-scale intensification of hourly rainfall extremes. *Nature Climate Change*, *8*(9), 803–807. https://doi.org/10.1038/s41558-018-0245-3

Haerter, J. O., & Berg, P. (2009). Unexpected rise in extreme precipitation caused by a shift in rain type? *Nature Geoscience*, *2*(6), 372–373. https://doi.org/10.1038/ngeo523

Hardwick Jones, R., Westra, S., & Sharma, A. (2010). Observed relationships between extreme sub-daily precipitation, surface temperature, and relative humidity. *Geophysical Research Letters*, *37*, L22805. https://doi.org/10.1029/2010GL045081

Hawkins, E., & Sutton, R. (2009). The potential to narrow uncertainty in regional climate predictions. *Bulletin of the American Meteorological Society*, *90*(8), 1095–1108. https://doi.org/10.1175/2009BAMS2607.1

Hegerl, G. C., Zwiers, F. W., Stott, P. A., & Kharin, V. v. (2004). Detectability of anthropogenic changes in annual temperature and precipitation extremes. *Journal of Climate*, *17*(19), 3683–3700. https://doi.org/10.1175/1520-0442(2004)017<3683:DOACIA>2.0.CO;2

Held, I. M., & Soden, B. J. (2006). Robust responses of the hydrological cycle to global warming. *Journal of Climate*, *19*(21), 5686–5699. https://doi.org/10.1175/JCLI3990.1

Hodnebrog, Ø., Marelle, L., Alterskjær, K., Wood, R. R., Ludwig, R., Fischer, E. M., et al. (2019). Intensification of summer precipitation with shorter time-scales in Europe. *Environmental Research Letters*, *14*(12), 124,050. https://doi.org/10.1088/1748-9326/ab549c

Innocenti, S., Mailhot, A., Frigon, A., Cannon, A. J., & Leduc, M. (2019). Observed and simulated precipitation over northeastern North America: How do daily and sub-daily extremes scale in space and time? *Journal of Climate. Advance online publication.*, *32*(24), 8563–8582. https://doi.org/10.1175/JCLI-D-19-0021.1

Kain, J. S., & Fritsch, J. M. (1990). A one-dimensional entraining/detraining plume model and its application in convective parameterization. *Journal of the Atmospheric Sciences*, *47*(23), 2784–2802. https://doi.org/10.1175/1520-0469(1990)047<2784:AODEPM>2.0.CO;2

Kay, J. E., Deser, C., Phillips, A., Mai, A., Hannay, C., Strand, G., et al. (2015). The Community Earth System Model (CESM) large ensemble project: A community resource for studying climate change in the presence of internal climate variability. *Bulletin of the American Meteorological Society*, *96*(8), 1333–1349. https://doi.org/10.1175/BAMS-D-13-00255.1

Kendon, E. J., Ban, N., Roberts, N. M., Fowler, H. J., Roberts, M. J., Chan, S. C., et al. (2017). Do convection-permitting regional climate models improve projections of future precipitation change? *Bulletin of the American Meteorological Society*, *98*(1), 79–93. https://doi.org/10.1175/BAMS-D-15-0004.1

Kendon, E. J., Blenkinsop, S., & Fowler, H. J. (2018). When will we detect changes in short-duration precipitation extremes? *Journal of Climate*, *31*(7), 2945–2964. https://doi.org/10.1175/JCLI-D-17-0435.1

Kendon, E. J., Roberts, N. M., Fowler, H. J., Roberts, M. J., Chan, S. C., & Senior, C. A. (2014). Heavier summer downpours with climate change revealed by weather forecast resolution model. *Nature Climate Change*, *4*(7), 570–576. https://doi.org/10.1038/nclimate2258

Kendon, E. J., Rowell, D. P., Jones, R. G., & Buonomo, E. (2008). Robustness of future changes in local precipitation extremes. *Journal of Climate*, *21*(17), 4280–4297. https://doi.org/10.1175/2008JCLI2082.1

Kendon, E. J., Stratton, R. A., Tucker, S., Marsham, J. H., Berthou, S., Rowell, D. P., & Senior, C. A. (2019). Enhanced future changes in wet and dry extremes over Africa at convection-permitting scale. *Nature Communications*, *10*(1), 1794. https://doi.org/10.1038/s41467-019-09776-9

Kjellström, E., Thejll, P., Rummukainen, M., Christensen, J. H., Boberg, F., Christensen, O. B., & Fox Maule, C. (2013). Emerging regional climate change signals for Europe under varying large-scale circulation conditions. *Climate Research*, *56*(2), 103–119. https://doi.org/10.3354/cr01146

Kotlarski, S., Keuler, K., Christensen, O. B., Colette, A., Déqué, M., Gobiet, A., et al. (2014). Regional climate modeling on European scales: A joint standard evaluation of the EURO-CORDEX RCM ensemble. *Geoscientific Model Development*, *7*(4), 1297–1333. https://doi.org/10.5194/gmd-7-1297-2014

Kröner, N., Kotlarski, S., Fischer, E. M., Lüthi, D., Zubler, E., & Schär, C. (2017). Separating climate change signals into thermodynamic, lapse-rate and circulation effects: Theory and application to the European summer climate. *Climate Dynamics*, *48*(9–10), 3425–3440. https://doi.org/10.1007/s00382-016-3276-3

Kuo, H. L. (1965). On formation and intensification of tropical cyclones through latent heat release by cumulus convection. *Journal of the Atmospheric Sciences*, *22*(1), 40–63. https://doi.org/10.1175/1520-0469(1965)022<0040:OFAIOT>2.0.CO;2

Leduc, M., Mailhot, A., Frigon, A., Martel, J.-L., Ludwig, R., Brietzke, G. B., et al. (2019). ClimEx project: A 50-member ensemble of climate change projections at 12-km resolution over Europe and northeastern North America with the Canadian Regional Climate Model (CRCM5). *Journal of Applied Meteorology and Climatology*, *58*(4), 663–693. https://doi.org/10.1175/JAMC-D-18-0021.1

Lehner, F., Deser, C., Maher, N., Marotzke, J., Fischer, E. M., Brunner, L., et al. (2020). Partitioning climate projection uncertainty with multiple large ensembles and CMIP5/6. *Earth System Dynamics*, *11*(2), 491–508. https://doi.org/10.5194/esd-11-491-2020

Lenderink, G., Barbero, R., Loriaux, J. M., & Fowler, H. J. (2017). Super-Clausius–Clapeyron scaling of extreme hourly convective precipitation and its relation to large-scale atmospheric conditions. *Journal of Climate*, *30*(15), 6037–6052. https://doi.org/10.1175/JCLI-D-16-0808.1

Lenderink, G., & van Meijgaard, E. (2008). Increase in hourly precipitation extremes beyond expectations from temperature changes. *Nature Geoscience*, *1*(8), 511–514. https://doi.org/10.1038/ngeo262

Madsen, H., Lawrence, D., Lang, M., Martinkova, M., & Kjeldsen, T. R. (2014). Review of trend analysis and climate change projections of extreme precipitation and floods in Europe. *Journal of Hydrology*, *519*, 3634–3650. https://doi.org/10.1016/j.jhydrol.2014.11.003

Maher, N., Milinski, S., Suarez-Gutierrez, L., Botzet, M., Dobrynin, M., Kornblueh, L., et al. (2019). The max Planck institute grand ensemble—Enabling the exploration of climate system variability. *Journal of Advances in Modeling Earth Systems*, *11*, 2050–2069. https://doi.org/10.1029/2019MS001639

Maraun, D., Wetterhall, F., Ireson, A. M., Chandler, R. E., Kendon, E. J., Widmann, M., et al. (2010). Precipitation downscaling under climate change: Recent developments to bridge the gap between dynamical models and the end user. *Reviews of Geophysics*, *48*, RG3003. https://doi.org/10.1029/2009RG000314

Marelle, L., Myhre, G., Hodnebrog, Ø., Sillmann, J., & Samset, B. H. (2018). The changing seasonality of extreme daily precipitation. *Geophysical Research Letters*, *45*, 11,352–11,360. https://doi.org/10.1029/2018GL079567

Martel, J.-L., Mailhot, A., & Brissette, F. (2019). Global and regional projected changes in 100-year sub-daily, daily and multi-day precipitation extremes estimated from three large ensembles of climate simulation. *Journal of Climate. Advance online publication*, *33*(3), 1089–1103. https://doi.org/10.1175/JCLI-D-18-0764.1

Martel, J.-L., Mailhot, A., Brissette, F., & Caya, D. (2018). Role of natural climate variability in the detection of anthropogenic climate change signal for mean and extreme precipitation at local and regional scales. *Journal of Climate*, *31*(11), 4241–4263. https://doi.org/10.1175/JCLI-D-17-0282.1

Martynov, A., Laprise, R., Sushama, L., Winger, K., Šeparović, L., & Dugas, B. (2013). Reanalysis-driven climate simulation over CORDEX North America domain using the Canadian Regional Climate Model, version 5: Model performance evaluation. *Climate Dynamics*, *41*(11–12), 2973–3005. https://doi.org/10.1007/s00382-013-1778-9

Meinshausen, M., Smith, S. J., Calvin, K., Daniel, J. S., Kainuma, M. L. T., Lamarque, J.-F., et al. (2011). The RCP greenhouse gas concentrations and their extensions from 1765 to 2300. *Climatic Change*, *109*(1–2), 213–241. https://doi.org/10.1007/s10584-011-0156-z

Milinski, S., Maher, N., & Olonscheck, D. (2019). How large does a large ensemble need to be? *Earth Syst. Dynam. Discuss. Advance online publication*. https://doi.org/10.5194/esd-2019-70

Min, S.-K., Zhang, X., Zwiers, F. W., & Hegerl, G. C. (2011). Human contribution to more-intense precipitation extremes. *Nature*, *470*(7334), 378–381. https://doi.org/10.1038/nature09763

Molnar, P., Fatichi, S., Gaál, L., Szolgay, J., & Burlando, P. (2015). Storm type effects on super Clausius–Clapeyron scaling of intense rainstorm properties with air temperature. *Hydrology and Earth System Sciences*, *19*(4), 1753–1766. https://doi.org/10.5194/hess-19-1753-2015

Pendergrass, A. G., & Hartmann, D. L. (2014). Changes in the distribution of rain frequency and intensity in response to global warming. *Journal of Climate*, *27*(22), 8372–8383. https://doi.org/10.1175/JCLI-D-14-00183.1

Pendergrass, A. G., Lehner, F., Sanderson, B. M., & Xu, Y. (2015). Does extreme precipitation intensity depend on the emissions scenario? *Geophysical Research Letters*, *42*, 8767–8774. https://doi.org/10.1002/2015GL065854

Pfahl, S., O'Gorman, P. A., & Fischer, E. M. (2017). Understanding the regional pattern of projected future changes in extreme precipitation. *Nature Climate Change*, *7*(6), 423–427. https://doi.org/10.1038/nclimate3287

Prein, A. F., Gobiet, A., Truhetz, H., Keuler, K., Goergen, K., Teichmann, C., et al. (2016). Precipitation in the EURO-CORDEX 0.11° and 0.44° simulations: High resolution, high benefits? *Climate Dynamics*, *46*(1–2), 383–412. https://doi.org/10.1007/s00382-015-2589-y

Prein, A. F., Langhans, W., Fosser, G., Ferrone, A., Ban, N., Goergen, K., et al. (2015). A review on regional convection-permitting climate modeling: Demonstrations, prospects, and challenges. *Reviews of Geophysics*, *53*, 323–361. https://doi.org/10.1002/2014RG000475

Prein, A. F., & Pendergrass, A. G. (2019). Can we constrain uncertainty in hydrologic cycle projections? *Geophysical Research Letters*, *46*, 3911–3916. https://doi.org/10.1029/2018GL081529

Rajczak, J., Pall, P., & Schär, C. (2013). Projections of extreme precipitation events in regional climate simulations for Europe and the Alpine Region. *Journal of Geophysical Research: Atmospheres*, *118*, 3610–3626. https://doi.org/10.1002/jgrd.50297

Sanderson, B. M., Oleson, K. W., Strand, W. G., Lehner, F., & O'Neill, B. C. (2018). A new ensemble of GCM simulations to assess avoided impacts in a climate mitigation scenario. *Climatic Change*, *146*(3–4), 303–318. https://doi.org/10.1007/s10584-015-1567-z

Šeparović, L., Alexandru, A., Laprise, R., Martynov, A., Sushama, L., Winger, K., et al. (2013). Present climate and climate change over North America as simulated by the fifth-generation Canadian regional climate model. *Climate Dynamics*, *41*(11–12), 3167–3201. https://doi.org/10.1007/s00382-013-1737-5

Sillmann, J., Kharin, V. V., Zwiers, F. W., Zhang, X., & Bronaugh, D. (2013). Climate extremes indices in the CMIP5 multimodel ensemble: Part 2. Future climate projections. *Journal of Geophysical Research: Atmospheres*, *118*, 2473–2493. https://doi.org/10.1002/jgrd.50188

Tang, T., Shindell, D., Samset, B. H., Boucher, O., Forster, P. M., Hodnebrog, Ø., et al. (2018). Dynamical response of Mediterranean precipitation to greenhouse gases and aerosols. *Atmospheric Chemistry and Physics*, *18*(11), 8439–8452. https://doi.org/10.5194/acp-18-8439-2018

Wentz, F. J., Ricciardulli, L., Hilburn, K., & Mears, C. (2007). How much more rain will global warming bring? *Science (New York, N.Y.)*, *317*(5835), 233–235. https://doi.org/10.1126/science.1140746

Westra, S., Alexander, L. V., & Zwiers, F. W. (2013). Global increasing trends in annual maximum daily precipitation. *Journal of Climate*, *26*(11), 3904–3918. https://doi.org/10.1175/JCLI-D-12-00502.1

Westra, S., Fowler, H. J., Evans, J. P., Alexander, L. V., Berg, P., Johnson, F., et al. (2014). Future changes to the intensity and frequency of short-duration extreme rainfall. *Reviews of Geophysics*, *52*, 522–555. https://doi.org/10.1002/2014RG000464

Xiao, C., Wu, P., Zhang, L., & Song, L. (2016). Robust increase in extreme summer rainfall intensity during the past four decades observed in China. *Scientific Reports*, *6*, 38,506. https://doi.org/10.1038/srep38506

Zappa, G., Hawcroft, M. K., Shaffrey, L., Black, E., & Brayshaw, D. J. (2015). Extratropical cyclones and the projected decline of winter Mediterranean precipitation in the CMIP5 models. *Climate Dynamics*, *45*(7–8), 1727–1738. https://doi.org/10.1007/s00382-014-2426-8

Zhang, W., Villarini, G., Scoccimarro, E., & Vecchi, G. A. (2017). Stronger influences of increased CO_2 on subdaily precipitation extremes than at the daily scale. *Geophysical Research Letters*, *44*, 7464–7471. https://doi.org/10.1002/2017GL074024

Zhang, X., Zwiers, F. W., Li, G., Wan, H., & Cannon, A. J. (2017). Complexity in estimating past and future extreme short-duration rainfall. *Nature Geoscience*, *10*(4), 255–259. https://doi.org/10.1038/ngeo2911

6 Role of mean and variability change for changes in European extreme precipitation events

This work has been submitted to the Journal *Earth System Dynamics*.

Wood, Raul R. (2022): Role of mean and variability change for changes in European annual and seasonal extreme precipitation events

Plain language Summary:

The frequency of precipitation extremes is set to change in response to a warming climate. The upper tail of the precipitation distribution (i.e., extremes) is thereby influenced by both the mean and variability. This means that any change to either of these properties will determine the probability of extremes in the distribution. How large the individual contributions from either of them (mean or variability) to the change in precipitation extremes are, is largely unknown. This is however relevant for a better understanding of how and why climate extremes change. The two previous publications show that the change in the mean and variability are not synchronized, implying that these changes are driven by different mechanisms. The probability risk ratio framework is used in regional large ensemble climate simulations at pre-industrial, current, and future climate conditions to determine the change in the probability of precipitation extremes over Europe. This framework is extended to partition the change in extreme event probability into contributions from a change in the mean and variability. The results reveal that the change in variability can be equally or even more important than the mean.

Author Contributions:

RRW is the single author of this paper. Hence, RRW designed the concept and methodology of the work, carried out the analysis including figures, and wrote the manuscript.

Journal:

"*Earth System Dynamics (ESD)* is a not-for-profit international scientific journal dedicated to the publication and public discussion of studies that take an interdisciplinary perspective of the functioning of the whole Earth system and global change. [...] such as the atmosphere, cryosphere, hydrosphere, oceans, pedosphere, lithosphere, and the inner Earth, but also by life and human activity. ESD solicits contributions that investigate these various interactions and the underlying mechanisms, ways how these can be conceptualized, modelled, and quantified, predictions of the overall system behavior to global changes, and the impacts for its habitability, humanity, and future Earth system management by human decision making." (Copernicus Publications 2021)

Journal Metrics	
Impact Factor	5.540
Impact Factor (5-Year)	5.241
CiteScore (2021)	8.8
CiteScore Rank (2021)	#11/191
	General Earth and Planetary Sciences

Role of mean and variability change for changes in European annual and seasonal extreme precipitation events

Raul R. Wood[1]

[1]Department of Geography, Ludwig-Maximilians Universität München, Munich, 80333, Germany

Correspondence to: Raul R. Wood (raul.wood@lmu.de)

Abstract. The frequency of precipitation extremes is set to change in response to a warming climate. Thereby, the change in precipitation extreme event occurrence is influenced by both a shift in the mean and a change in variability. How large the individual contributions from either of them (mean or variability) to the change in precipitation extremes are, is largely unknown. This is however relevant for a better understanding of how and why climate extremes change. For this study, two sets of forcing experiments from the regional CRCM5 initial-condition large ensemble are used. A set of 50 members with historical and RCP8.5 forcing as well as a 35-member (700 year) ensemble of pre-industrial natural forcing. The concept of the probability risk ratio is used to partition the change in extreme event occurrence into contributions from a change in mean climate or a change in variability. The results show that the contributions from a change in variability are in parts equally important to changes in the mean, and can even exceed them. The level of contributions shows high spatial variation which underlines the importance of regional processes for changes in extremes. While over Scandinavia or Mid-Europe the mean influences the increase in extremes more, reversely the increase is driven by changes in variability over France, the Iberian Peninsula, and the Mediterranean. For annual extremes the differences between the ratios of contribution of mean and variability are smaller, while on seasonal scales the difference in contributions becomes larger. In winter (DJF) the mean contributes more to an increase in extreme events, while in summer (JJA) the change in variability drives the change in extremes. The level of temporal aggregation (3h, 24h, 72h) has only a small influence on annual and winterly extremes, while in summer the contribution from variability can increase with longer durations. The level of extremeness for the event definition generally increases the role of variability. These results highlight the need for a better understanding of changes in climate variability to better understand the mechanisms behind changes in climate extremes.

1 Introduction

Climate extremes (i.e., droughts, heat waves and floods) are set to change in a warming climate (Böhnisch et al., 2021; Brunner et al., 2021; Suarez-Gutierrez et al., 2020; van der Wiel et al., 2022) and recent devastating extreme events are testing the resilience of society. The rapid attribution of recent devastating extremes, such as the July 2021 Flood in Western Germany (Kreienkamp et al., 2021) or the heat wave in British Columbia (Philip et al., 2021) emphasize an already quantifiable influence of climate change on the severity of these and other extreme events. In observational records

significant trends emerge for various extreme metrics (Contractor et al., 2021; Fischer and Knutti, 2016; Fowler et al., 2021; Guerreiro et al., 2018; Westra et al., 2013). The impact of a warming climate on future precipitation extremes is a well-studied research field (Martel et al., 2021) with a consensus that precipitation extremes are increasing in magnitude and frequency over most parts of the world. Over Europe, it is shown that the magnitude (i.e., mean state) of extreme or heavy precipitation is increasing in Central and Northern Europe in all seasons while the Mediterranean Region can show decreasing trends in summer (Aalbers et al., 2018; Hodnebrog et al., 2019; Poschlod and Ludwig, 2021; Rajczak and Schär, 2017; Rutgersson et al., 2022; Wood and Ludwig, 2020). At sub-daily timescales precipitation extremes can increase at higher rates then on daily timescales (Wood and Ludwig, 2020; Fowler et al., 2021). The general assumption is that the magnitude of precipitation extremes is likely to increase under a warming climate due to atmospheric warming and its inherent impact on the hydrological cycle (Allen and Ingram, 2002; Held and Soden, 2006). While mean precipitation is constrained by the Earth's energy budget and scales at 1-3%/K per degree of global surface temperature warming, extremes are not constrained and can scale at the rate of moisture change at around 6-7%/K (O'Gorman and Schneider, 2009). Regionally and seasonally it is shown that precipitation extremes can considerably deviate from these global scaling rates, by scaling at levels well above the 7%/K Clausius-Clapeyron scaling (Wood and Ludwig, 2020; Lenderink et al., 2017; Poschlod and Ludwig, 2021; Lenderink and van Meijgaard, 2008) or showing negative scaling rates for seasonal extremes in the Mediterranean (Wood and Ludwig, 2020; Bador and Alexander, 2022). The regional and seasonal response of extreme precipitation to global warming is thereby governed by thermodynamic and dynamic drivers (Brogli et al., 2019; Kröner et al., 2017; Pfahl et al., 2017; Norris et al., 2019; Vries et al., 2022).

Besides the change in the magnitude of extreme precipitation, the extreme event occurrence (i.e., frequency) is as well set to change under global warming (Martel et al., 2020; Myhre et al., 2019). Any changes to the distribution of precipitation, hence also extreme events at the tail of the distribution, are influenced by both a shift in the mean and a change in variability. Thereby, the changes in the mean and variability can have different driving mechanisms (Pendergrass et al., 2017; van der Wiel and Bintanja, 2021; Bintanja and Selten, 2014; Bintanja et al., 2020). The variability connects the swings between extreme climatic states (Swain et al., 2018) and even when taking an evolving mean climate into account the change in variability influences the occurrence of extremes (Suarez-Gutierrez et al., 2020). Precipitation variability has been shown to increase at a higher rate than mean precipitation with regionally diverse patterns (Pendergrass et al., 2017; Wood et al., 2021). In global climate model simulations, van der Wiel and Bintanja (2021) show that the contributions of climate variability to the change in monthly extreme precipitation is considerable and that the contribution shows strong regional variations. However, to analyze the contributions on the European scale, higher resolution regional climate simulations are required. Higher resolution regional climate models yield lower biases and show added-value in representing local climate (Prein et al., 2016; Poschlod, 2021).

Extreme events with its rare occurrence are the most discernible manifestation of internal climate variability and more broadly precipitation projections are strongly influenced by the uncertainty of internal climate variability even far into the future (Lehner et al., 2020), especially on regional scales (Lehner et al., 2020; Wood and Ludwig, 2020). Hence, climate

simulations from a regional single model initial-condition large ensemble (SMILE) are used for a more robust sampling of extreme events under pre-industrial, current, and future climate conditions. The benefit of using SMILEs for the robust quantification of extreme event metrics has been asserted in many studies for numerous types of extremes. For example, the added-value of SMILEs for a better quantification of rare flood events (van der Wiel et al., 2019; Brunner et al., 2021; Kelder et al., 2022), the change in magnitude and frequency of precipitation extremes (Aalbers et al., 2018; Hodnebrog et al., 2019; Martel et al., 2020; Poschlod and Ludwig, 2021; Wood and Ludwig, 2020; Thompson et al., 2017), or droughts (Aalbers et al., 2022; Böhnisch et al., 2021; van der Wiel et al., 2022). SMILEs are also beneficial for studying changes in precipitation variability (e.g., Maher et al., 2021b; Pendergrass et al., 2017; Wood et al., 2021), the changes in the driving modes of climate variability (e.g., ENSO or NAO; Maher et al., 2018; McKenna and Maycock, 2021), and the robust quantification of changes in weather patterns (Mittermeier et al., 2019; Mittermeier et al., 2022). An overview of other applications using SMILEs can be found in Deser et al. (2020) and Maher et al. (2021a).

Here the probability risk ratio is used in regional large-ensemble climate simulations to partition the changes in extreme annual and seasonal precipitation events into contributions from changes in mean climate and climate variability. It is further analysed whether the contributions are influenced by the warming level, season, level of extremeness, or level of temporal aggregation (3h-72h).

2 Data and Methods

2.1 Climate simulations

For this study, two sets of forcing experiments (ALL and NAT) with the Canadian Regional Climate Model version 5 (CRCM5) are used. The ALL forcing experiment originate from the CRCM5 large ensemble (CRCM5-LE; Leduc et al., 2019). The CRCM5-LE is a regional 50 member initial-condition large ensemble, which was produced by dynamically downscaling the 50 member CanESM2 large ensemble (Canadian Earth System Model version 2 large ensemble; Fyfe et al., 2017; Kirchmeier-Young et al., 2017) with the regional climate model CRCM5 (v.3.3.3.1; Martynov et al., 2013; Šeparović et al., 2013) to the EURO-CORDEX 0.11° grid in a one-way nesting setup. All 50-member use combined anthropogenic (CO2 and non-CO2 GHGs, aerosols, and land cover) and natural (solar and volcanic influences) forcing (ALL forcings). Historical forcing is applied before 2006, and RCP8.5 (Meinshausen et al., 2011) is used for 2006 until 2100. The differences among the individual CRCM5 members are due to the macro and micro initialization in the driving CanESM2-LE and can be interpreted as natural climate variability.

For the NAT forcing experiment, the CRCM5 uses the CanESM2 pre-industrial control simulations (Arora et al., 2011) as its driving data. The pre-industrial simulations represent a climate state in 1850 without anthropogenic global warming at constant atmospheric CO_2 levels of 284.7ppm. From this 1000-year CanESM2 pre-industrial continuous simulation, 35 non overlapping time slices of each 22 years were selected and used as boundary conditions for the CRCM5 resulting in 35 pre-industrial control members. From each of the 35 CRCM5 members, the first two years were discarded as spin-up, resulting

in an ensemble of 700 years (35 members x 20 years). The CRCM5 setup used for this pre-industrial ensemble is identical to the setup used in Leduc et al. (2019) for the CRCM5-LE. Both CRCM5 experiments share the same model parameterization of deep convection (Kain and Fritsch, 1990) and shallow convection (Kuo, 1965; Bélair et al., 2005) providing hourly precipitation outputs. At a resolution of 0.11° a discrete modelling of convection is not possible and needs to be parameterized within the regional climate model.

The CRCM5-LE precipitation data was evaluated in various studies, showing a good representation of the timing of maximum annual precipitation (Wood and Ludwig, 2020), as well as good agreement for ten-year return levels of 3h-24h annual maxima with observations (Poschlod et al., 2021) over Europe. The CRCM5-LE is further capable of simulating synoptic weather pattern (i.e., Vb-cyclone) which are relevant for long-lasting high impact rainfall events triggering floods in the Alpine Region (Mittermeier et al., 2019). Over Eastern North America, the CRCM5-LE also yields a good representation of the annual and daily cycle (Innocenti et al., 2019). An analysis of the general biases of the CRCM5 setup can be found in (Leduc et al., 2019). Future projections of the annual maximum precipitation in the CRCM5-LE over Europe show similar patterns and magnitudes to the 16-member EC-Earth-RACMO large ensemble (Aalbers et al., 2018; Wood and Ludwig, 2020). The CRCM5-LE also shows a comparable spread of internal variability to other regional SMILEs and a good agreement of interannual variability with observations (von Trentini et al., 2020). The good representation of interannual variability can also be asserted to the driving CanESM2-LE (Wood et al., 2021). The large-scale NAO teleconnections, which are relevant for the interannual to multi-annual variability over Europe, are properly propagated from the driving CanESM2-LE to the CRCM5-LE (Böhnisch et al., 2020). For the CanESM2 statistically robust NAO patterns have been evaluated under current climate conditions (Böhnisch et al., 2020).

2.2 Methods

Here the probability risk ratio is used in regional large-ensemble climate simulations to partition the changes in extreme annual and seasonal precipitation events into contributions from changes in mean climate and climate variability. The basis for the analysis is annual (seasonal) maximum precipitation, which is defined as the maximum precipitation sum within a season (DJF or JJA) and year. Precipitation sums are calculated with a rolling window of size 3h, 24h and 72h accounting for partial overlaps with preceding/trailing seasons (years) to receive the absolute annual (seasonal) maximum precipitation. Annual (seasonal) maxima are calculated for each ensemble member and grid cell separately.

2.2.1 Event probability

The probability risk ratio is a widely used metric in attribution studies (Kirchmeier-Young et al., 2019a; Kirchmeier-Young et al., 2019b; Otto et al., 2018b; Swain et al., 2020) to analyse the change in event probability. It requires event probabilities from two different climate simulations (Figure 1a), which are defined here as the number of annual (seasonal) maxima exceeding a local event threshold. The event threshold is valid for both simulations and is based on the NAT simulations,

calculated for each season separately. For the threshold definition, all 700 annual (seasonal) values are pooled and normalized by its mean (see Eq. 1).

$$RX_{norm} = (RX_i - RX_{NAT}) / RX_{NAT} \text{ (Eq. 1)}$$

Where RX_{norm} is the normalised annual (seasonal) maximum precipitation, RX_{NAT} the mean annual (seasonal) maximum precipitation in the NAT simulation, and RX_i the values to be normalised. The normalization (Eq. 1) is valid for both NAT and ALL simulations by replacing RX_i with ALL (NAT) values. A normalization is applied to receive a comparable threshold across the domain and season. Thresholds based on absolute values without a normalization can show high spatial and seasonal variability. After normalization the standard-deviation over all values is calculated and events exceeding two-times (three-times) the standard-deviation are considered for the event probability (Figure 1a).

$$\text{Threshold} = N*\text{std}(RX_{norm,\,NAT}) \text{ (Eq. 2)}$$

Calculations of the threshold and event probabilities are performed for each grid cell separately. To ensure the same sample size in the NAT and ALL simulations, 35 random members have been picked from the full 50-member ALL simulations. The random sampling without replacement has no effect on the results and different sets of random samples will produce only very small marginal differences.

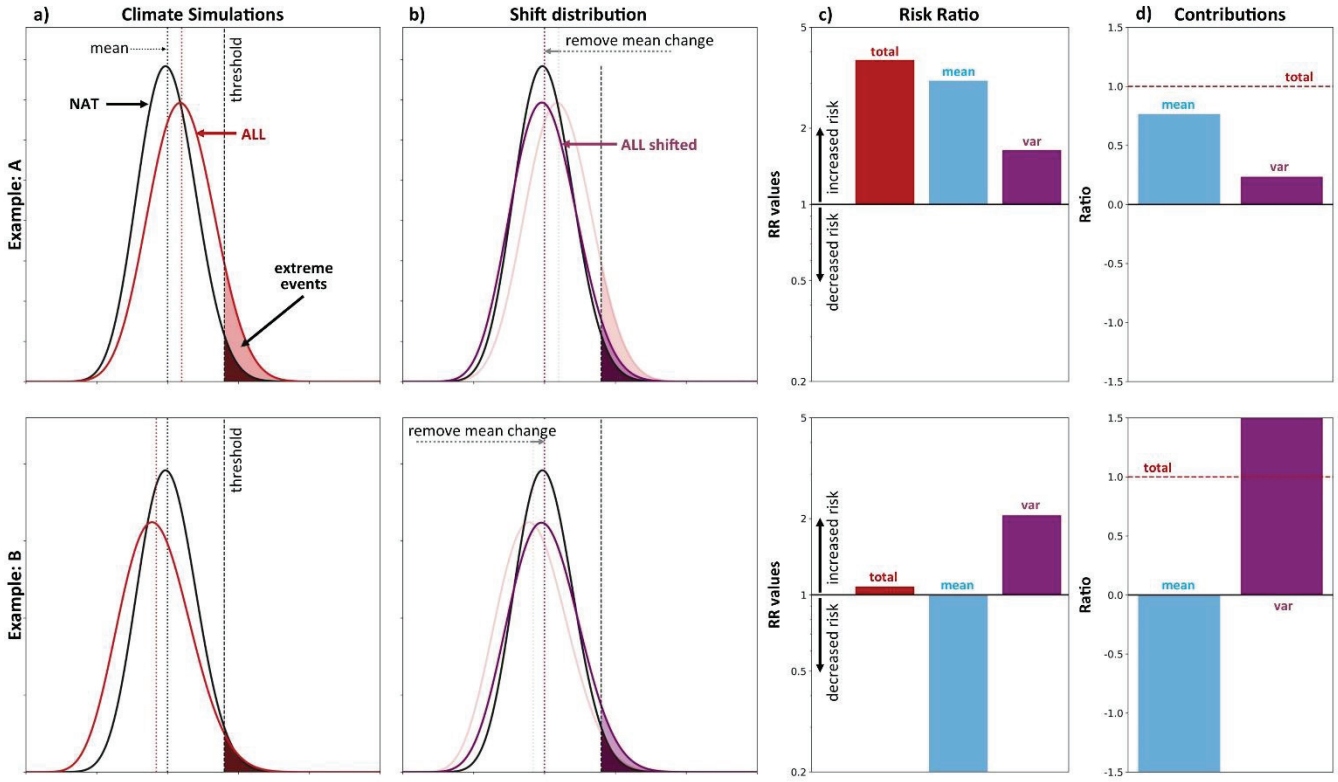

Figure 1: Schematic of the probability risk ratio framework for separating contributions from mean and variability. Two examples are given. In example A both mean and variability contribute to an increase in event probability. Example B shows contrasting contributions from mean and variability. a) Shows two different climate simulations (NAT and ALL) for which the

PRtotal is calculated based on the number of events exceeding the threshold in both distributions. b) Any change in the mean is removed by shifting the ALL distribution to match the mean in the NAT distributions, the shifted ALL simulation is then used to determine the PRvar based on the events exceeding the threshold. c) The PRmean can be determined from an adapted probability risk ratio relationship, giving the PR-values for PRtotal, PRmean, and PRvar. d) The ratio of contribution is determined from the individual contributions from PRmean and PRvar to the PRtotal, which sum up to 1. For more details see the methods (section 2.2).

2.2.2 Probability risk ratios

To assess the change in event probability, the framework of the probability risk ratio is applied. The conventional risk ratio as used in many attribution studies is calculated as follows:

$$PR = P_{ALL} / P_{NAT} \quad \text{(Eq. 3)}$$

with PR=1 indicating no change in extreme event probability, PR>1 indicates an increase in event probability and PR<1 a decrease in probability. Here, the event probabilities (P_{ALL}, P_{NAT}) are given as the number of extreme events in the ALL and NAT dataset and as described above. The conventional risk ratio framework is extended, as proposed by van der Wiel and Bintanja (2021) to separate the contributions from changes in the mean and changes in variability. The PR_{Total} is calculated in the classical way by following Eq.3. The PR_{Total} includes both the contributions from a change in the mean and variability and therefore concludes the total change. To quantify the role of a change in variability (widening of the distribution), the influence of any change in the mean is first removed by shifting the entire distribution of ALL to match the mean of NAT (Figure 1b). The shifting is achieved by subtracting the difference in the mean of ALL and NAT. The shifting of the distribution is done prior to the normalization of the ALL precipitation values (i.e., Eq 1). The number of extreme events is determined in the new distribution and used to calculate the risk ratio PR_{var}, representing the change in event occurrence due to the change in variability. From the two risk ratios PR_{Total} and PR_{var}, the risk ratio for PR_{mean} can be calculated following the new risk ratio relationship:

$$PR_{Total} = PR_{mean} + PR_{var} - 1 \quad \text{(Eq. 4)}$$

In this relationship subtracting by 1 is necessary because the reference PR-value is 1 (no change). The PR-values should be evaluated on a logarithmic scale, where PR=2 and PR=0.5 indicate a similar change in magnitude (Figure 1c).

2.2.3 Contributions from mean and variability

To quantify the relative contributions attributable to the change in the mean (PR_{mean}) and change in variability (PR_{var}) to the total risk change (PR_{Total}), a simple ratio of contribution is calculated as proposed by van der Wiel and Bintanja (2021):

$$C_{mean} = (PR_{mean} - 1) / (PR_{Total} - 1) \quad \text{(Eq.5)}$$

Which is equivalent for variability (C_{var}) by replacing PR_{mean} with PR_{var}. The two contributions C_{mean} and C_{var} sum up to 1. Thereby, they can either result in the same sign, which means that both mean and variability contribute to an increase (decrease) in the risk ratio (see Example A in Figure 1d), or they can have opposite signs showing opposing contributions (see Example B in Figure 1d). For the regional analysis the probability risk ratios (total, mean, and var) are averaged across

grid cells falling within the region boundaries (inclusion is based on cell centre points) before the ratio of contribution is calculated based on the regionally averaged PR-values.

2.2.4 Warming levels

Lastly, the risk ratios and their contributions are analysed for different warming levels. The warming levels are calculated from the driving CanESM2-LE dataset with a rolling window of 20 years with the pi-Control CanESM2 simulation as the reference. The ensemble mean warming is used to identify the 20-year periods closest to 1°C, 2°C, 3° and 4°C. Thereby, the 1°C warming level is considered as the current climate.

3 Results

3.1 Probability risk ratio and ratio of contribution in annual extremes

3.1.2 Current climate

Compared to a stable pre-industrial climate the present-day climate (+1°C) in the CRCM5-LE shows a widespread increase in the mean 3-hourly annual maximum (AX3h) precipitation by 4.6 % K^{-1} over land (Figure 2a). The regionally averaged scaling rates differ between 3.6 and 5.9 % K^{-1} among the different subregions. The standard deviation (i.e., variability) of the AX3h has increased by 8.9 % K^{-1} over all land area within the same time (Figure 2b). The increase in variability is larger than the change in the mean AX3h in all subregions. The total probability risk ratio (PRtotal) of AX3h events larger than 2-sigma has also increased slightly by 1.36 averaged over all land areas (Figure 2e, Figure 4). This total change is influenced by both the change in the mean and variability. When the probability risk ratio is calculated based on the mean and variability separately, then slightly higher risk ratios can be seen for the PRvar (1.2) than for PRmean (1.16) (Figure 2c-d). The individual ratios of contribution for mean and variability to the total risk ratio show that the increase in the PRtotal can to a larger part be attributed to a change in variability (0.55 when averaged over all land area) and to a slightly lesser extend due to the mean (0.45) (Figure 2f-g, Figure 5). Within all subregions the contribution from variability varies between 0.48 and 0.63.

Other studies show that the observational records reveal an increased risk of extreme precipitation, at least when taking the change in mean extremes as a proxy (Westra et al., 2013; Westra et al., 2014; Donat et al., 2016; Sippel et al., 2017). Which in parts fits the trend seen in the CRCM5-LE, since the mean contributes to roughly 0.45 to the increase in extreme events. Although trends in single realizations (i.e., observations) could be underestimated since changes in variability are difficult to quantify from the limited sample size, studies from the detection and attribution community show that climate change is now detectable in everyday weather events (Sippel et al., 2020) and that recent extreme events over Europe have been amplified by climate change (Kreienkamp et al., 2021; Otto et al., 2018a), which makes the results from the CRCM5-LE for the seem plausible.

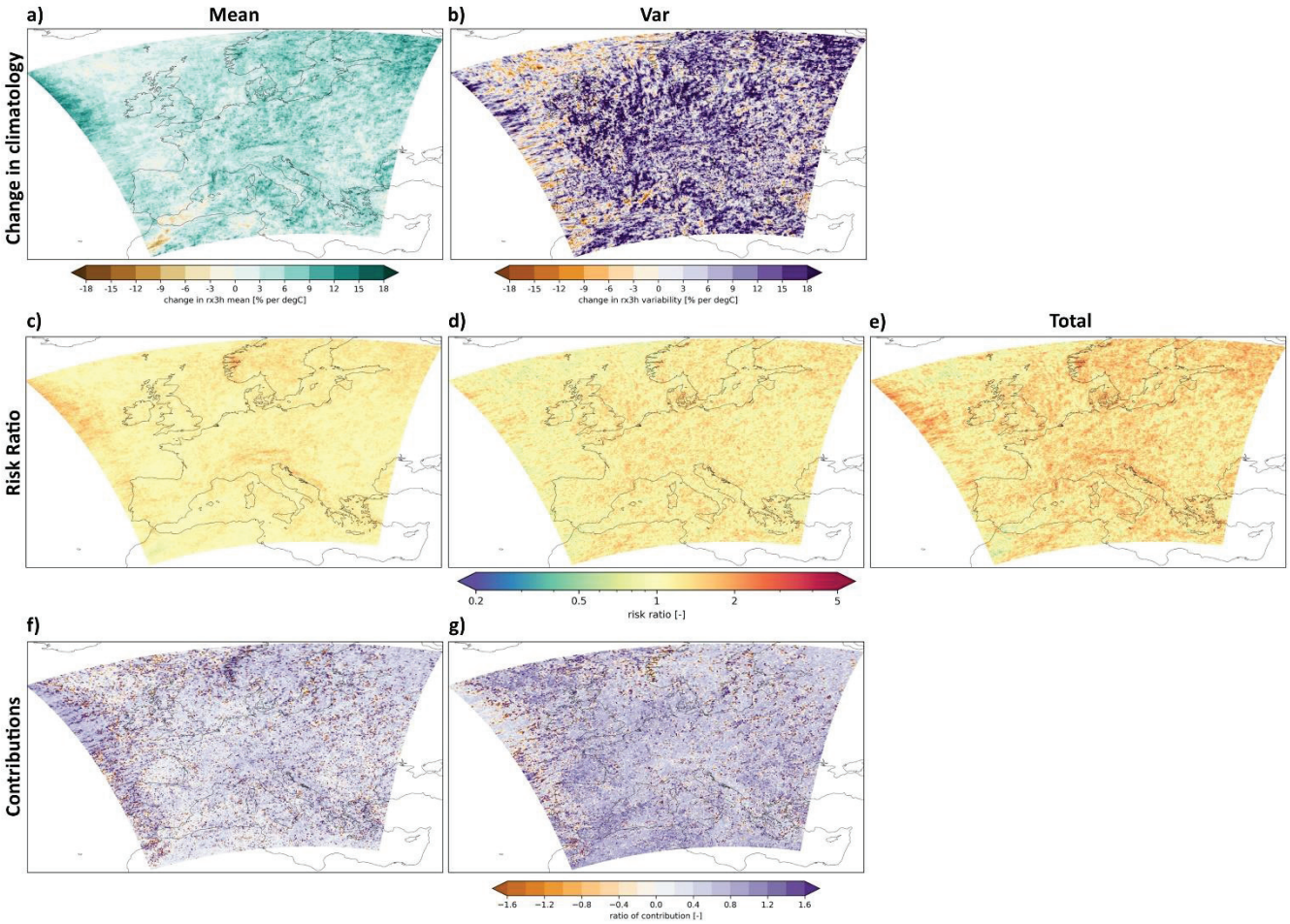

Figure 2: Changes in the current climate (+1°C) compared to a stable pre-industrial climate in the CRCM5-LE simulations. a) Change in the mean annual rx3h. b) Change in the variability (i.e., standard deviation of annual rx3h). c) PRmean, d) PRvar and e) PRtotal values for 2-sigma events. f) ratio of contribution for changes in the mean. g) ratio of contribution for changes in variability.

3.1.2 Future climates

In a two-degree (+2°C) warmer world, the probability risk ratio continues to increase to 1.77 showing a doubling of 2-sigma extreme events in roughly 29 percent of the land area (Figure 3a). The strongest increases in the total risk ratio can be seen in the Scandinavian region with an average increase in the PRtotal by 2.1 with roughly 56 percent of grid cells showing a doubling in events. By a change of mean or variability alone, a considerably smaller percentage of land area would show a doubling in extreme events in Scandinavia (mean: 13 %, var: 6.3 %), and over all land areas (mean: 4 %, var: 3.5 %). This emphasizes the joint role that changes in mean and variability have for shaping the total change in extremes. Both the Scandinavian region and the Alps are clearly visible in the PRmean maps while the PRvar show a more widespread increase in the risk ratio throughout the entire domain (Figure 3b-c).

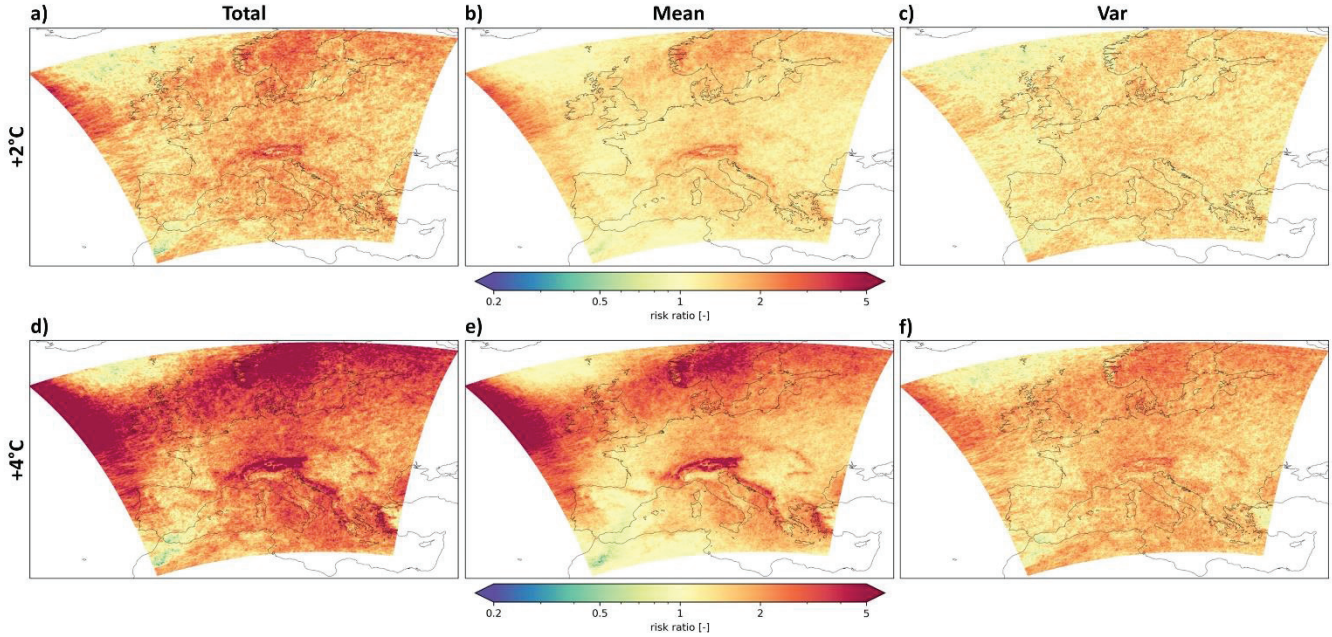

Figure 3: Probability risk ratios for annual rx3h for extreme events larger than 2-sigma in a +2 °Cand +4 °C warmer world. a) + d) PRtotal. b) + e) PRmean. c) + f) PRvar. a) – c) +2 °C climate. d) – f) +4 °C climate. All probabilities relative to the pre-industrial climate.

In a four-degree (+4 °C) warmer world, the risk of 2-sigma extreme events becomes more likely with roughly 69 percent of land grid cells showing at least a doubling of events with an average increase in PRtotal of 2.7 (Figure 3d-f). While the PRvar is generally still increasing more widespread, the PRmean shows a more contrasting picture with regions, such as the Alps and Scandinavia, showing a very large increase in PR-values, while other regions show PR-values closer to one (i.e., no change), such as parts of the Iberian Peninsula or France. Figure 4 shows the regional average PR-values (total, mean, and var) for all PRUDENCE subregions at different warming levels, and reveals that in most regions the PRmean and PRvar develop similar. In Mid-Europe, Eastern Europe, and the Mediterranean both the PRmean and PRvar develop very closely and show almost identical PR-values. Over the British Isles the PRmean starts to increase steeper towards the +4°C warming level, diverging from the PRvar which shows a continued increase but at a lower level. In Scandinavia and the Alps, where the change in the PRtotal is most pronounced, the PRmean diverges already at +2°C from the PRvar and increases at considerably higher rates. Over France and the Iberian Peninsula, where overall PRtotal values are lower than in other regions, the PRvar remains throughout all warming levels slightly above the increase in PRmean. In all subdomains the probability of more extremes increases no matter if this is driven by a change in the mean or variability.

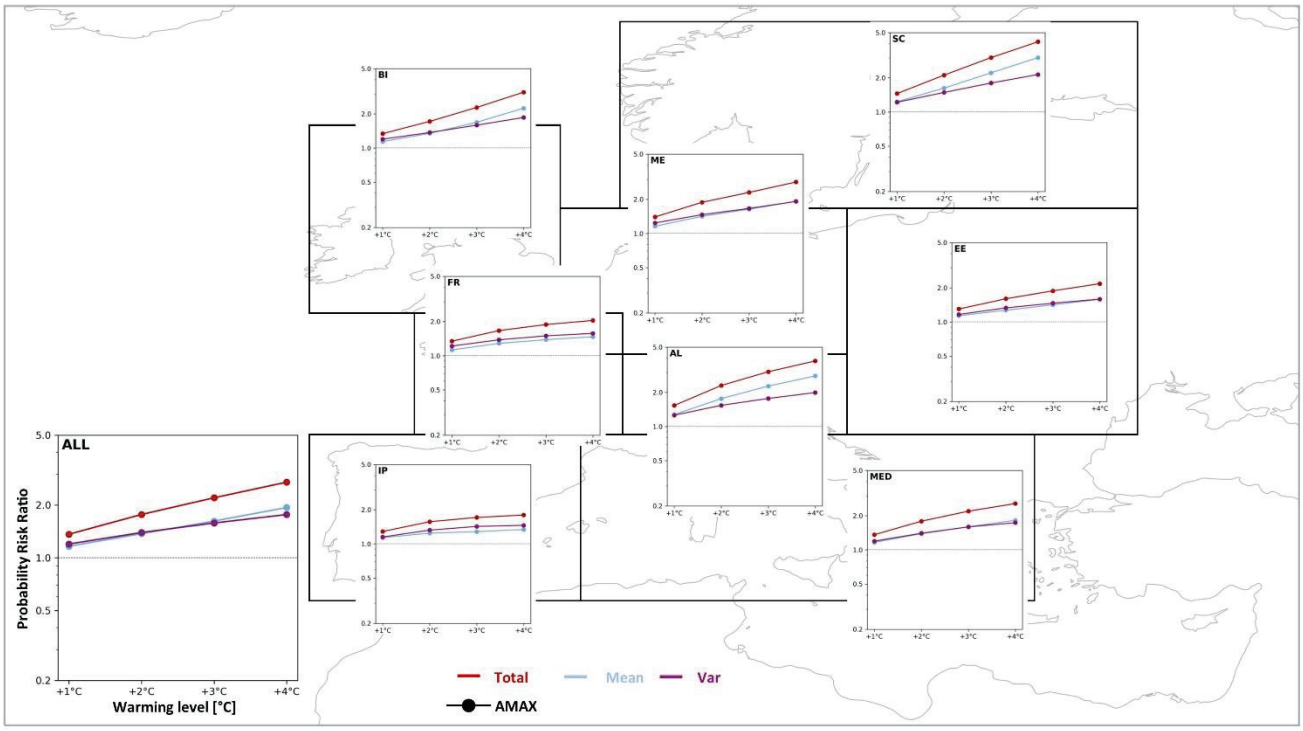

Figure 4: Regional averaged PR-values (total, mean, and var) for the PRUDENCE regions at different warming levels for annual rx3h events larger than 2-sigma. PRtotal (red), PRmean (blue), and PRvar (purple) values (y-axis) at warming levels (+1, +2, +3, +4 °C) (x-axis). The lower left panel shows the aggregation over all land grid cells and shows axis labels.

In Figure 5, the individual contributions from PRmean and PRvar to the total change (PRtotal) are shown for the subregions. Generalized over all land areas the contributions reveal that the change in variability attributes slightly more (approx. 0.55) in the current climate (+1°C) and the contributions steadily reduce to approx. 0.45 in the +4°C warmer world. This means the contributions from mean and variability develop diagonally to each other with the mean gaining in importance. On the regional scale however, there are distinct differences among the regions. The British Isles show a similar development to the domain average, but slightly more pronounced with the variability contributing by 0.58 in the current climate and by 0.41 at +4°C. In the Mediterranean this is less pronounced, and both contribute close to equally in the current and future climates. In Mid-Europe and Eastern Europe, the contributions from variability and mean converge with continued warming. In the current climate the variability has a higher contribution. Over Eastern Europe the converging takes slightly longer than over Mid-Europe where both (mean and variability) contribute equally from a +2°C climate onwards. In France, both contributions tend to converge, however the contributions from variability remain higher than the mean (0.55-0.63). In contrast, over Scandinavia and the Alps the contributions are approximately equal at current levels and diverge throughout the future warming with the mean gaining in importance (0.64 in both regions). Over the Iberian Peninsula the variability gains in importance towards a +3°C world (0.6) and slightly converges towards the end but remains higher than the mean.

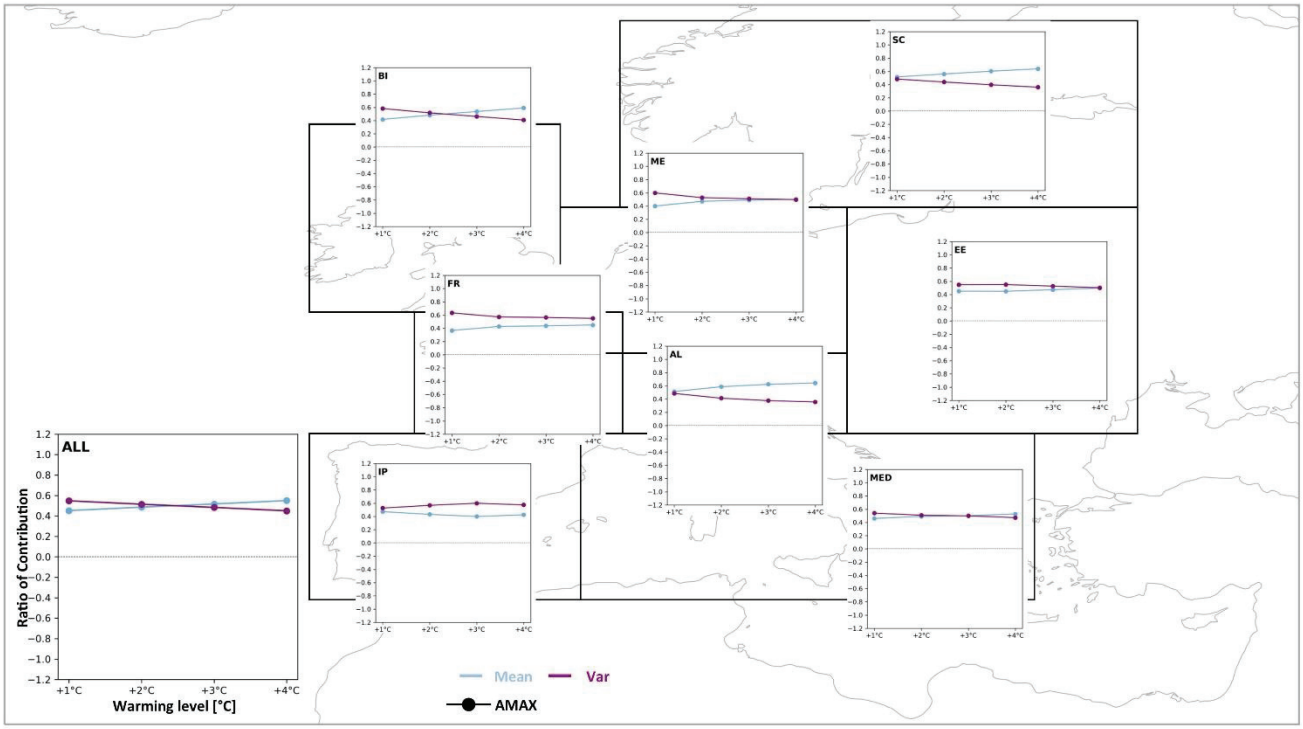

Figure 5: Individual contributions from PRmean and PRvar to the PRtotal in the different PRUDENCE regions at different warming levels. Ratio of contributions from PR-values in Figure 4. Contribution from the mean in blue and contributions from variability in purple. Ratio of contribution on the y-axis and different warming levels on the x-axis. Warming levels: +1, +2, +3, +4 °C; The lower left panel shows the aggregation over all land grid cells and shows axis labels.

3.2 Extremes on seasonal scales

3.2.1 Probability Risk Ratios

Looking at the seasonal scales which can be relevant for decision-makers the patterns reveal some interesting and diverse characteristics. Figure 6 shows maps of the probability risk ratios (PRtotal, PRmean, and PRvar) in the +4°C world for the two seasons winter (DJF) and summer (JJA) in comparison to the annual scale (as seen in Figure 3). The two seasons have been chosen since they show a strong seasonal contrast in the forced response of mean seasonal maximum precipitation as well as seasonal total precipitation amounts (Wood and Ludwig, 2020; Christensen et al., 2019; Matte et al., 2019; Rajczak et al., 2013).

In winter the increase in total risk ratio is in many parts of the domain larger than on the annual scales. Over Eastern Europe, the Greater Alps, the Balkan region as well as over the Iberian Peninsula more intense and widespread increases can be seen compared to the annual scale. Also, in winter the contrast between PRmean and PRvar is more pronounced with the mean projecting a higher probability of extremes. While the winter shows large widespread increases, in summer more grid cells

emerge that show a decrease, no change or only a marginal increase in the PRtotal. In general, the pattern of PRtotal follows the expected North-South gradient with increases in the north and decreases in the south. However, despite the summerly decrease in PRmean over France, Italy, Eastern Europe, the Balkan, and the Pyrenees, which clearly follows the decrease in the mean JJAx3h (see Figure S1 in the supplementary material), the PRtotal is still increasing in parts of these regions. Which means that the number of extremes is increasing even though the mean is decreasing and would project a decline in extremes. Here, the decline in the risk ratio is compensated by the change in variability which is showing the opposite and shows an increase in the PRvar in these areas. This clearly highlights that the mean change is not always a sufficient proxy for the change in the probability of extremes. Especially over the Mediterranean and the Iberian Peninsula a widespread decline in the mean summerly average extremes is projected, however due to the change in the variability the probability of summerly extremes greater than 2-sigma remains and can even increase locally. Other clearly visible features in summer are the Alps and Scandinavia, which are also apparent features in winter and on the annual scale.

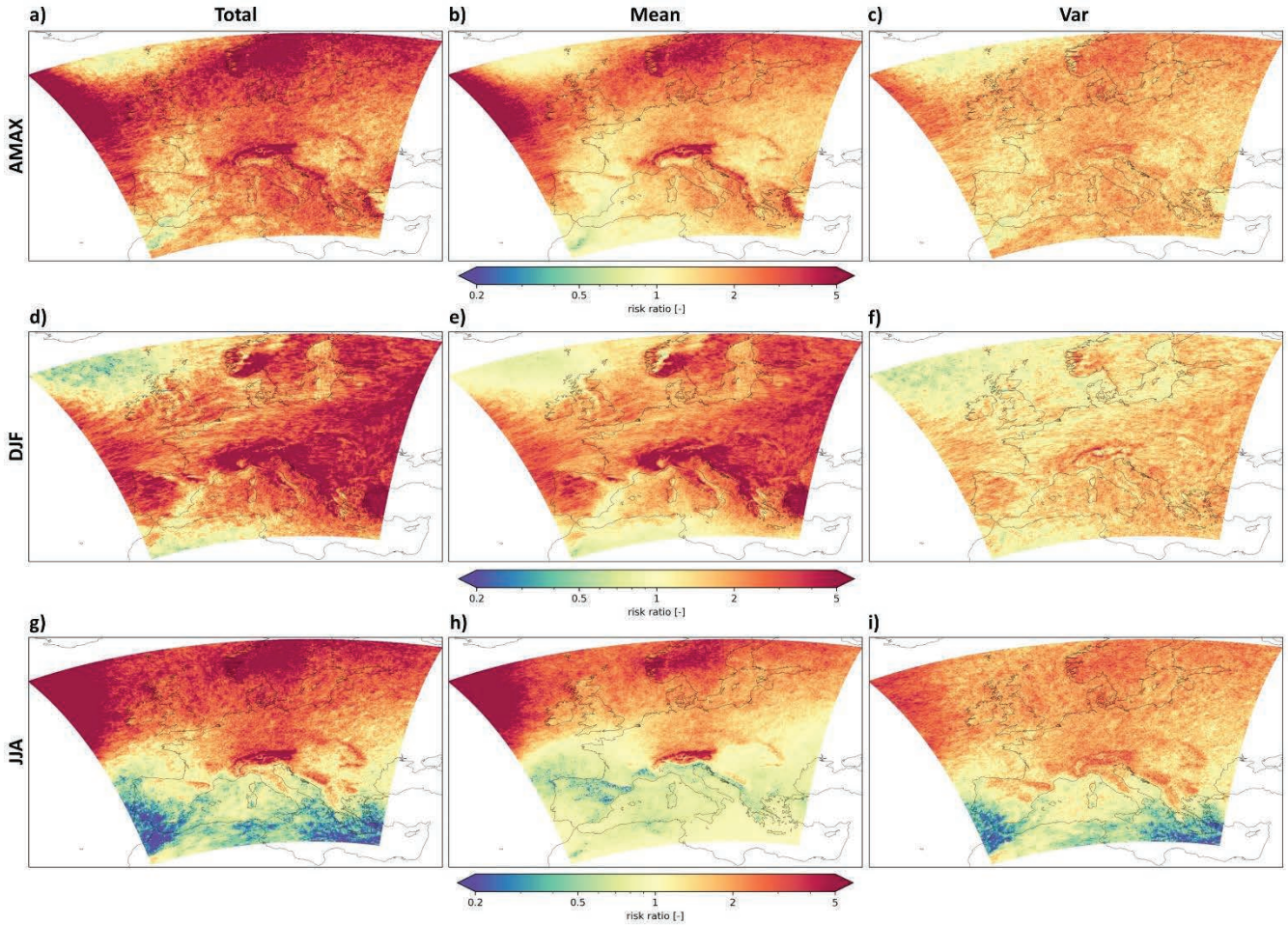

Figure 6: Annual probability risk ratios of rx3h events compared to seasonal DJF and JJA PR-values at +4 °C warming. a) – c) Annual PR-values; d) – f) DJF PR-values; g) – i) JJA PR-values; a) + d) + g) PRtotal; b) + e) + h) PRmean; c) + f) + i) PRvar.

Through the regional aggregation some generalized statements can be formulated. Aggregated over all land areas, the PRtotal increase is strongest in DJF (3.34) compared to the annual scale (2.7) and lowest in JJA (2.06) at +4°C warming (Figure 7). Generally, this can also be shown for France (DJF: 2.8, AMAX: 2.04, JJA: 1.6), the Alps (DJF: 5.6, AMAX: 3.78, JJA: 3), and Eastern Europe (DJF: 4.18, AMAX: 2.17, JJA: 1.6). In these regions the PRtotal increases for the two seasons and the annual values. Also, the Iberian Peninsula and the Mediterranean show the same order of strongest to lowest increases, but with the unique characteristic that in JJA the PRtotal is decreasing in the Iberian Peninsula (0.71) and declining towards no change in the Mediterranean.

A different order can be seen over Scandinavia and Mid-Europe where the PRtotal in JJA and the annual scale are basically identical in their progression with warming. In Scandinavia, the PRtotal in DJF remains below JJA and the annual values for all warming levels. In Mid-Europe, values of JJA remain below DJF and the annual values until the +4°C world where all three values converge to approx. 2.7-2.8 (PRtotal). In the British Isles, the PRtotal is largest on the annual scale and is closely followed by JJA and shows a weaker increase in winter.

Generally, when comparing the evolution of PRmean and PRvar it can be stated, that in summer the PRvar is above the PRmean, and in winter vice versa. Except for Scandinavia where PRmean is always larger than PRvar. On annual scales, both the PRmean and PRvar are generally quite similar except for the Alps and Scandinavia where PRmean is considerably larger than PRvar.

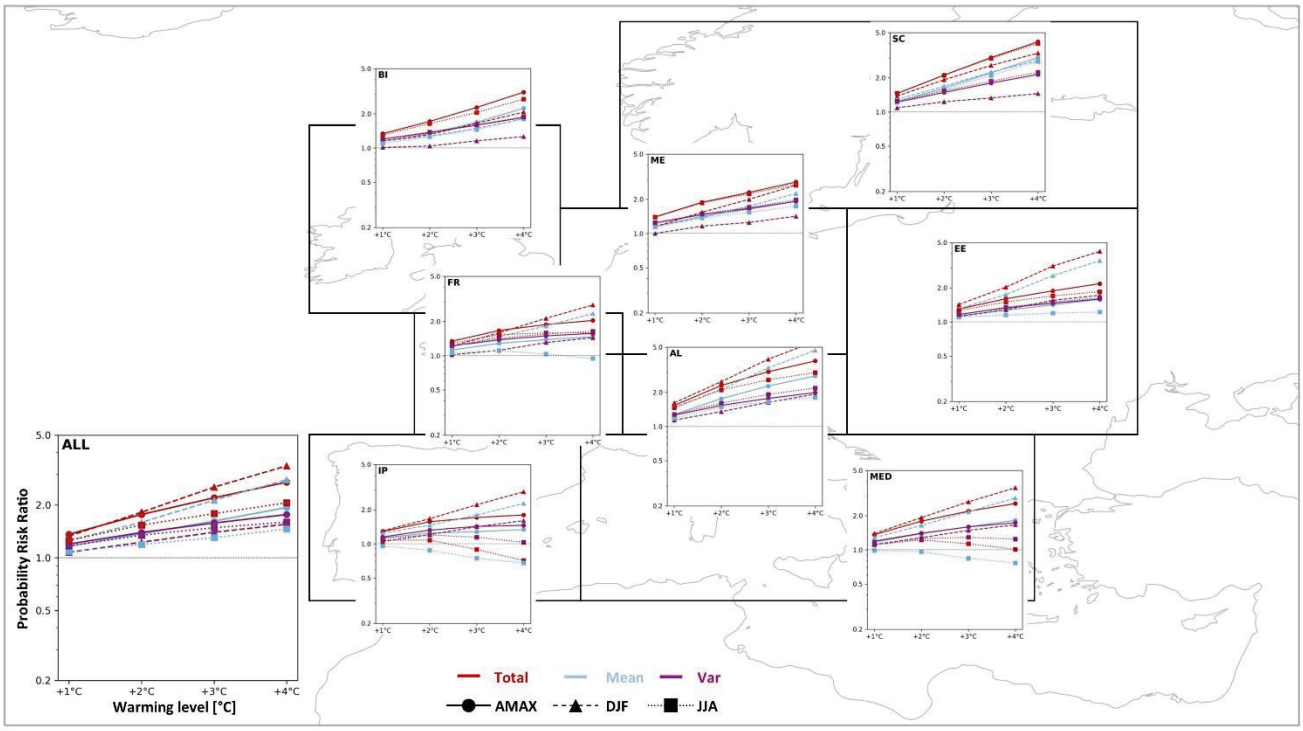

Figure 7: Comparison of regional averaged annual and seasonal PR-values (total, mean, and var) at different warming levels. The panels show PRtotal (red), PRmean (blue), and PRvar (purple) values (y-axis) at warming levels (+1, +2, +3, +4 °C) (x-axis). The solid lines with the circle marker represent annual PR-values (same as in Figure 4); the dashed lines with the triangle marker represent PR-values in winter (DJF); the dotted lines with the square marker represent PR-values in summer (JJA). The lower left panel shows the aggregation over all land grid cells and shows axis labels.

3.2.2 Ratio of Contribution from mean and variability

In Figure 8 the ratios of contribution for JJA, DJF and the annual scale are compared. All regions, except for Scandinavia show the general behaviour that the variability contributes to a large extent to the change in extremes in summer, while in winter this relation is opposite (i.e., mean > var). Aggregated over all land areas, the variability attributes to 0.56-0.66 of the change in summer while the mean only contributes to 0.34-0.44 of the change. In winter, the contribution of the variability only contributes to roughly a quarter (0.23-0.28) while the mean dominates the change in probability by roughly three-quarters (0.72-0.78). In comparison on the annual scale either the mean or variability contribute closer to equal by 0.45-0.55. Over the British Isles, the change in variability initially contributes to 0.7 (mean: 0.3) of the current change in the probability of summerly extremes before the contribution of both variability and mean converge to roughly equal contributions in a +4°C world. In winter, the mean initially contributes to most of the change with roughly 0.9 (var: 0.1) and slowly reduces to 0.76 (var: 0.24).

Over the Alps the ratios of contribution are very stable across all warming levels within their respective season. In summer, the variability contributes to a higher degree with roughly 0.6 compared to 0.4 from the mean. In winter, the change in probability is dominated by the change in the mean contributing by 0.8 (var: 0.2).

Also, in Scandinavia the ratio of contribution remains very stable across the warming levels in winter, with the mean contributing roughly by 0.8 to the overall change (var: 0.2). In summer, both the mean and variability initially contribute almost equally to the change and diverge to roughly 0.6 attributable to the change in the mean compared to 0.4 by the variability.

Over Eastern Europe, the variability attributes roughly to 0.6 (mean: 0.4) of the current change in summer and increases to 0.7 (mean: 0.3) in future climates. In winter, the contributions are stable across warming levels and the mean attributes to roughly 0.75 (var: 0.25) of the change.

Over Mid-Europe, the difference in contributions between mean and variability is initially larger, and they slightly converge in a warmer climate. In summer, the variability contributes to 0.63 (mean: 0.37) of the total change before the two contributions converge slightly. In winter, the current change is predominantly driven by the change in the mean (close to 1.0) before the variability slightly gains in importance with roughly 0.25 (mean: 0.75) in warmer climates.

Over France, the ratios of contribution are experiencing considerable changes throughout the different warming levels and seasons. In winter, the mean contributes by 0.9 to the current change before reducing slightly to 0.75. In the same time contributions from variability increase from 0.1 to 0.25. In summer, the variability is the main driver of change with 0.8 at current climate levels and increasing beyond 1 in the future climate. A contribution beyond 1 is possible because the mean contributes negatively to the change in the total risk ratio while variability shows an increase in extremes attributing to an overall increase in summerly extremes. This exemplifies that the change in the mean and variability can not only amplify the change in event probability, but in some cases counteract each other.

Over the Iberian Peninsula, the decline in the mean is responsible for the overall decline in the probability of extremes in summer. While the mean contributes to a decline throughout all warming levels, the variability can initially offset the overall decline in summerly extremes but can't compensate for the strong decline in the mean in warmer climates. Note that the change in the sign of contributions in JJA is due to a change in the PRtotal shifting from an increase (>1) to a decrease (<1). However, locally in the northern parts of the Iberian Peninsula increases in the probability of extremes in summer can still occur due to the change in variability even though the mean is strongly decreasing (as seen in Figure 6). In winter, for which the PRtotal is continuously increasing, the mean contributes initially with 0.83 (var: 0.17) and is subsequently lower in warmer climates (0.66-0.69).

Also, over the Mediterranean the mean contributes continuously to a decline in summerly extremes, however here the change in variability can initially offset the decline and lead to an increase in the probability of extremes in summer before the reversal of the trend towards no change of extremes in the +4°C world which is slowed by the presence of variability. In winter the mean attributes to roughly 0.7 of the change while variability by 0.3. The contributions are thereby stable across all warming levels.

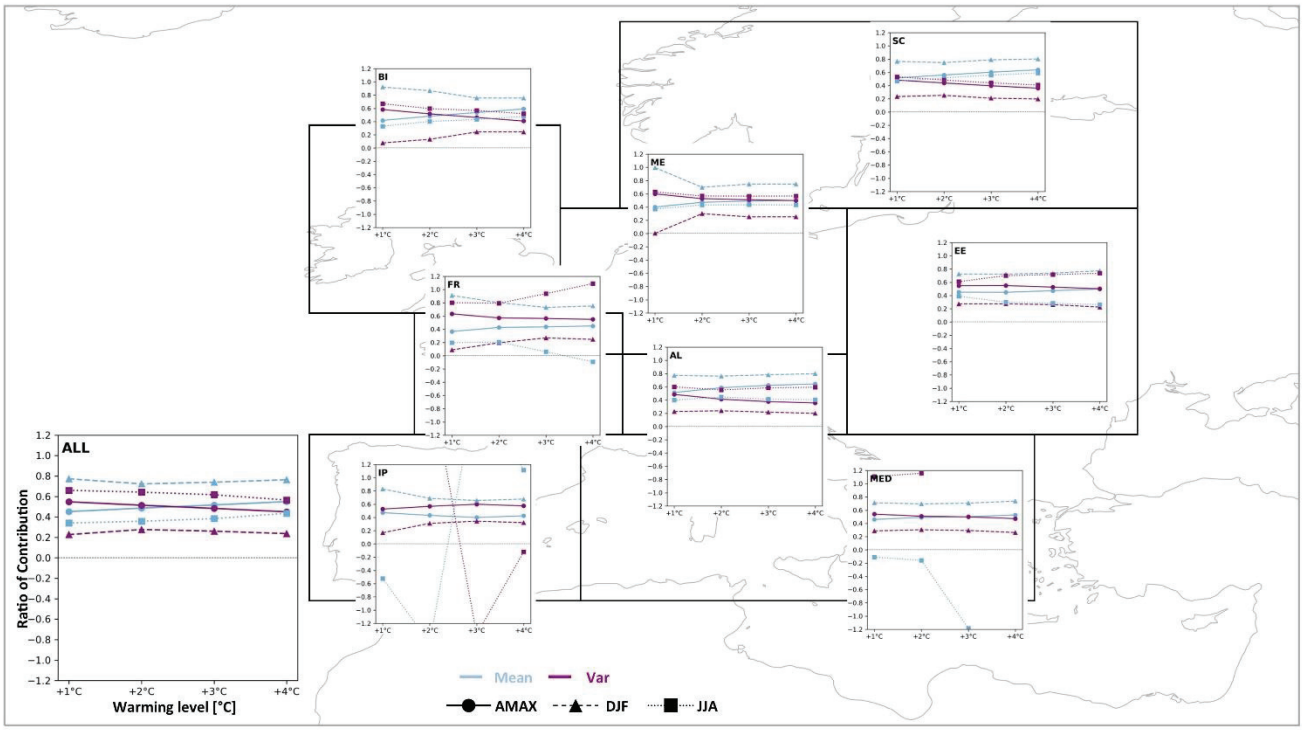

Figure 8: Comparison of individual contributions of annual and seasonal PRmean and PRvar to the PRtotal at different warming levels. Ratio of contributions from PR-values in Figure 7. Contribution from the mean in blue and contributions from variability in purple. Ratio of contribution on the y-axis with different warming levels on the x-axis (+1, +2, +3, +4 °C). The solid lines with the circle marker represent annual ratio of contributions (same as in Figure 5); the dashed lines with the triangle marker represent ratios in winter (DJF); the dotted lines with the square marker represent ratios in summer (JJA). The lower left panel shows the aggregation over all land grid cells and shows axis labels.

3.3 Influence of the temporal aggregation

Until now, all results shown are for an aggregation level of three hours raising the question whether the level of aggregation (i.e., 24-hours, 72-hours) has any influence on the ratio of contribution. First, looking at the probability risk ratios of annual extremes reveals that the level of temporal aggregation influences the magnitude of the probability risk ratios of total, mean and variability. In general, the PR-values of subdaily extremes (3-hours) are in most regions and aggregated over all land area higher than for 24-hours and 72-hours. Only over France the 3-hourly and 24-hourly PRtotal values develop close to identical with the 72-hours showing slightly lower values before all three aggregations converge in a similar PRtotal at +4°C. In Scandinavia, both the 24- and 72-hour extremes show near identical PR-values well below the 3-hour aggregation.

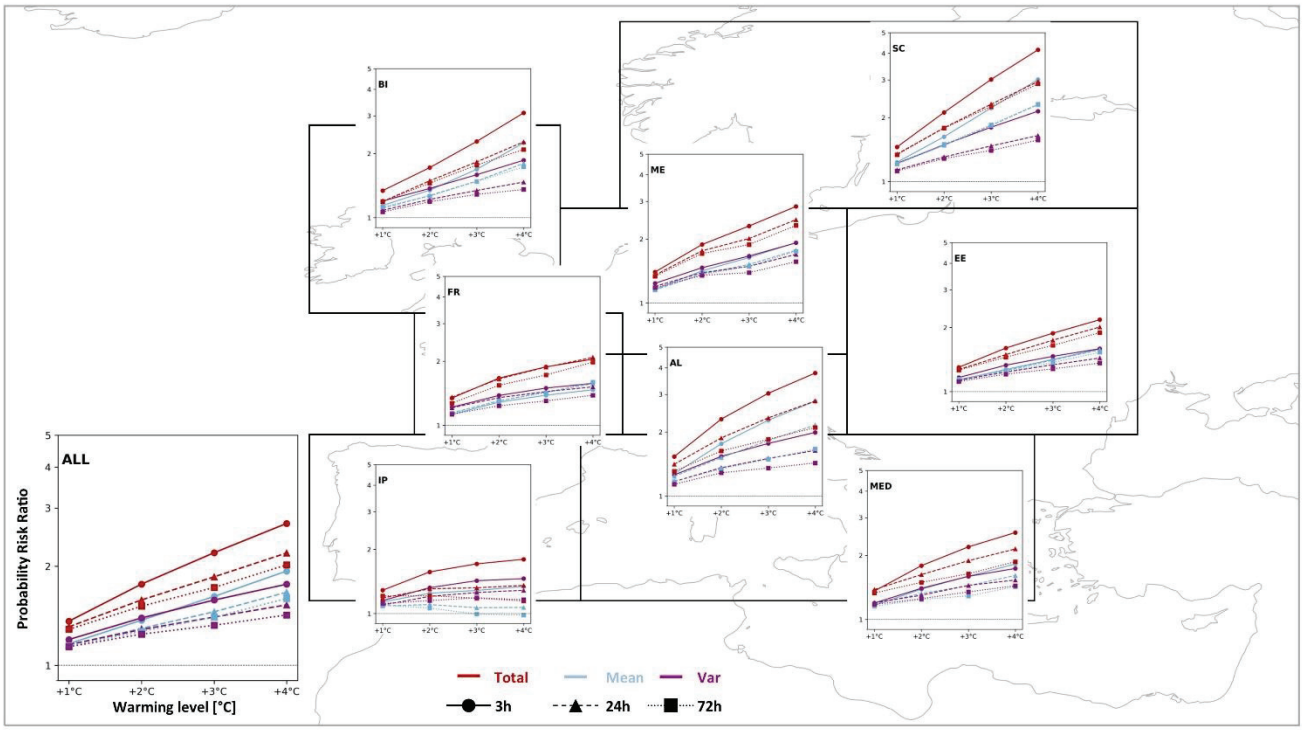

Figure 9: Regional probability risk ratios for different temporal aggregation levels (3h, 24h, 72h) on annual scales. The panels show PRtotal (red), PRmean (blue), and PRvar (purple) values (y-axis) at warming levels (+1, +2, +3, +4 °C) (x-axis). The solid lines with the circle marker represent PR-values for 3-hour temporal aggregation (same as in Figure 4); the dashed lines with the triangle marker represent PR-values for 24-hours; the dotted lines with the square marker represent PR-values for 72-hours. The lower left panel shows the aggregation over all land grid cells and shows axis labels.

The level of temporal aggregation has however only a very marginal influence on the ratio of contribution and the main takeaways from the previous sections remain true. Only in the Iberian Peninsula the influence of the variability considerably gains in importance. This is caused by a decrease in the PRmean in the 24-hour and 72-hour extremes. In the 3-hour data all PRtotal, PRmean, and PRvar show an increase, while in the 24h and 72h the PRmean shows a downward trend and in the 72h even a decrease in the PRmean from +3°C warming on. In comparison, the PRvar continues to increase in the 24h and increases then decreases in the 72h data.

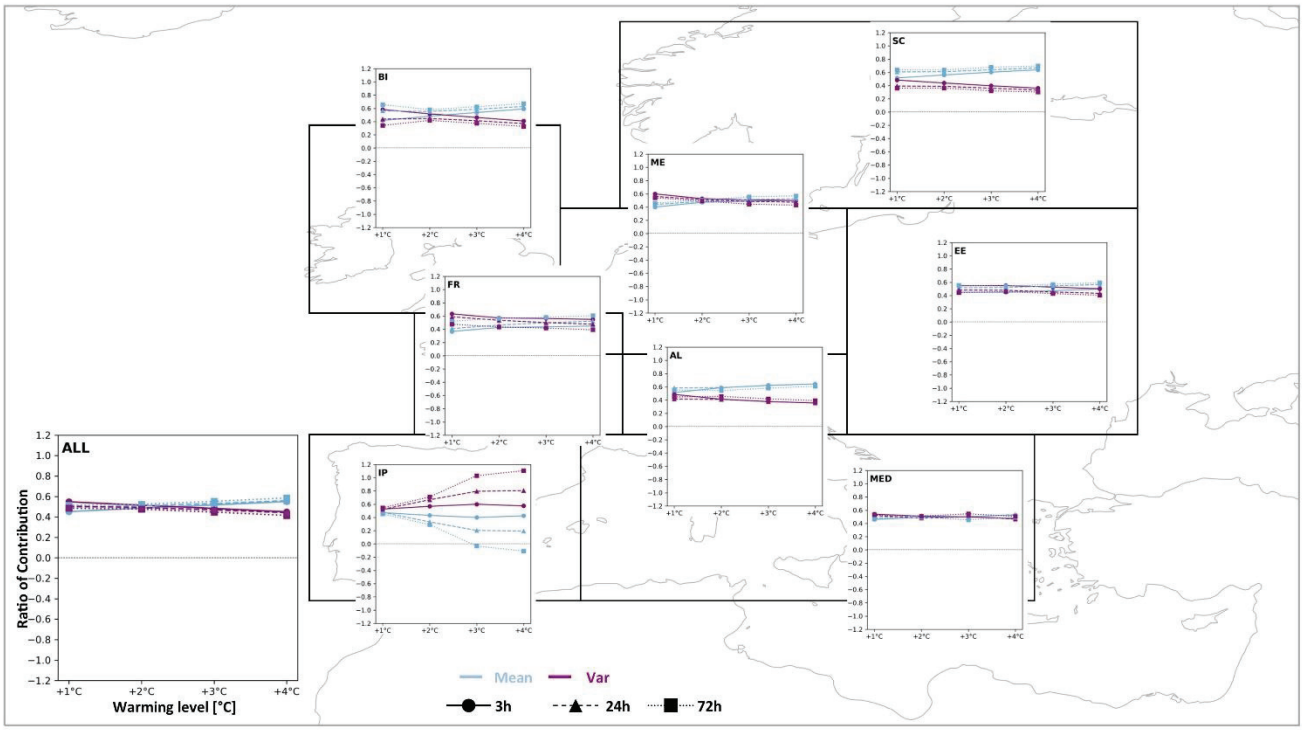

Figure 10: Regional ratios of contribution based on different levels of temporal aggregation (3h, 24h, and 72h) for annual maxima. Ratio of contributions from PR-values in Figure 9. Contribution from the mean in blue and contributions from variability in purple. Ratio of contribution on the y-axis with different warming levels on the x-axis (+1, +2, +3, +4 °C). The solid lines with the circle marker represent individual contributions for 3-hour temporal aggregation (same as in Figure 5); the dashed lines with the triangle marker represent contributions for 24-hours; the dotted lines with the square marker represent contributions for 72-hours. The lower left panel shows the aggregation over all land grid cells and shows axis labels.

Winter shows generally the same influence of temporal aggregation as seen on the annual scales. The PR-values are generally lower in the longer durations then in the subdaily extremes (Figure S2). In the British-Isles, Mid-Europe, Eastern Europe and over all land areas the three aggregation levels produce very similar PR-values throughout. Only in Scandinavia the longer durations show considerably higher PR-values then on the subdaily scale (PRtotal for 3h: 3.3, 24h: 4.2, 72h: 4.4). Over the Alps (PRtotal, 3h: 5.6, 24h: 3.6, 72h: 2.8) and the Iberian Peninsula (PRtotal, 3h: 2.9, 24h: 1.5, 72h: 1.3) the longer duration PR-values are markedly lower. Also, over France and the Mediterranean the PR-values are lower in the 24h and 72h data. However, these differences in the PR-values have only a low influence on the overall ratio of contributions which remain almost unaffected in the subregions of Scandinavia, Eastern Europe, the Alps, and the Mediterranean as well as aggregated over all land area (Figure S3). Over Mid-Europe the influence of the variability gains in importance for explaining the changes in the current (3h: ~0, 24/72h: ~0.3) and near-term future climate (3h: ~0.3, 24/72h: ~0.4). In the +3 and +4°C climates the ratios of contribution are near identical on all temporal aggregation levels. In the British-Isles the mean contributes more to the changes in the current climate in both the 24 and 72h data. In the future climates ratios are

similar across aggregation levels. In France, the variability in the 24-hours gains slightly in importance in the current climate compared to the 3-hours. In the 72h data the mean gains in importance in current climate and slightly in future climates. In the Iberian Peninsula the 3h and 24h ratios are near identical, but in the 72h data the variability loses in importance especially in the +4°C climate due to the decrease in PRvar towards no change (1) from a previous increase (>1).

However, in summer the ratio of contribution is markedly influenced by the level of temporal aggregation (Figure S5). Aggregated over all land area this results in the variability contributing by 0.7-0.76 in the 24h data and 0.74-0.87 in the 72h data compared to 0.56-0.66 in the 3h data. The gain in importance of the variability for changes in the probability of extremes with the level of aggregation can be seen in all regions. Differences due to the level of aggregation are less defined in the regions of Scandinavia and Mid-Europe, but very noticeable in France, the Alps, Eastern Europe, the Iberian Peninsula, and the Mediterranean. These differences in the ratio of contribution can be explained by the mean showing progressively decreasing PR-values (<1) or values closer to no-change with longer durations. The PRmean values of the 24h and 72h are markedly lower than for the 3h data, while the temporal aggregation produces less of a difference in the PRvar values (Figure S4). As a result, the importance of the variability for the future changes in extreme event probability increases with temporal aggregation in summer.

3.4 Influence of the level of extremeness

The level of extremeness (2-sigma or 3-sigma) does in general not change the overall conclusions of the importance of both the mean and variability for the total change in extreme events. The regions largely show the same order of importance by either the mean or variability. For example, regions where the mean contributes more to a change in event probability then the variability will also show this behaviour with a higher threshold for the event definition. However, the level of extremeness does in general increase the ratio of contribution for variability and respectively lowers the ratio of the mean. This increase in the ratio of contribution for variability is true for the annual scales (Figure S6) as well as the seasonal scales (Figure S7, S8). Further, this can also be shown for the different temporal aggregations (Figure S9, S10). On the seasonal scale the order of contribution is unchanged with the mean showing higher contributions in winter, and the variability showing higher contributions in summer. On the annual scales where the ratios of contribution are relatively similar anyway the increase in the ratio for variability can change the major contributor from mean to variability. In regions where the mean and variability contributed near equal (e.g., Mid-Europe, Mediterranean) the contributions from the variability remain above the mean with the 3-sigma threshold. Regions where the main contributor switched throughout continued warming from variability to mean (e.g., British-Isles, all land area) also show for the 3-sigma events that the contribution from variability remains larger than the mean, but the ratios converge to near equal in the +4°C world.

4 Discussion

In this study, only one regional large ensemble has been used which makes it difficult to evaluate the importance of model uncertainty on these results. Using multiple global SMILEs van der Wiel and Bintanja (2021) have shown that the model uncertainty seems to only play a minor role for the contributions of mean and variability to the extreme event occurrence. However, different models will influence the magnitude of the probability risk ratios. On the local scale different regional climate models can show different land-atmosphere feedbacks, due to a difference in model components or parameterization, which can influence the evolution of local precipitation extremes (e.g., Ritzhaupt and Maraun, 2023). Other regional SMILEs are necessary to analyse the impact of model uncertainty on the results. However, the availability of other regional SMILEs is limited. The only two other regional SMILES over Europe (to the knowledge of the author) differ in the extent of the domain (Aalbers et al., 2018) or the model resolution (Brönnimann et al., 2018; Addor and Fischer, 2015). von Trentini et al. (2020) have analyzed the three regional SMILEs and show that the three SMILEs reveal comparable changes in interannual variability of various climate indicators. Comparing projections for seasonal maximum precipitation in the 50-member CRCM5-LE (Wood and Ludwig, 2020) and the 16-member EC-Earth-RACMO ensemble (Aalbers et al., 2018) reveals very comparable forced changes in the mean magnitudes. This might indicate that the findings in van der Wiel and Bintanja (2021) of a small influence of model uncertainty on the ratio of contribution could potentially also be true for regional SMILEs.

Over the Mediterranean region, including the Iberian Peninsula, it has been shown that the magnitude of the drying trend especially for total summerly precipitation as well as mean extreme magnitudes can be model dependant, however there is a high model agreement on an overall drying (e.g., Ritzhaupt and Maraun, 2023; Zittis et al., 2021). However, it has also been shown that lower likelihood precipitation extremes still increase in the northern parts of the Mediterranean region (e.g., Zittis et al., 2021). Both, the reduction in mean climate characteristics while upper tails increase, fit the results shown in this study and strengthen the hypothesis that the increase in lower likelihood precipitation events is mainly driven by an increase in the variability. Most regional climate simulations place the French domain within a transitional zone between a drying signal of summerly precipitation in the south and a wetting in the north of Europe (e.g., Aalbers et al., 2018; Ritzhaupt and Maraun, 2023; Wood and Ludwig, 2020), largely showing no-change or a slight decrease in mean-state extremes, which is consistent with the results here. This means that any increase in the upper tails is dependent on the change in variability.

Scenario uncertainty could also have an influence. However, by using warming levels instead of fixed time periods and under the assumption that there is a physical basis for the connection of level of warming and climate system response, the scenario uncertainty can be reduced at least for the warming levels which are reachable by both lower and higher emission scenarios. To fully address the influence of scenario uncertainty on the presented results, a regional SMILE with multiple dynamically downscaled emission scenarios from the same global model would be necessary. Unfortunately, such a multi scenario regional SMILE ensemble does not exist.

Several studies have highlighted that convection permitting climate models (CPM) are better in representing precipitation extremes compared to regional climate models on non-convection resolving resolutions, especially in summer for convective events (e.g., Ban et al., 2014; Kendon et al., 2017; Pichelli et al., 2021). These studies are however often only a single model with a single short time slice simulation. Progress is being made on the availability of a multi-model CPM ensemble (Coppola et al., 2020; Pichelli et al., 2021). However, these simulations will only cover a small part of the Pan-European domain and will rely on short time slice simulations of single climate realizations. These single decadal climate realizations will however be strongly influenced by natural climate variability (Lehner et al., 2020; Leduc et al., 2019; Deser et al., 2012; Hawkins and Sutton, 2009). Poschlod (2021) has shown the suitability of the CRCM5-LE and highlights the added value of using a regional SMILE for the analysis of precipitation extremes even on non-convection permitting resolutions. Other studies have shown that the CRCM5-LE, even though convection is parameterized, can show a good representation of the timing of maximum annual precipitation (Wood and Ludwig, 2020), as well as good agreement for ten-year return levels of 3h-24h annual maxima with observations (Poschlod et al., 2021) over Europe. Concerning overall patterns of precipitation change in CPM compared to RCM ensembles, Pichelli et al. (2021) have shown that both ensembles are largely in agreement on the patterns of the change (over the Alps and northern Mediterranean) but that differences might occur in the magnitudes. This will likely entail that the magnitudes of the probability risk ratios will be different in the CPM models. However, this does not necessarily mean a change in the relation between the influences of the mean and variability. The level of temporal aggregations or the level of extremeness also influence the magnitudes of the PR-values, but do not necessarily entail a change in the ratios of contribution. Further, Kendon et al. (2017) have shown that CPM and RCM simulations agree on many aspects of the change in future precipitation projections.

5 Conclusion

In this study, climate simulations from the regional CRCM5 initial-condition large ensemble are used to analyse the general drivers for the change in extreme annual and seasonal precipitation event probability. The concept of the probability risk ratio is used to partition the change in extreme event occurrence into individual contributions from a change in mean climate and a change in variability. The results reveal that for the increase in event probability of annual maxima larger than 2-sigma, both the change in the mean and variability contribute near equally to the total change. For seasonal extremes in winter (DJF) the change in the mean is the major contributor to the total change. In summer the contribution from the change in variability is larger than the mean, and in some regions, variability is the sole driver of an increase in extreme event occurrence. Over France, the Iberian Peninsula, and the Mediterranean the change in variability can lead to an increase in extreme event probability despite a strong decline in extreme precipitation events as projected by the mean. The strong decrease in the mean would likely entail a decrease in the probability of extreme precipitation events, but due to an increase in variability the overall probability can still increase or remain at current levels. The level of extremeness in the event definition (2-sigma or 3-sigma) does in general not change the overall results of this study. Also, the level of temporal

aggregation is generally not changing the results. However, both do tend to increase the importance of the variability slightly.

Data availability

The CRCM5-LE data for the historical and RCP8.5 simulations are available through https://climex-data.srv.lrz.de/Public/. The CRCM5-LE pre-industrial control simulations are available upon reasonable request.

Author contribution

RRW designed the study concept, performed all analysis including visualization of results, and wrote the manuscript.

Competing interests

The author declares that there is no conflict of interest.

Acknowledgments

CRCM5 was developed by the ESCER Centre of Université du Québec à Montréal (UQAM) in collaboration with Environment and Climate Change Canada. We acknowledge Environment and Climate Change Canada's Canadian Centre for Climate Modelling and Analysis for executing and making available the CanESM2 Large Ensemble simulations used in this study, and the Canadian Sea Ice and Snow Evolution Network for proposing the simulations. Computations with CRCM5 for the ClimEx project were made on the SuperMUC supercomputer at the Leibniz Supercomputing Centre (LRZ) of the Bavarian Academy of Sciences and Humanities. The operation of this supercomputer is funded via the Gauss Centre for Supercomputing (GCS) by the German Federal Ministry of Education and Research and the Bavarian State Ministry of Education, Science and the Arts. The CRCM5-LE simulations used here were produced for the ClimEx project funded by the Bavarian State Ministry of the Environment and Consumer Protection (grant no. 81-0270-024570/2015).

References

Aalbers, E. E., Lenderink, G., van Meijgaard, E., and van den Hurk, B. J. J. M.: Local-scale changes in mean and heavy precipitation in Western Europe, climate change or internal variability?, Clim Dyn, 50, 4745–4766, https://doi.org/10.1007/s00382-017-3901-9, 2018.

Aalbers, E. E., van Meijgaard, E., Lenderink, G., Vries, H. de, and van den Hurk, B. J. J. M.: The 2018 west-central European drought projected in a warmer climate: how much drier can it get?, 2022.

Addor, N. and Fischer, E. M.: The influence of natural variability and interpolation errors on bias characterization in RCM simulations, J. Geophys. Res. Atmos., 120, https://doi.org/10.1002/2014JD022824, 2015.

Allen, M. R. and Ingram, W. J.: Constraints on future changes in climate and the hydrologic cycle, Nature, 419, 224–232, https://doi.org/10.1038/nature01092, 2002.

Arora, V. K., Scinocca, J. F., Boer, G. J., Christian, J. R., Denman, K. L., Flato, G. M., Kharin, V. V., Lee, W. G., and Merryfield, W. J.: Carbon emission limits required to satisfy future representative concentration pathways of greenhouse gases, Geophys Res Lett, 38, n/a-n/a, https://doi.org/10.1029/2010GL046270, 2011.

Bador, M. and Alexander, L. V.: Future Seasonal Changes in Extreme Precipitation Scale With Changes in the Mean, Earth's Future, 10, https://doi.org/10.1029/2022EF002979, 2022.

Ban, N., Schmidli, J., and Schär, C.: Evaluation of the convection-resolving regional climate modeling approach in decade-long simulations, J. Geophys. Res. Atmos., 119, 7889–7907, https://doi.org/10.1002/2014JD021478, 2014.

Bélair, S., Mailhot, J., Girard, C., and Vaillancourt, P.: Boundary Layer and Shallow Cumulus Clouds in a Medium-Range Forecast of a Large-Scale Weather System, Monthly Weather Review, 133, 1938–1960, https://doi.org/10.1175/MWR2958.1, 2005.

Bintanja, R. and Selten, F. M.: Future increases in Arctic precipitation linked to local evaporation and sea-ice retreat, Nature, 509, 479–482, https://doi.org/10.1038/nature13259, 2014.

Bintanja, R., van der Wiel, K., van der Linden, E. C., Reusen, J., Bogerd, L., Krikken, F., and Selten, F. M.: Strong future increases in Arctic precipitation variability linked to poleward moisture transport, Science advances, 6, eaax6869, https://doi.org/10.1126/sciadv.aax6869, 2020.

Böhnisch, A., Mittermeier, M., Leduc, M., and Ludwig, R.: Hot Spots and Climate Trends of Meteorological Droughts in Europe–Assessing the Percent of Normal Index in a Single-Model Initial-Condition Large Ensemble, Front. Water, 3, https://doi.org/10.3389/frwa.2021.716621, 2021.

Böhnisch, A., Ludwig, R., and Leduc, M.: Using a nested single-model large ensemble to assess the internal variability of the North Atlantic Oscillation and its climatic implications for central Europe, Earth Syst. Dynam., 11, 617–640, https://doi.org/10.5194/esd-11-617-2020, 2020.

Brogli, R., Kröner, N., Sørland, S. L., Lüthi, D., and Schär, C.: The Role of Hadley Circulation and Lapse-Rate Changes for the Future European Summer Climate, Journal of Climate, 32, 385–404, https://doi.org/10.1175/JCLI-D-18-0431.1, 2019.

Brönnimann, S., Rajczak, J., Fischer, E. M., Raible, C. C., Rohrer, M., and Schär, C.: Changing seasonality of moderate and extreme precipitation events in the Alps, Nat. Hazards Earth Syst. Sci., 18, 2047–2056, https://doi.org/10.5194/nhess-18-2047-2018, 2018.

Brunner, M. I., Swain, D. L., Wood, R. R., Willkofer, F., Done, J. M., Gilleland, E., and Ludwig, R.: An extremeness threshold determines the regional response of floods to changes in rainfall extremes, Commun Earth Environ, 2, https://doi.org/10.1038/s43247-021-00248-x, 2021.

Christensen, J. H., Larsen, M. A. D., Christensen, O. B., Drews, M., and Stendel, M.: Robustness of European climate projections from dynamical downscaling, Clim Dyn, 53, 4857–4869, https://doi.org/10.1007/s00382-019-04831-z, 2019.

Contractor, S., Donat, M. G., and Alexander, L. V.: Changes in Observed Daily Precipitation over Global Land Areas since 1950, J. Climate, 34, 3–19, https://doi.org/10.1175/JCLI-D-19-0965.1, 2021.

Coppola, E., Sobolowski, S., Pichelli, E., Raffaele, F., Ahrens, B., Anders, I., Ban, N., Bastin, S., Belda, M., Belusic, D., Caldas-Alvarez, A., Cardoso, R. M., Davolio, S., Dobler, A., Fernandez, J., Fita, L., Fumiere, Q., Giorgi, F., Goergen, K., Güttler, I., Halenka, T., Heinzeller, D., Hodnebrog, Ø., Jacob, D., Kartsios, S., Katragkou, E., Kendon, E., Khodayar, S., Kunstmann, H., Knist, S., Lavín-Gullón, A., Lind, P., Lorenz, T., Maraun, D., Marelle, L., van Meijgaard, E., Milovac, J., Myhre, G., Panitz, H.-J., Piazza, M., Raffa, M., Raub, T., Rockel, B., Schär, C., Sieck, K., Soares, P. M. M., Somot, S., Srnec, L., Stocchi, P., Tölle, M. H., Truhetz, H., Vautard, R., Vries, H. de, and Warrach-Sagi, K.: A first-of-its-kind multi-model convection permitting ensemble for investigating convective phenomena over Europe and the Mediterranean, Clim Dyn, 55, 3–34, https://doi.org/10.1007/s00382-018-4521-8, 2020.

Deser, C., Lehner, F., Rodgers, K. B., Ault, T., Delworth, T. L., DiNezio, P. N., Fiore, A., Frankignoul, C., Fyfe, J. C., Horton, D. E., Kay, J. E., Knutti, R., Lovenduski, N. S., Marotzke, J., McKinnon, K. A., Minobe, S., Randerson, J., Screen, J. A., Simpson, I. R., and Ting, M.: Insights from Earth system model initial-condition large ensembles and future prospects, Nature Clim Change, 10, 277–286, https://doi.org/10.1038/s41558-020-0731-2, 2020.

Deser, C., Phillips, A., Bourdette, V., and Teng, H.: Uncertainty in climate change projections: the role of internal variability, Clim Dyn, 38, 527–546, https://doi.org/10.1007/s00382-010-0977-x, 2012.

Donat, M. G., Lowry, A. L., Alexander, L. V., O'Gorman, P. A., and Maher, N.: More extreme precipitation in the world's dry and wet regions, Nature Clim Change, 6, 508–513, https://doi.org/10.1038/nclimate2941, 2016.

Fischer, E. M. and Knutti, R.: Observed heavy precipitation increase confirms theory and early models, Nature Clim Change, 6, 986–991, https://doi.org/10.1038/NCLIMATE3110, 2016.

Fowler, H. J., Lenderink, G., Prein, A. F., Westra, S., Allan, R. P., Ban, N., Barbero, R., Berg, P., Blenkinsop, S., Do, H. X., Guerreiro, S., Haerter, J. O., Kendon, E. J., Lewis, E., Schaer, C., Sharma, A., Villarini, G., Wasko, C., and Zhang, X.: Anthropogenic intensification of short-duration rainfall extremes, Nat Rev Earth Environ, 2, 107–122, https://doi.org/10.1038/s43017-020-00128-6, 2021.

Fyfe, J. C., Derksen, C., Mudryk, L., Flato, G. M., Santer, B. D., Swart, N. C., Molotch, N. P., Zhang, X., Wan, H., Arora, V. K., Scinocca, J., and Jiao, Y.: Large near-term projected snowpack loss over the western United States, Nature communications, 8, 14996, https://doi.org/10.1038/ncomms14996, 2017.

Guerreiro, S. B., Fowler, H. J., Barbero, R., Westra, S., Lenderink, G., Blenkinsop, S., Lewis, E., and Li, X.-F.: Detection of continental-scale intensification of hourly rainfall extremes, Nature Clim Change, 8, 803–807, https://doi.org/10.1038/s41558-018-0245-3, 2018.

Hawkins, E. and Sutton, R.: The Potential to Narrow Uncertainty in Regional Climate Predictions, Bull. Amer. Meteor. Soc., 90, 1095–1108, https://doi.org/10.1175/2009BAMS2607.1, 2009.

Held, I. M. and Soden, B. J.: Robust Responses of the Hydrological Cycle to Global Warming, Journal of Climate, 19, 5686–5699, https://doi.org/10.1175/JCLI3990.1, 2006.

Hodnebrog, Ø., Marelle, L., Alterskjær, K., Wood, R. R., Ludwig, R., Fischer, E. M., Richardson, T. B., Forster, P. M., Sillmann, J., and Myhre, G.: Intensification of summer precipitation with shorter time-scales in Europe, Environ. Res. Lett., 14, 124050, https://doi.org/10.1088/1748-9326/ab549c, 2019.

Innocenti, S., Mailhot, A., Frigon, A., Cannon, A. J., and Leduc, M.: Observed and Simulated Precipitation over Northeastern North America: How Do Daily and Subdaily Extremes Scale in Space and Time?, Journal of Climate, 32, 8563–8582, https://doi.org/10.1175/JCLI-D-19-0021.1, 2019.

Kain, J. S. and Fritsch, J. M.: A One-Dimensional Entraining/Detraining Plume Model and Its Application in Convective Parameterization, J. Atmos. Sci., 47, 2784–2802, https://doi.org/10.1175/1520-0469(1990)047<2784:AODEPM>2.0.CO;2, 1990.

Kelder, T., Wanders, N., van der Wiel, K., Marjoribanks, T. I., Slater, L. J., Wilby, R. l., and Prudhomme, C.: Interpreting extreme climate impacts from large ensemble simulations—are they unseen or unrealistic?, Environ. Res. Lett., 17, 44052, https://doi.org/10.1088/1748-9326/ac5cf4, 2022.

Kendon, E. J., Ban, N., Roberts, N. M., Fowler, H. J., Roberts, M. J., Chan, S. C., Evans, J. P., Fosser, G., and Wilkinson, J. M.: Do Convection-Permitting Regional Climate Models Improve Projections of Future Precipitation Change?, Bull. Amer. Meteor. Soc., 98, 79–93, https://doi.org/10.1175/BAMS-D-15-0004.1, 2017.

Kirchmeier-Young, M. C., Zwiers, F. W., and Gillett, N. P.: Attribution of Extreme Events in Arctic Sea Ice Extent, J. Climate, 30, 553–571, https://doi.org/10.1175/JCLI-D-16-0412.1, 2017.

Kirchmeier-Young, M. C., Gillett, N. P., Zwiers, F. W., Cannon, A. J., and Anslow, F. S.: Attribution of the Influence of Human-Induced Climate Change on an Extreme Fire Season, Earth's Future, 7, 2–10, https://doi.org/10.1029/2018EF001050, 2019a.

Kirchmeier-Young, M. C., Wan, H., Zhang, X., and Seneviratne, S. I.: Importance of Framing for Extreme Event Attribution: The Role of Spatial and Temporal Scales, Earth's Future, 7, 1192–1204, https://doi.org/10.1029/2019EF001253, 2019b.

Kreienkamp, F., Philip, S. Y., Tradowsky, J. S., Kew, S. F., Lorenz, P., Arrighi, J., Belleflamme, A., Bettmann, T., Caluwaerts, S., Chan, S. C., Ciavarella, A., Cruz, L. de, Vries, H. de, Demuth, N., Ferrone, A., Fischer, r. M., Fowler, H. J., Goergen, K., Heinrich, D., Henrichs, Y., Lenderink, G., Kaspar, F., Nilson, E., Otto, F. E. L., Ragone, F., Seneviratne, S. I., Singh, R. K., Skålevåg, A., Termonia, P., Thalheimer, L., van Aalst, M., van den Bergh, J., van de Vyver, H., Vannitsem, S., van Oldenborgh, G. J., van Schaeybroeck, B., Vautard, R., Vonk, D., and Wanders, N.: Rapid attribution of heavy rainfall events leading to the severe flooding in Western Europe during July 2021, available at: https://www.worldweatherattribution.org/heavy-rainfall-which-led-to-severe-flooding-in-western-europe-made-more-likely-by-climate-change/, last access: 25 February 2022, 2021.

Kröner, N., Kotlarski, S., Fischer, E., Lüthi, D., Zubler, E., and Schär, C.: Separating climate change signals into thermodynamic, lapse-rate and circulation effects: theory and application to the European summer climate, Clim Dyn, 48, 3425–3440, https://doi.org/10.1007/s00382-016-3276-3, 2017.

Kuo, H. L.: On Formation and Intensification of Tropical Cyclones Through Latent Heat Release by Cumulus Convection, J. Atmos. Sci., 22, 40–63, https://doi.org/10.1175/1520-0469(1965)022<0040:OFAIOT>2.0.CO;2, 1965.

Leduc, M., Mailhot, A., Frigon, A., Martel, J.-L., Ludwig, R., Brietzke, G. B., Giguère, M., Brissette, F., Turcotte, R., Braun, M., and Scinocca, J.: The ClimEx Project: A 50-Member Ensemble of Climate Change Projections at 12-km Resolution over Europe and Northeastern North America with the Canadian Regional Climate Model (CRCM5), Journal of Applied Meteorology and Climatology, 58, 663–693, https://doi.org/10.1175/JAMC-D-18-0021.1, 2019.

Lehner, F., Deser, C., Maher, N., Marotzke, J., Fischer, E. M., Brunner, L., Knutti, R., and Hawkins, E.: Partitioning climate projection uncertainty with multiple large ensembles and CMIP5/6, Earth Syst. Dynam., 11, 491–508, https://doi.org/10.5194/esd-11-491-2020, 2020.

Lenderink, G., Barbero, R., Loriaux, J. M., and Fowler, H. J.: Super-Clausius–Clapeyron Scaling of Extreme Hourly Convective Precipitation and Its Relation to Large-Scale Atmospheric Conditions, J. Climate, 30, 6037–6052, https://doi.org/10.1175/JCLI-D-16-0808.1, 2017.

Lenderink, G. and van Meijgaard, E.: Increase in hourly precipitation extremes beyond expectations from temperature changes, Nature Geosci, 1, 511–514, https://doi.org/10.1038/ngeo262, 2008.

Maher, N., Matei, D., Milinski, S., and Marotzke, J.: ENSO Change in Climate Projections: Forced Response or Internal Variability?, Geophys Res Lett, 45, https://doi.org/10.1029/2018GL079764, 2018.

Maher, N., Milinski, S., and Ludwig, R.: Large ensemble climate model simulations: introduction, overview, and future prospects for utilising multiple types of large ensemble, Earth Syst. Dynam., 12, 401–418, https://doi.org/10.5194/esd-12-401-2021, 2021a.

Maher, N., Power, S. B., and Marotzke, J.: More accurate quantification of model-to-model agreement in externally forced climatic responses over the coming century, Nature communications, 12, 788, https://doi.org/10.1038/s41467-020-20635-w, 2021b.

Martel, J.-L., Brissette, F. P., Lucas-Picher, P., Troin, M., and Arsenault, R.: Climate Change and Rainfall Intensity–Duration–Frequency Curves: Overview of Science and Guidelines for Adaptation, J. Hydrol. Eng., 26, 3121001, https://doi.org/10.1061/(ASCE)HE.1943-5584.0002122, 2021.

Martel, J.-L., Mailhot, A., and Brissette, F.: Global and Regional Projected Changes in 100-yr Subdaily, Daily, and Multiday Precipitation Extremes Estimated from Three Large Ensembles of Climate Simulations, Journal of Climate, 33, 1089–1103, https://doi.org/10.1175/JCLI-D-18-0764.1, 2020.

Martynov, A., Laprise, R., Sushama, L., Winger, K., Šeparović, L., and Dugas, B.: Reanalysis-driven climate simulation over CORDEX North America domain using the Canadian Regional Climate Model, version 5: model performance evaluation, Clim Dyn, 41, 2973–3005, https://doi.org/10.1007/s00382-013-1778-9, 2013.

Matte, D., Larsen, M. A. D., Christensen, O. B., and Christensen, J. H.: Robustness and Scalability of Regional Climate Projections Over Europe, Front. Environ. Sci., 6, https://doi.org/10.3389/fenvs.2018.00163, 2019.

McKenna, C. M. and Maycock, A. C.: Sources of Uncertainty in Multimodel Large Ensemble Projections of the Winter North Atlantic Oscillation, Geophys Res Lett, 48, https://doi.org/10.1029/2021GL093258, 2021.

Meinshausen, M., Smith, S. J., Calvin, K., Daniel, J. S., Kainuma, M. L. T., Lamarque, J.-F., Matsumoto, K., Montzka, S. A., Raper, S. C. B., Riahi, K., Thomson, A., Velders, G. J. M., and van Vuuren, D. P.: The RCP greenhouse gas concentrations and their extensions from 1765 to 2300, Climatic Change, 109, 213–241, https://doi.org/10.1007/s10584-011-0156-z, 2011.

Mittermeier, M., Weigert, M., Rügamer, D., Küchenhoff, H., and Ludwig, R.: A deep learning based classification of atmospheric circulation types over Europe: projection of future changes in a CMIP6 large ensemble, Environ. Res. Lett., 17, 84021, https://doi.org/10.1088/1748-9326/ac8068, 2022.

Mittermeier, M., Braun, M., Hofstätter, M., Wang, Y., and Ludwig, R.: Detecting Climate Change Effects on Vb Cyclones in a 50-Member Single-Model Ensemble Using Machine Learning, Geophys Res Lett, 46, 14653–14661, https://doi.org/10.1029/2019GL084969, 2019.

Myhre, G., Alterskjær, K., Stjern, C. W., Hodnebrog, Ø., Marelle, L., Samset, B. H., Sillmann, J., Schaller, N., Fischer, E., Schulz, M., and Stohl, A.: Frequency of extreme precipitation increases extensively with event rareness under global warming, Scientific reports, 9, 16063, https://doi.org/10.1038/s41598-019-52277-4, 2019.

Norris, J., Chen, G., and Neelin, J. D.: Thermodynamic versus Dynamic Controls on Extreme Precipitation in a Warming Climate from the Community Earth System Model Large Ensemble, J. Climate, 32, 1025–1045, https://doi.org/10.1175/JCLI-D-18-0302.1, 2019.

O'Gorman, P. A. and Schneider, T.: Scaling of Precipitation Extremes over a Wide Range of Climates Simulated with an Idealized GCM, J. Climate, 22, 5676–5685, https://doi.org/10.1175/2009JCLI2701.1, 2009.

Otto, F. E. L., van der Wiel, K., van Oldenborgh, G. J., Philip, S., Kew, S. F., Uhe, P., and Cullen, H.: Climate change increases the probability of heavy rains in Northern England/Southern Scotland like those of storm Desmond—a real-time event attribution revisited, Environ. Res. Lett., 13, 24006, https://doi.org/10.1088/1748-9326/aa9663, 2018a.

Otto, F. E. L., Philip, S., Kew, S., Li, S., King, A., and Cullen, H.: Attributing high-impact extreme events across timescales—a case study of four different types of events, Climatic Change, 149, 399–412, https://doi.org/10.1007/s10584-018-2258-3, 2018b.

Pendergrass, A. G., Knutti, R., Lehner, F., Deser, C., and Sanderson, B. M.: Precipitation variability increases in a warmer climate, Scientific reports, 7, 17966, https://doi.org/10.1038/s41598-017-17966-y, 2017.

Pfahl, S., O'Gorman, P. A., and Fischer, E. M.: Understanding the regional pattern of projected future changes in extreme precipitation, Nature Clim Change, 7, 423–427, https://doi.org/10.1038/nclimate3287, 2017.

Philip, S. Y., Kew, S. F., van Oldenborgh, G. J., Anslow, F. S., Seneviratne, S. I., Vautard, R., Coumou, D., Ebi, K. L., Arrighi, J., Singh, R., van Aalst, M., Pereira Marghidan, C., Wehner, M., Yang, W., Li, S., Schumacher, D. L., Hauser,

M., Bonnet, R., Luu, L. N., Lehner, F., Gillett, N., Tradowsky, J., Vecchi, G. A., Rodell, C., Stull, R. B., Howard, R., and Otto, F. E. L.: Rapid attribution analysis of the extraordinary heatwave on the Pacific Coast of the US and Canada June 2021, 2021.

Pichelli, E., Coppola, E., Sobolowski, S., Ban, N., Giorgi, F., Stocchi, P., Alias, A., Belušić, D., Berthou, S., Caillaud, C., Cardoso, R. M., Chan, S., Christensen, O. B., Dobler, A., Vries, H. de, Goergen, K., Kendon, E. J., Keuler, K., Lenderink, G., Lorenz, T., Mishra, A. N., Panitz, H.-J., Schär, C., Soares, P. M. M., Truhetz, H., and Vergara-Temprado, J.: The first multi-model ensemble of regional climate simulations at kilometer-scale resolution part 2: historical and future simulations of precipitation, Clim Dyn, 56, 3581–3602, https://doi.org/10.1007/s00382-021-05657-4, 2021.

Poschlod, B.: Using high-resolution regional climate models to estimate return levels of daily extreme precipitation over Bavaria, Nat. Hazards Earth Syst. Sci., 21, 3573–3598, https://doi.org/10.5194/nhess-21-3573-2021, 2021.

Poschlod, B. and Ludwig, R.: Internal variability and temperature scaling of future sub-daily rainfall return levels over Europe, Environ. Res. Lett., 16, 64097, https://doi.org/10.1088/1748-9326/ac0849, 2021.

Poschlod, B., Ludwig, R., and Sillmann, J.: Ten-year return levels of sub-daily extreme precipitation over Europe, Earth Syst. Sci. Data, 13, 983–1003, https://doi.org/10.5194/essd-13-983-2021, 2021.

Prein, A. F., Gobiet, A., Truhetz, H., Keuler, K., Goergen, K., Teichmann, C., Fox Maule, C., van Meijgaard, E., Déqué, M., Nikulin, G., Vautard, R., Colette, A., Kjellström, E., and Jacob, D.: Precipitation in the EURO-CORDEX 0.11° and 0.44° simulations: high resolution, high benefits?, Clim Dyn, 46, 383–412, https://doi.org/10.1007/s00382-015-2589-y, 2016.

Rajczak, J., Pall, P., and Schär, C.: Projections of extreme precipitation events in regional climate simulations for Europe and the Alpine Region, J. Geophys. Res. Atmos., 118, 3610–3626, https://doi.org/10.1002/jgrd.50297, 2013.

Rajczak, J. and Schär, C.: Projections of Future Precipitation Extremes Over Europe: A Multimodel Assessment of Climate Simulations, J. Geophys. Res. Atmos., 122, 10,773-10,800, https://doi.org/10.1002/2017JD027176, 2017.

Ritzhaupt, N. and Maraun, D.: Consistency of Seasonal Mean and Extreme Precipitation Projections Over Europe Across a Range of Climate Model Ensembles, J. Geophys. Res. Atmos., 128, https://doi.org/10.1029/2022JD037845, 2023.

Rutgersson, A., Kjellström, E., Haapala, J., Stendel, M., Danilovich, I., Drews, M., Jylhä, K., Kujala, P., Larsén, X. G., Halsnæs, K., Lehtonen, I., Luomaranta, A., Nilsson, E., Olsson, T., Särkkä, J., Tuomi, L., and Wasmund, N.: Natural hazards and extreme events in the Baltic Sea region, Earth Syst. Dynam., 13, 251–301, https://doi.org/10.5194/esd-13-251-2022, 2022.

Šeparović, L., Alexandru, A., Laprise, R., Martynov, A., Sushama, L., Winger, K., Tete, K., and Valin, M.: Present climate and climate change over North America as simulated by the fifth-generation Canadian regional climate model, Clim Dyn, 41, 3167–3201, https://doi.org/10.1007/s00382-013-1737-5, 2013.

Sippel, S., Meinshausen, N., Fischer, E. M., Székely, E., and Knutti, R.: Climate change now detectable from any single day of weather at global scale, Nature Clim Change, 10, 35–41, https://doi.org/10.1038/s41558-019-0666-7, 2020.

Sippel, S., Zscheischler, J., Heimann, M., Lange, H., Mahecha, M. D., van Oldenborgh, G. J., Otto, F. E. L., and Reichstein, M.: Have precipitation extremes and annual totals been increasing in the world's dry regions over the last 60 years?, Hydrol. Earth Syst. Sci., 21, 441–458, https://doi.org/10.5194/hess-21-441-2017, 2017.

Suarez-Gutierrez, L., Müller, W. A., Li, C., and Marotzke, J.: Dynamical and thermodynamical drivers of variability in European summer heat extremes, Clim Dyn, 54, 4351–4366, https://doi.org/10.1007/s00382-020-05233-2, available at: https://link.springer.com/article/10.1007/s00382-020-05233-2#citeas, 2020.

Swain, D. L., Singh, D., Touma, D., and Diffenbaugh, N. S.: Attributing Extreme Events to Climate Change: A New Frontier in a Warming World, One Earth, 2, 522–527, https://doi.org/10.1016/j.oneear.2020.05.011, 2020.

Swain, D. L., Langenbrunner, B., Neelin, J. D., and Hall, A.: Increasing precipitation volatility in twenty-first-century California, Nature Clim Change, 8, 427–433, https://doi.org/10.1038/s41558-018-0140-y, 2018.

Thompson, V., Dunstone, N. J., Scaife, A. A., Smith, D. M., Slingo, J. M., Brown, S., and Belcher, S. E.: High risk of unprecedented UK rainfall in the current climate, Nature communications, 8, 107, https://doi.org/10.1038/s41467-017-00275-3, 2017.

van der Wiel, K., Wanders, N., Selten, F. M., and Bierkens, M. F. P.: Added Value of Large Ensemble Simulations for Assessing Extreme River Discharge in a 2 °C Warmer World, Geophys Res Lett, 46, 2093–2102, https://doi.org/10.1029/2019GL081967, 2019.

van der Wiel, K. and Bintanja, R.: Contribution of climatic changes in mean and variability to monthly temperature and precipitation extremes, Commun Earth Environ, 2, https://doi.org/10.1038/s43247-020-00077-4, 2021.

van der Wiel, K., Batelaan, T. J., and Wanders, N.: Large increases of multi-year droughts in north-western Europe in a warmer climate, Clim Dyn, https://doi.org/10.1007/s00382-022-06373-3, 2022.

von Trentini, F., Aalbers, E. E., Fischer, E. M., and Ludwig, R.: Comparing interannual variability in three regional single-model initial-condition large ensembles (SMILEs) over Europe, Earth Syst. Dynam., 11, 1013–1031, https://doi.org/10.5194/esd-11-1013-2020, 2020.

Vries, H. de, Lenderink, G., van der Wiel, K., and van Meijgaard, E.: Quantifying the role of the large-scale circulation on European summer precipitation change, Clim Dyn, 59, 2871–2886, https://doi.org/10.1007/s00382-022-06250-z, 2022.

Westra, S., Fowler, H. J., Evans, J. P., Alexander, L. V., Berg, P., Johnson, F., Kendon, E. J., Lenderink, G., and Roberts, N. M.: Future changes to the intensity and frequency of short-duration extreme rainfall, Rev. Geophys., 52, 522–555, https://doi.org/10.1002/2014RG000464, 2014.

Westra, S., Alexander, L. V., and Zwiers, F. W.: Global Increasing Trends in Annual Maximum Daily Precipitation, Journal of Climate, 26, 3904–3918, https://doi.org/10.1175/JCLI-D-12-00502.1, 2013.

Wood, R. R. and Ludwig, R.: Analyzing Internal Variability and Forced Response of Subdaily and Daily Extreme Precipitation Over Europe, Geophys. Res. Lett., 47, https://doi.org/10.1029/2020GL089300, 2020.

Wood, R. R., Lehner, F., Pendergrass, A. G., and Schlunegger, S.: Changes in precipitation variability across time scales in multiple global climate model large ensembles, Environ. Res. Lett., 16, 84022, https://doi.org/10.1088/1748-9326/ac10dd, 2021.

Zittis, G., Bruggeman, A., and Lelieveld, J.: Revisiting future extreme precipitation trends in the Mediterranean, Weather and Climate Extremes, 34, 100380, https://doi.org/10.1016/j.wace.2021.100380, 2021.

7 Conclusion

The three publications contribute to a better understanding of the global to local precipitation response to a changing climate. Multiple global SMILEs and one regional SMILE have been used to analyze precipitation in current and future climate conditions regarding changes in the mean, the variability, and the upper tail (i.e., extremes) of its distribution. By applying the SMILE framework, the intrinsic uncertainty of internal climate variability could implicitly be accounted for. In the following the key findings of the three publications with respect to the posed research questions and hypothesis are discussed.

In the *first publication* (Wood et al. 2021) seven global SMILEs from the multi-model large ensemble archive were used to analyze changes in interannual to decadal precipitation variability in a warming climate. It is the first paper to evaluate the SMILEs collectively regarding their representation of interannual precipitation variability compared to observed variability. The evaluation reveals a possible influence of the ensemble size on the representation of interannual variability. The main focus of the paper is the future change of precipitation variability on interannual to decadal timescales.

H1: *Precipitation variability is non-stationary and increases with rising global mean surface temperature on interannual to decadal timescales.*

The findings from Wood et al. (2021) confirm the hypothesis. The results show implicit evidence that precipitation variability is non-stationary and changing in response to rising global mean surface temperatures. Thereby, the changes on interannual to decadal timescales are markedly similar.

RQ1.1: (a) *Are SMILEs capable of capturing observed interannual variability? (b) Does the ensemble size influence the representation of variability?*

The evaluation of interannual precipitation variability generally reveals that the seven global SMILEs show a better representation of variability over the Northern compared to the Southern Hemisphere. Most SMILEs capture interannual variability well over North and Central America, Europe, and Western Russia. Over tropical regions model differences are apparent, especially over South America where some SMILEs show an overestimation of variability, while others show an underestimation. The intercomparison of evaluation results revealed a tendency of smaller ensemble sizes to underestimate interannual variability more widespread. To test this hypothesis, multiple artificial small (16-member) and medium (30-member) size ensembles were randomly sampled from the 100-member MPI large ensemble, to quantify the influence of the ensemble size on precipitation variability. The results indicate a possible ensemble size dependance over northern hemisphere mid- to high-latitudes, with

smaller ensembles showing an underestimation of variability. For the High Latitudes a large ensemble size of +40 members is recommended. An underestimation of variability over South America, East Asia, South-East Asia, and Northern Australia could partly be ensemble size dependent. Results over other regions, such as Africa, the Amazon, the Middle East, or India are likely not ensemble size dependent, but rather model dependent.

RQ1.2: *Is precipitation variability increasing with an increase in global surface temperature and are the changes in variability comparable on interannual to decadal timescales?*

The results from the multi-SMILE analysis show implicit evidence for an increase in precipitation variability on interannual to decadal timescales in response to a warming climate. The multi-SMILE average shows an increase in interannual variability globally by 4 % K^{-1} (percentage change per one degree of global surface temperature increase) and markedly similar rates for multiyear (3.7 % K^{-1}) and decadal variability (4 % K^{-1}). Over land, the increase in variability is slightly larger (4.5-4.7 % K^{-1}). Locally, increases can exceed the global scaling rates which will have considerable relevance for local adaptation plans. The increase in precipitation variability is larger than the projected increase in mean-state precipitation (2.5 % K^{-1}) which implies that the changes are governed by different mechanisms.

RQ1.3: *Are changes in precipitation variability robust across SMILEs and if not where are the areas with high structural uncertainty?*

In this publication the robustness of results is determined where five out of six SMILEs agree on the sign of change. Areas that do not meet this definition are considered to have high structural (i.e., model) uncertainty. Changes in interannual precipitation variability are robust in 75 percent of gridcells globally with slightly higher agreement over land than over ocean. The model agreement is also high for decadal variability with 66 percent of all gridcells showing agreement on the sign. Over the mid- to high latitudes the model agreement is even higher showing agreement in 80-100 percent of gridcells. SMILES generally disagree over the land area of Central and South America, the Sahel Region, the Middle East, and Australia. As well as over the tropical Atlantic Ocean, the Southern Indian Ocean, and parts of the sub-tropical Pacific. These areas are dominated by large model uncertainty.

What is the broader impact of these results?

On the scientific side this work has contributed to the large ensemble community by evaluating interannual precipitation variability in a suite of multiple SMILEs from the multi-model large ensemble archive and adding new insights for the discussion of 'how large must a large ensemble be?'. Further, this work confirms and extends previous studies delivering implicit evidence that precipitation variability is increasing with global warming and where

this change is robust across models. For society an increase in precipitation variability implies an increase in precipitation volatility with an enhanced risk of swings between dry and wet conditions. Society is adapted to current levels of variability and any changes will likely pose severe challenges for local communities that rely on precipitation as a primary water source.

In the *second publication* (Wood and Ludwig 2020), a single regional SMILE, the CRCM5-LE, was used to analyze future changes in seasonal and annual maximum precipitation over Europe. Alongside the forced changes in the magnitude of maximum precipitation, the change in the internal variability was analyzed to determine the time-of-emergence when the forced signal robustly emerges from the uncertainty of internal climate variability.

H2: *The magnitude of heavy precipitation is increasing over Europe in a warming climate with changes emerging from internal variability.*

The findings from Wood and Ludwig (2020) can partly confirm the hypothesis. On the annual scale the hypothesis can be confirmed. Annual maximum precipitation is increasing in magnitude throughout Europe with changes emerging from internal variability. However, on seasonal scales the forced changes show a strong seasonal contrast between winter (widespread increase) and summer (widespread decrease). This means in summer the hypothesis needs to be rejected in many parts of Europe.

RQ2.1: *(a) Is seasonal and annual maximum precipitation changing over Europe? (b) Is the magnitude of change dependent on the season and temporal aggregation?*

Annual maximum precipitation is increasing throughout Europe showing generally higher increases on subdaily (3h) than on daily (1d, 5d) temporal scales. On seasonal scales, there is a noticeable difference between changes in summer and all other seasons. There is generally a widespread increase in the maximum precipitation in all seasons besides summer. In summer, there is an apparent north-south gradient of increases in Northern Europe including the British Isles, and continuously decreasing trends moving south. Thereby, the transition zone moves further north with increasing temporal aggregation. In subdaily (3h) and daily (1d) extremes, Central Europe shows summerly increases, while for multi-day extremes (5d) there is no significant change. Over France, South-Eastern Europe, and the Mediterranean region there is however a large difference between a decrease in summer and an increase in winter (and other seasons).

RQ2.2: *Do the changes in seasonal and annual extremes follow the Clausius-Clapeyron scaling?*

The climate simulations show widespread scaling rates of subdaily and daily extremes above the Clausius-Clapeyron (CC) scaling (~7% per 1°C of warming) over mainly Northern, Eastern and South-Eastern Europe. Locally scaling rates above CC are also possible in other regions.

Scaling rates above CC are however dependent on the season and temporal aggregation. Generally, subdaily extremes show larger areas with above CC-scaling and overall scaling rates than daily extremes. Northern Europe show above CC-scaling throughout all seasons while other regions mainly show above CC-scaling for winter (DJF) and spring (MAM). Extremes scaling near and above CC indicate a strong role of the thermodynamic component in explaining the increase in magnitude. Areas with low or negative scaling rates indicate that changes are partly or mainly driven by other effects than thermodynamics (i.e., dynamic changes). Looking at the Bowen Ratio indicates that the local moisture availability might be limiting the thermodynamic component in these regions. The Bowen Ratio determines the relationship between the sensible and latent heat flux. The change in the relationship between the two fluxes indicates a shift towards a stronger sensible heat flux and reduced latent heat flux, which means a lack of moisture from the surface and indicates an increase in aridity. The preceding season already shows a decrease in mean precipitation which can amplify the lack of moisture. Over Central, Northern, and Eastern Europe, as well as the British Isles, the Bowen ratio indicates continued sufficient local moisture content in summer which correlates with positive scaling rates near or above CC.

RQ2.3: *When can we expect changes in extreme precipitation to robustly emerge from internal variability?*

Robust emergence of the forced change from internal variability is determined by the signal-to-noise ratio exceeding and remaining above one standard-deviation. In this analysis the internal variability (i.e., noise) is defined as the standard-deviation of the individual trends from all 50 member, and the forced response (i.e., signal) is the mean of all 50 trends. In most regions the time-of-emergence is reached before or by the middle of the 21st century. Generally, subdaily extremes emerge earlier than daily extremes, as well as extremes in winter compared to other seasons. However, the results show that internal variability can remain an important source of uncertainty throughout the end of the century.

What is the broader impact of these results?

This work has further strengthened the theory that subdaily extremes change at faster rates than daily extremes. It further contributes to a growing literature of research indicating local and regional scaling rates above Clausius-Clapeyron. The strong increase in subdaily precipitation extremes calls for an enhanced adaptation planning in urban areas. Especially new infrastructure projects should include climate information into the planning and dimensioning. In urban areas or areas with low permeability, a strong increase in the total precipitation sums of subdaily extremes can potentially cause local flash flooding. This work

further highlights that the uncertainty of internal variability can be large on regional scales even far into the future.

In the publications one and two, it has been established that precipitation variability in general as well as the variability of seasonal/annual maximum precipitation, and mean maximum precipitation is changing. This means that all these individual changes will likely influence the probability of extreme precipitation events occurring and will likely contribute to the change thereof. Therefore, the third publication (Wood 2023) explores the individual contributions from changes in the mean and variability to changes in the total change in extreme precipitation event probability. The analysis is based on climate simulations from the same regional SMILE (CRCM5-LE) used in the second publication as well as data from its driving global SMILE (CanESM2-LE), which was used in the first publication.

H3: *Changes in the probability of extreme precipitation events are governed by changes in both the mean and variability.*

This hypothesis can be confirmed. Changes in the mean and variability collectively contribute to a change in the extreme event probability. The individual contributions from either the mean or variability can thereby jointly contribute to an amplification of event probability or counteract each other.

RQ3.1: *(a) Do current climate projections over Europe already show an increase in the probability of extreme precipitation events? (b) Will the risk of extreme precipitation events continue to increase in future climates?*

The results reveal that current climate simulations (i.e., climate simulations at +1°C of global warming) already show an increase in the total probability risk ratio by 1.36 over all land area in Europe compared to pre-industrial climate simulations. A probability risk ratio above one indicates an increase in the risk of annual 3-hourly extreme precipitation events occurring or in other words that the frequency of such events has increased. Thereby, the increase in the total probability risk ratio is influenced by both the change in the mean and variability. In this study, extreme events are defined as annual extremes greater than two standard deviations (i.e., 2-sigma). An additional warming until +2°C will further increase the total probability risk ratio to 1.77. In a +2°C warmer world, roughly 29 percent of all land area in Europe will already show a doubling of 2-sigma extreme events. With continued warming the probability risk ratio will further increase. By +4°C of warming already 69 percent of land grid cells are likely to show at least a doubling of the probability risk ratio with a European average of 2.7 over land. In winter the increase is generally larger than on the annual scale. In summer patterns are more complex with regions showing increases, decreases, and no-change in extremes. However, despite a strong decrease of the mean in some regions, such as France, the Iberian

Peninsula, the Mediterranean, or South-East Europe, the total risk ratio continues to increase due to changes in variability.

RQ3.2: *(a) What are the individual contributions from changes in the mean and variability to the total change in probability risk ratio? (b) Are the individual contributions dependent on the season, level of aggregation, or level of extremeness?*

On annual scales the change in the mean and variability both contribute approximately equal to an increase in the total risk ratio. In winter the change in the mean dominates the increase in extreme events by attributing for roughly three-quarters of the total change. In summer, the relation is opposite (i.e., variability > mean) and variability accounts for up-to two-thirds of the change. In regions that show a strong decline in the mean, such as France, the Iberian Peninsula, the Mediterranean, and South-Eastern Europe, the change in variability can be the sole driver of the increase in extreme events. These results have also been tested for different temporal aggregation levels (i.e., 24-hours, 72-hours). On the annual scale and in winter the level of temporal aggregation has only a minor influence. In summer the level of contribution from variability increases with the level of temporal aggregation. This can be explained by the stronger and more widespread decrease in mean maximum precipitation in summer at longer timescales, while the variability continues to increase in summer. The results have also been tested for a different level of extremeness (3-sigma compared to 2-sigma) and it can be stated that the overall conclusions of the importance of both the mean and variability for the total change in extreme events does not change. In some cases, the change in variability gains in importance.

What is the broader impact of these results?

The fact that the number of extreme events can continue to increase, due to the presence and increase of precipitation variability, while the average extreme declines is an important information for the communication of climate risk at regional and local scales. The large contribution from the change in the mean extremes in winter means that if we can explain the mechanisms for the change in the mean extremes, we can also largely explain the increase in extreme events in winter. However, in summer we will need to understand the mechanisms in variability to fully explain the change in extremes. Hence, to better understand the change in seasonal and annual extreme event frequency the drivers of a change in extreme precipitation variability needs to be further explored.

8 Discussion and perspectives for future research

A commonly raised statement when precipitation extremes are analyzed in the context of GCM and RCM simulations is that convection permitting climate models (CPM) are better at representing precipitation extremes compared to non-convection resolving resolutions. This has been shown in numerous studies and is certainly true especially for convective events in summer (e.g., Pichelli et al. 2021; Ban et al. 2014; Kendon et al. 2017). Despite the increased precision in convective events, the currently available CPM simulations have the large drawback of mainly consisting of only a single climate realization for a short time slice, and mostly only covering a small part of the Pan-European domain. Which is a result of the very high computational cost of running and storing CPM simulations. There is progress being made on developing a multi-model CPM ensemble (Coppola et al. 2020; Pichelli et al. 2021) which however will only be based on decadal time slices as well. These single decadal climate realizations will likely be strongly influenced by large uncertainties from internal variability (Leduc et al. 2019; Lehner et al. 2020; Hawkins and Sutton 2009; Deser et al. 2012). Further, Giorgi (2019) argues that there is increased noise at CPM resolutions which requires an ensemble of climate simulations. Hence, regional SMILEs remain a valuable tool to study extremes on regional to local scales in the presence of large internal variability. A key question that needs to be answered is whether we truly require large ensembles of CPM simulations or whether we can infer the information of internal climate variability onto the CPM simulations from RCM SMILEs.

A possible way of bringing together the two existing modeling tools (i.e., large ensembles and CPM models) could be the event based dynamical downscaling of extreme events detected within the large ensemble by using a CPM model (e.g., Huang et al. 2020). Going even a step further, this could potentially be extended by using the ensemble boosting approach (Gessner et al. 2021, 2022). In ensemble boosting regular SMILEs are used to detect relevant extreme events, for which then additional ensemble runs are re-initialized at certain lead times by adding small perturbations at the initialization to create a boosted ensemble (i.e., even larger ensemble) of possible realizations of the same extreme event. This approach could potentially also be implemented on the CPM scale. Here higher resolution GCM large ensembles or RCM large ensembles could be used to detect high impact low likelihood events on the coarser scale and only run the CPM model for the selected extreme events from the large ensembles. This way we could merge the benefits of both worlds and wouldn't require long transient CPM simulations.

Lastly, for the impact modeling community it has been challenging to use SMILEs within the scope of the established modeling environments, due to the overwhelming amount of data

and computational requirements. Dynamic impact modeling requires intense post-processing work (i.e., bias correction and spatial downscaling) to deliver a higher level of detail needed on the local scale. In the case of physically and spatially explicit impact models this means long runtimes with a high computational cost. However, the emerging field of storylines (e.g., Sillmann et al. 2021; Shepherd et al. 2018) could open new opportunities for the impact modeling community. Thereby, physically consistent analogues of past events (e.g., the 2018 drought, van der Wiel et al. 2021) can be searched in SMILEs under future climate conditions (e.g., in a +2 or +3°C climate) to retrieve a limited set of extreme events which can then be processed and evaluated within the impact models. In such a setup, the benefits from the SMILE framework (i.e., robust quantification of extreme events) are retained while adding increased detail through the impact model and having the possibility to test adaptation strategies for such extreme events.

9 Scientific outreach

Besides the three papers directly connected to this dissertation I have contributed to multiple scientific papers related to the fields of climatology, hydrometeorology, and hydrology:

> M. I. Brunner, D. L. Swain, **R. R. Wood**, F. Willkofer, J. M. Done, E. Gilleland, R. Ludwig (2021): *An extremeness threshold determines the regional response of floods to changes in rainfall extremes*, Communications Earth & Environment 2(1):173, 10.1038/s43247-021-00248-x

In this paper, we analyzed how changes in extreme precipitation and changes in flood magnitude and frequency are connected. For Bavaria, we show that an increase in precipitation extremes is not directly inferring an increase in floods. We found that there exists an extremeness threshold for above which increased flood magnitude and frequency is driven by the increase in extreme precipitation, and below the threshold the flood response is modulated by land surface processes even though extreme precipitation is increasing. This partly reconciles the lack of trends in the observations.

> F. Willkofer, **R. R. Wood**, F. von Trentini, J. Weissmüller, B. Poschlod, R. Ludwig (2020): *A Holistic Modelling Approach for the Estimation of Return Levels of Peak Flows in Bavaria*, Water, 12 (9), https://doi.org/10.3390/w12092349

This paper proposes a new holistic modeling approach for hydrological impact studies. In most impact studies the impact model (i.e., hydrological model) is set up for each individual catchment with the goal of optimizing the parameter space for each individual location. However, this can result in many different parameter sets which might react differently to external changes. Hence, with a single global parameter set any changes in response to climate change should therefore be more comparable across catchments, since differences should only rely on the change in climate and not due to differences in the parameter set.

> B. Poschlod, J. Zscheischler, J. Sillmann, **R. R. Wood**, R. Ludwig (2020): *Climate change effects on hydrometeorological compound events over southern Norway*, Weather and Climate Extremes, Volume 28, 2020, https://doi.org/10.1016/j.wace.2020.100253

This paper highlights the use of the CRCM5 large ensemble to study compound climate events. The large ensemble framework allows for the analysis of rare multivariate compound climate extremes, due to its large sample size. Over Norway two compound events that can trigger flooding have been analyzed. Rain on snow events as well as heavy precipitation on saturated soils.

J. Leandro, K.-F. Chen, **R. R. Wood**, R. Ludwig (2020): *A scalable flood-resilience-index for measuring climate change adaptation: Munich city*, Water Research, 173, https://doi.org/10.1016/j.watres.2020.115502

In this paper, we used the CRCM5 large ensemble precipitation data to derive future changes to the intensity-duration frequency (IDF) curves of precipitation over Maxvorstadt (Munich). The future IDF curves were used to simulate future extreme precipitation events to study flood resilience in the urban area of Maxvorstadt.

Ø. Hodnebrog, L. Marelle, K. Alterskjær, **R. R. Wood**, R. Ludwig, E. M. Fischer, T. B. Richardson, P. M. Forster, J. Sillmann, G. Myhre (2019): *Intensification of summer precipitation with shorter timescales in Europe*, Environmental Research Letters, 14 (12), https://doi.org/10.1088/1748-9326/ab549c

In this paper, WRF simulations at convection-permitting scales over four different regions in Europe have been compared to a set of regional SMILEs alongside their driving SMILEs. Summerly extremes have been analyzed regarding the temperature scaling rates. Scaling rates close to Clausius-Clapeyron could be detected however no super-CC scaling due to the pronounced and robust summer drying over many regions.

B. Poschlod, Ø. Hodnebrog, **R. R. Wood**, K. Altersjær, R. Ludwig, G. Myhre, J. Sillmann (2018): *Comparison and Evaluation of Statistical Rainfall Disaggregation and High-Resolution Dynamical Downscaling over Complex Terrain*, Journal of Hydrometeorology, Vol. 19, No. 12, 2018, https://doi.org/10.1175/JHM-D-18-0132.1

Lastly, in this paper a statistical method for the rainfall disaggregation from daily to hourly timescales has been compared to the result of a convection-permitting model run and observations.

Acknowledgments

First and foremost, I would like to thank my doctor father Prof. Ralf Ludwig without whom I probably would never have pursued the path of science and a PhD. Thank you for all the encouragement and trust throughout the years. The many opportunities to visit workshops and conferences helped me to develop my professional network. I am grateful for the many years of funding which enabled me to grow as a scientist.

Secondly, I would like to thank my other supervisor, Prof. Flavio Lehner, for the guidance throughout the last years. Thank you for the opportunity to meet and interact with the colleagues at NCAR and ETH.

Further, I want to thank my working group, current or alumni, for the many years of fun interactions, Feierabendbier, discussions, and help throughout the years. Without the comradery and solidarity I would have suffered much more. I especially want to thank Fabi and Flo, whom I started my PhD with. And of course, I cannot forget Vera the heart and soul of our working group. I will miss our lunches and without your stockpile of sweets I wouldn't have survived my last years.

I also want to thank my SMILE colleagues (Nic, Seb, Andrea, and Flavio) for the great years of hosting the SMILE webinars and many AGU and EGU sessions. It was always something to look forward to even when project work and papers kept piling up.

My PhD and my scientific involvement in the SMILE community wouldn't have been possible without the ClimEx project. So, thank you ClimEx team (Bavarian and Québecois) for a great project and the scientific momentum that I have greatly profited from.

Lastly, I want to thank my friends and family.

References

Aalbers, Emma E.; Lenderink, Geert; van Meijgaard, Erik; van den Hurk, Bart J. J. M. (2018): Local-scale changes in mean and heavy precipitation in Western Europe, climate change or internal variability? In *Clim Dyn* 50 (11-12), pp. 4745–4766. DOI: 10.1007/s00382-017-3901-9.

Aalbers, Emma Elizabeth; van Meijgaard, Erik; Lenderink, Geert; Vries, Hylke de; van den Hurk, Bart J. J. M. (2022): The 2018 west-central European drought projected in a warmer climate: how much drier can it get? In *EGUsphere [preprint]*. DOI: 10.5194/egusphere-2022-954.

Addor, Nans; Fischer, Erich M. (2015): The influence of natural variability and interpolation errors on bias characterization in RCM simulations. In *J. Geophys. Res. Atmos.* 120 (19). DOI: 10.1002/2014JD022824.

Alexander, Lisa V.; Bador, Margot; Roca, Rémy; Contractor, Steefan; Donat, Markus G.; Nguyen, Phuong Loan (2020): Intercomparison of annual precipitation indices and extremes over global land areas from in situ, space-based and reanalysis products. In *Environ. Res. Lett.* 15 (5), p. 55002. DOI: 10.1088/1748-9326/ab79e2.

Allan, Richard P.; Barlow, Mathew; Byrne, Michael P.; Cherchi, Annalisa; Douville, Hervé; Fowler, Hayley J. et al. (2020): Advances in understanding large-scale responses of the water cycle to climate change. In *Annals of the New York Academy of Sciences* 1472 (1), pp. 49–75. DOI: 10.1111/nyas.14337.

Allen, Myles R.; Ingram, William J. (2002): Constraints on future changes in climate and the hydrologic cycle. In *Nature* 419 (6903), pp. 224–232. DOI: 10.1038/nature01092.

Ban, Nikolina; Schmidli, Juerg; Schär, Christoph (2014): Evaluation of the convection-resolving regional climate modeling approach in decade-long simulations. In *J. Geophys. Res. Atmos.* 119 (13), pp. 7889–7907. DOI: 10.1002/2014JD021478.

Berg, Peter; Christensen, Ole B.; Klehmet, Katharina; Lenderink, Geert; Olsson, Jonas; Teichmann, Claas; Yang, Wei (2019): Summertime precipitation extremes in a EURO-CORDEX 0.11° ensemble at an hourly resolution. In *Nat. Hazards Earth Syst. Sci.* 19 (4), pp. 957–971. DOI: 10.5194/nhess-19-957-2019.

Bevacqua, Emanuele; Zappa, Giuseppe; Lehner, Flavio; Zscheischler, Jakob (2022): Precipitation trends determine future occurrences of compound hot–dry events. In *Nature Clim Change* 12 (4), pp. 350–355. DOI: 10.1038/s41558-022-01309-5.

Bevacqua, Emanuele; Zappa, Giuseppe; Shepherd, Theodore G. (2020): Shorter cyclone clusters modulate changes in European wintertime precipitation extremes. In *Environ. Res. Lett.* 15 (12), p. 124005. DOI: 10.1088/1748-9326/abbde7.

Bintanja, R.; van der Wiel, K.; van der Linden, E. C.; Reusen, J.; Bogerd, L.; Krikken, F.; Selten, F. M. (2020): Strong future increases in Arctic precipitation variability linked to poleward moisture transport. In *Sci. Adv.* 6 (7), Article eaax6869. DOI: 10.1126/sciadv.aax6869.

Blauhut, Veit; Stoelzle, Michael; Ahopelto, Lauri; Brunner, Manuela I.; Teutschbein, Claudia; Wendt, Doris E. et al. (2022): Lessons from the 2018–2019 European droughts: a collective need for unifying drought risk management. In *Nat. Hazards Earth Syst. Sci.* 22 (6), pp. 2201–2217. DOI: 10.5194/nhess-22-2201-2022.

Böhnisch, Andrea; Ludwig, Ralf; Leduc, Martin (2020): Using a nested single-model large ensemble to assess the internal variability of the North Atlantic Oscillation and its climatic implications for central Europe. In *Earth Syst. Dynam.* 11 (3), pp. 617–640. DOI: 10.5194/esd-11-617-2020.

Böhnisch, Andrea; Mittermeier, Magdalena; Leduc, Martin; Ludwig, Ralf (2021): Hot Spots and Climate Trends of Meteorological Droughts in Europe–Assessing the Percent of Normal Index in a Single-Model Initial-Condition Large Ensemble. In *Front. Water* 3, Article 716621. DOI: 10.3389/frwa.2021.716621.

Brogli, Roman; Kröner, Nico; Sørland, Silje Lund; Lüthi, Daniel; Schär, Christoph (2019): The Role of Hadley Circulation and Lapse-Rate Changes for the Future European Summer Climate. In *Journal of Climate* 32 (2), pp. 385–404. DOI: 10.1175/JCLI-D-18-0431.1.

Brunner, Manuela I.; Swain, Daniel L.; Wood, Raul R.; Willkofer, Florian; Done, James M.; Gilleland, Eric; Ludwig, Ralf (2021): An extremeness threshold determines the regional response of floods to changes in rainfall extremes. In *Commun Earth Environ* 2 (1). DOI: 10.1038/s43247-021-00248-x.

Cammalleri, C.; Naumann, G.; Mentaschi, L.; Formetta, G.; Forzieri, G.; Gosling, S. et al. (2020): Global warming and drought impacts in the EU. JRC PESETA IV project : Task 7. Edited by Joint Research Centre (European Commission). Publications Office.

Chan, Steven C.; Kendon, Elizabeth J.; Fowler, Hayley J.; Kahraman, Abdullah; Crook, Julia; Ban, Nikolina; Prein, Andreas F. (2023): Large-scale dynamics moderate impact-relevant changes to organised convective storms. In *Commun Earth Environ* 4 (1). DOI: 10.1038/s43247-022-00669-2.

Collins, M.; Knutti, R.; Arblaster, J.; Dufresne, J.-L.; Fichefet, T.; Friedlingstein, P. et al. (2013): Long-term Climate Change: Projections, Commitments and Irreversibility. In T. F. Stocker, D. Qin, G.-K. Plattner, M. Tignor, S. K. Allen, J. Boschung et al. (Eds.): Climate Change 2013: The Physical Science Basis. Contribution of Working Group I to the Fifth Assessment Report of the Intergovernmental Panel on Climate Change. Cambridge, United Kingdom and New York, NY, USA: Cambridge University Press.

Contractor, Steefan; Donat, Markus G.; Alexander, Lisa V. (2021): Changes in Observed Daily Precipitation over Global Land Areas since 1950. In *J. Climate* 34 (1), pp. 3–19. DOI: 10.1175/JCLI-D-19-0965.1.

Contractor, Steefan; Donat, Markus G.; Alexander, Lisa V.; Ziese, Markus; Meyer-Christoffer, Anja; Schneider, Udo et al. (2020): Rainfall Estimates on a Gridded Network (REGEN) – a global land-based gridded dataset of daily precipitation from 1950 to 2016. In *Hydrol. Earth Syst. Sci.* 24 (2), pp. 919–943. DOI: 10.5194/hess-24-919-2020.

Copernicus Publications (Ed.) (2021): Earth System Dynamics. Available online at https://www.earth-system-dynamics.net/, checked on 12/29/2021.

Coppola, Erika; Sobolowski, Stefan; Pichelli, E.; Raffaele, F.; Ahrens, B.; Anders, I. et al. (2020): A first-of-its-kind multi-model convection permitting ensemble for investigating convective phenomena over Europe and the Mediterranean. In *Clim Dyn* 55 (1-2), pp. 3–34. DOI: 10.1007/s00382-018-4521-8.

Coumou, Dim; Lehmann, Jascha; Beckmann, Johanna (2015): Climate change. The weakening summer circulation in the Northern Hemisphere mid-latitudes. In *Science (New York, N.Y.)* 348 (6232), pp. 324–327. DOI: 10.1126/science.1261768.

Cubasch, U.; Wuebbles, D.; Chen, D.; Facchini, M. C.; Frame, D.; Mahowald, N. and Winther J.-G. (2013): Introduction. In T. F. Stocker, D. Qin, G.-K. Plattner, M. Tignor, S. K. Allen, J. Boschung et al. (Eds.): Climate Change 2013: The Physical Science Basis. Contribution of Working Group I to the Fifth Assessment Report of the Intergovernmental Panel on Climate Change. Cambridge, United Kingdom and New York, NY, USA: Cambridge University Press.

Deser, C.; Lehner, F.; Rodgers, K. B.; Ault, T.; Delworth, T. L.; DiNezio, P. N. et al. (2020): Insights from Earth system model initial-condition large ensembles and future prospects. In *Nature Clim Change* 10 (4), pp. 277–286. DOI: 10.1038/s41558-020-0731-2.

Deser, Clara; Phillips, Adam; Bourdette, Vincent; Teng, Haiyan (2012): Uncertainty in climate change projections: the role of internal variability. In *Clim Dyn* 38 (3-4), pp. 527–546. DOI: 10.1007/s00382-010-0977-x.

Deser, Clara; Terray, Laurent; Phillips, Adam S. (2016): Forced and Internal Components of Winter Air Temperature Trends over North America during the past 50 Years: Mechanisms and Implications*. In *Journal of Climate* 29 (6), pp. 2237–2258. DOI: 10.1175/JCLI-D-15-0304.1.

Di Chen; Norris, Jesse; Thackeray, Chad; Hall, Alex (2022): Increasing precipitation whiplash in climate change hotspots. In *Environ. Res. Lett.* 17 (12), p. 124011. DOI: 10.1088/1748-9326/aca3b9.

Di Luca, Alejandro; Argüeso, Daniel; Evans, Jason P.; Elía, Ramón; Laprise, René (2016): Quantifying the overall added value of dynamical downscaling and the contribution from different spatial scales. In *J. Geophys. Res. Atmos.* 121 (4), pp. 1575–1590. DOI: 10.1002/2015JD024009.

Di Virgilio, Giovanni; Evans, Jason P.; Di Luca, Alejandro; Grose, Michael R.; Round, Vanessa; Thatcher, Marcus (2020): Realised added value in dynamical downscaling of Australian climate change. In *Clim Dyn* 54 (11-12), pp. 4675–4692. DOI: 10.1007/s00382-020-05250-1.

Dickinson, RobertE.; Errico, RonaldM.; Giorgi, Filippo; Bates, GaryT. (1989): A regional climate model for the western United States. In *Climatic Change* 15 (3). DOI: 10.1007/BF00240465.

Douville, H.; Raghavan, K.; Renwick, J.; Allan, R. P.; Arias, P. A.; Barlow, M. et al. (2021): Water Cycle Changes. In V. Masson-Delmotte, P. Zhai, A. Pirani, S. L. Connors, C. Péan, S. Berger et al. (Eds.): Climate Change 2021: The Physical Science Basis. Contribution of Working Group I to the Sixth Assessment Report of the Intergovernmental Panel on Climate Change. Cambridge, United Kingdom and New York, NY, USA: Cambridge University Press.

DWD (2020): DWD Climate Data Center (CDC): Hourly station observations of precipitation amount in mm for Germany, version v19.3. German Weather Service (DWD), checked on 7/20/2020.

Endris, Hussen Seid; Omondi, Philip; Jain, Suman; Lennard, Christopher; Hewitson, Bruce; Chang'a, Ladislaus et al. (2013): Assessment of the Performance of CORDEX Regional Climate Models in Simulating East African Rainfall. In *J. Climate* 26 (21), pp. 8453–8475. DOI: 10.1175/JCLI-D-12-00708.1.

England, Mark R. (2021): Are Multi-Decadal Fluctuations in Arctic and Antarctic Surface Temperatures a Forced Response to Anthropogenic Emissions or Part of Internal Climate Variability? In *Geophys. Res. Lett.* 48 (6). DOI: 10.1029/2020GL090631.

Fischer, E. M.; Beyerle, U.; Knutti, R. (2013): Robust spatially aggregated projections of climate extremes. In *Nature Clim Change* 3 (12), pp. 1033–1038. DOI: 10.1038/nclimate2051.

Fischer, E. M.; Knutti, R. (2016): Observed heavy precipitation increase confirms theory and early models. In *Nature Clim Change* 6 (11), pp. 986–991. DOI: 10.1038/NCLIMATE3110.

Fowler, Hayley J.; Lenderink, Geert; Prein, Andreas F.; Westra, Seth; Allan, Richard P.; Ban, Nikolina et al. (2021): Anthropogenic intensification of short-duration rainfall extremes. In *Nat Rev Earth Environ* 2 (2), pp. 107–122. DOI: 10.1038/s43017-020-00128-6.

Frankcombe, Leela M.; England, Matthew H.; Kajtar, Jules B.; Mann, Michael E.; Steinman, Byron A. (2018): On the Choice of Ensemble Mean for Estimating the Forced Signal in the Presence of Internal Variability. In *J. Climate* 31 (14), pp. 5681–5693. DOI: 10.1175/JCLI-D-17-0662.1.

Frankcombe, Leela M.; England, Matthew H.; Mann, Michael E.; Steinman, Byron A. (2015): Separating Internal Variability from the Externally Forced Climate Response. In *J. Climate* 28 (20), pp. 8184–8202. DOI: 10.1175/JCLI-D-15-0069.1.

Freire-González, Jaume; Decker, Christopher; Hall, Jim W. (2017): The Economic Impacts of Droughts: A Framework for Analysis. In *Ecological Economics* 132, pp. 196–204. DOI: 10.1016/j.ecolecon.2016.11.005.

Fyfe, John C.; Derksen, Chris; Mudryk, Lawrence; Flato, Gregory M.; Santer, Benjamin D.; Swart, Neil C. et al. (2017): Large near-term projected snowpack loss over the western United States. In *Nature communications* 8, p. 14996. DOI: 10.1038/ncomms14996.

Gampe, David; Schmid, Josef; Ludwig, Ralf (2019): Impact of Reference Dataset Selection on RCM Evaluation, Bias Correction, and Resulting Climate Change Signals of Precipitation. In *Journal of Hydrometeorology* 20 (9), pp. 1813–1828. DOI: 10.1175/JHM-D-18-0108.1.

Gessner, Claudia; Fischer, Erich M.; Beyerle, Urs; Knutti, Reto (2021): Very rare heat extremes: quantifying and understanding using ensemble re-initialization. In *J. Climate*, pp. 1–46. DOI: 10.1175/JCLI-D-20-0916.1.

Gessner, Claudia; Fischer, Erich M.; Beyerle, Urs; Knutti, Reto (2022): Multi-year drought storylines for Europe and North America from an iteratively perturbed global climate model. In *Weather and Climate Extremes* 38, p. 100512. DOI: 10.1016/j.wace.2022.100512.

Gherardi, Laureano A.; Sala, Osvaldo E. (2019): Effect of interannual precipitation variability on dryland productivity: A global synthesis. In *Global change biology* 25 (1), pp. 269–276. DOI: 10.1111/gcb.14480.

Giorgi, Filippo (2019): Thirty Years of Regional Climate Modeling: Where Are We and Where Are We Going next? In *J. Geophys. Res. Atmos.* DOI: 10.1029/2018JD030094.

Giorgi, Filippo; Bates, Gary T. (1989): The Climatological Skill of a Regional Model over Complex Terrain. In *Mon. Wea. Rev.* 117 (11), pp. 2325–2347. DOI: 10.1175/1520-0493(1989)117%3C2325:TCSOAR%3E2.0.CO;2.

Giorgi, Filippo; Gutowski, William J. (2015): Regional Dynamical Downscaling and the CORDEX Initiative. In *Annu. Rev. Environ. Resour.* 40 (1), pp. 467–490. DOI: 10.1146/annurev-environ-102014-021217.

Giorgi, Filippo; Torma, Csaba; Coppola, Erika; Ban, Nikolina; Schär, Christoph; Somot, Samuel (2016): Enhanced summer convective rainfall at Alpine high elevations in response to climate warming. In *Nature Geosci* 9 (8), pp. 584–589. DOI: 10.1038/ngeo2761.

Guerreiro, Selma B.; Fowler, Hayley J.; Barbero, Renaud; Westra, Seth; Lenderink, Geert; Blenkinsop, Stephen et al. (2018): Detection of continental-scale intensification of hourly rainfall extremes. In *Nature Clim Change* 8 (9), pp. 803–807. DOI: 10.1038/s41558-018-0245-3.

Haarsma, Reindert J.; Roberts, Malcolm J.; Vidale, Pier Luigi; Senior, Catherine A.; Bellucci, Alessio; Bao, Qing et al. (2016): High Resolution Model Intercomparison Project (HighResMIP v1.0) for CMIP6. In *Geosci. Model Dev.* 9 (11), pp. 4185–4208. DOI: 10.5194/gmd-9-4185-2016.

Harvey, B. J.; Cook, P.; Shaffrey, L. C.; Schiemann, R. (2020): The Response of the Northern Hemisphere Storm Tracks and Jet Streams to Climate Change in the CMIP3, CMIP5, and CMIP6 Climate Models. In *J. Geophys. Res. Atmos.* 125 (23). DOI: 10.1029/2020JD032701.

Haszpra, Tímea; Herein, Mátyás; Bódai, Tamás (2020): Investigating ENSO and its teleconnections under climate change in an ensemble view – a new perspective. In *Earth Syst. Dynam.* 11 (1), pp. 267–280. DOI: 10.5194/esd-11-267-2020.

Hattermann, Fred F.; Wortmann, Michel; Liersch, Stefan; Toumi, Ralf; Sparks, Nathan; Genillard, Christopher et al. (2018): Simulation of flood hazard and risk in the Danube basin with the Future Danube Model. In *Climate Services* 12, pp. 14–26. DOI: 10.1016/j.cliser.2018.07.001.

Hawkins, Ed; Smith, Robin S.; Gregory, Jonathan M.; Stainforth, David A. (2016): Irreducible uncertainty in near-term climate projections. In *Clim Dyn* 46 (11-12), pp. 3807–3819. DOI: 10.1007/s00382-015-2806-8.

Hawkins, Ed; Sutton, Rowan (2009): The Potential to Narrow Uncertainty in Regional Climate Predictions. In *Bull. Amer. Meteor. Soc.* 90 (8), pp. 1095–1108. DOI: 10.1175/2009BAMS2607.1.

Hazeleger, Wilco; Severijns, Camiel; Semmler, Tido; Ştefănescu, Simona; Yang, Shuting; Wang, Xueli et al. (2010): EC-Earth. In *Bull. Amer. Meteor. Soc.* 91 (10), pp. 1357–1364. DOI: 10.1175/2010BAMS2877.1.

Hedemann, Christopher; Mauritsen, Thorsten; Jungclaus, Johann; Marotzke, Jochem (2017): The subtle origins of surface-warming hiatuses. In *Nature Clim Change* 7 (5), pp. 336–339. DOI: 10.1038/nclimate3274.

Heinze-Deml, Christina; Sippel, Sebastian; Pendergrass, Angeline G.; Lehner, Flavio; Meinshausen, Nicolai (2021): Latent Linear Adjustment Autoencoder v1.0: a novel method for estimating and emulating dynamic precipitation at high resolution. In *Geosci. Model Dev.* 14 (8), pp. 4977–4999. DOI: 10.5194/gmd-14-4977-2021.

Held, Isaac M.; Soden, Brian J. (2006): Robust Responses of the Hydrological Cycle to Global Warming. In *Journal of Climate* 19 (21), pp. 5686–5699. DOI: 10.1175/JCLI3990.1.

Huang, Xingying; Swain, Daniel L.; Hall, Alex D. (2020): Future precipitation increase from very high resolution ensemble downscaling of extreme atmospheric river storms in California. In *Sci. Adv.* 6 (29), eaba1323. DOI: 10.1126/sciadv.aba1323.

Hurrell, James W.; Deser, Clara (2010): North Atlantic climate variability: The role of the North Atlantic Oscillation. In *Journal of Marine Systems* 79 (3-4), pp. 231–244. DOI: 10.1016/j.jmarsys.2009.11.002.

IOP Publishing (Ed.) (2021): Environmental Research Letters. Available online at https://publishingsupport.iopscience.iop.org/journals/environmental-research-letters/about-environmental-research-letters/, checked on 12/29/2021.

Jacob, Daniela; Petersen, Juliane; Eggert, Bastian; Alias, Antoinette; Christensen, Ole Bøssing; Bouwer, Laurens M. et al. (2014): EURO-CORDEX: new high-resolution climate change projections for European impact research. In *Reg Environ Change* 14 (2), pp. 563–578. DOI: 10.1007/s10113-013-0499-2.

Jeffrey, S.; Rotstayn, L.; Collier, M.; Dravitzki, S.; Hamalainen, C.; Moeseneder, C. et al. (2013): Australia's CMIP5 submission using the CSIRO-Mk3.6 model. In *a* 63 (1), pp. 1–14. DOI: 10.22499/2.6301.001.

Kahraman, Abdullah; Kendon, Elizabeth J.; Chan, Steven C.; Fowler, Hayley J. (2021): Quasi-Stationary Intense Rainstorms Spread Across Europe Under Climate Change. In *Geophys Res Lett* 48 (13). DOI: 10.1029/2020GL092361.

Kay, J. E.; Deser, C.; Phillips, A.; Mai, A.; Hannay, C.; Strand, G. et al. (2015): The Community Earth System Model (CESM) Large Ensemble Project: A Community Resource for Studying Climate Change in the Presence of Internal Climate Variability. In *Bull. Amer. Meteor. Soc.* 96 (8), pp. 1333–1349. DOI: 10.1175/BAMS-D-13-00255.1.

Kendon, Elizabeth J.; Ban, Nikolina; Roberts, Nigel M.; Fowler, Hayley J.; Roberts, Malcolm J.; Chan, Steven C. et al. (2017): Do Convection-Permitting Regional Climate Models Improve Projections of Future Precipitation Change? In *Bull. Amer. Meteor. Soc.* 98 (1), pp. 79–93. DOI: 10.1175/BAMS-D-15-0004.1.

Kharin, V. V.; Flato, G. M.; Zhang, X.; Gillett, N. P.; Zwiers, F.; Anderson, K. J. (2018): Risks from Climate Extremes Change Differently from 1.5°C to 2.0°C Depending on Rarity. In *Earth's Future* 6 (5), pp. 704–715. DOI: 10.1002/2018EF000813.

Kirchmeier-Young, Megan C.; Zwiers, Francis W.; Gillett, Nathan P. (2017): Attribution of Extreme Events in Arctic Sea Ice Extent. In *Journal of Climate* 30 (2), pp. 553–571. DOI: 10.1175/JCLI-D-16-0412.1.

Kjellström, E.; Thejll, P.; Rummukainen, M.; Christensen, J. H.; Boberg, F.; Christensen, O. B.; Fox Maule, C. (2013): Emerging regional climate change signals for Europe under varying large-scale circulation conditions. In *Clim. Res.* 56 (2), pp. 103–119. DOI: 10.3354/cr01146.

Kotlarski, S.; Keuler, K.; Christensen, O. B.; Colette, A.; Déqué, M.; Gobiet, A. et al. (2014): Regional climate modeling on European scales: a joint standard evaluation of the EURO-CORDEX RCM ensemble. In *Geosci. Model Dev.* 7 (4), pp. 1297–1333. DOI: 10.5194/gmd-7-1297-2014.

Kreienkamp, Frank; Philip, Sjoukje Y.; Tradowsky, Jordis S.; Kew, Sarah F.; Lorenz, Philip; Arrighi, Julie et al. (2021): Rapid attribution of heavy rainfall events leading to the severe flooding in Western Europe during July 2021. Available online at https://www.worldweatherattribution.org/heavy-rainfall-which-led-to-severe-flooding-in-western-europe-made-more-likely-by-climate-change/, checked on 2/25/2022.

Kröner, Nico; Kotlarski, Sven; Fischer, Erich; Lüthi, Daniel; Zubler, Elias; Schär, Christoph (2017): Separating climate change signals into thermodynamic, lapse-rate and circulation effects: theory and application to the European summer climate. In *Clim Dyn* 48 (9-10), pp. 3425–3440. DOI: 10.1007/s00382-016-3276-3.

Laprise, René (2008): Regional climate modelling. In *Journal of Computational Physics* 227 (7), pp. 3641–3666. DOI: 10.1016/j.jcp.2006.10.024.

Leduc, Martin; Mailhot, Alain; Frigon, Anne; Martel, Jean-Luc; Ludwig, Ralf; Brietzke, Gilbert B. et al. (2019): The ClimEx Project: A 50-Member Ensemble of Climate Change

Projections at 12-km Resolution over Europe and Northeastern North America with the Canadian Regional Climate Model (CRCM5). In *Journal of Applied Meteorology and Climatology* 58 (4), pp. 663–693. DOI: 10.1175/JAMC-D-18-0021.1.

Lehner, Flavio; Deser, Clara; Maher, Nicola; Marotzke, Jochem; Fischer, Erich M.; Brunner, Lukas et al. (2020): Partitioning climate projection uncertainty with multiple large ensembles and CMIP5/6. In *Earth Syst. Dynam.* 11 (2), pp. 491–508. DOI: 10.5194/esd-11-491-2020.

Lehner, Flavio; Deser, Clara; Terray, Laurent (2017): Toward a New Estimate of "Time of Emergence" of Anthropogenic Warming: Insights from Dynamical Adjustment and a Large Initial-Condition Model Ensemble. In *J. Climate* 30 (19), pp. 7739–7756. DOI: 10.1175/JCLI-D-16-0792.1.

Lenderink, G.; Barbero, R.; Loriaux, J. M.; Fowler, H. J. (2017): Super-Clausius–Clapeyron Scaling of Extreme Hourly Convective Precipitation and Its Relation to Large-Scale Atmospheric Conditions. In *J. Climate* 30 (15), pp. 6037–6052. DOI: 10.1175/JCLI-D-16-0808.1.

Lenderink, Geert; van Meijgaard, Erik (2008): Increase in hourly precipitation extremes beyond expectations from temperature changes. In *Nature Geosci* 1 (8), pp. 511–514. DOI: 10.1038/ngeo262.

Liu, Junzhi; Ma, Xuanlong; Duan, Zheng; Jiang, Jingchao; Reichstein, Markus; Jung, Martin (2020): Impact of temporal precipitation variability on ecosystem productivity. In *WIREs Water* 7 (6). DOI: 10.1002/wat2.1481.

Madakumbura, Gavin D.; Kim, Hyungjun; Utsumi, Nobuyuki; Shiogama, Hideo; Fischer, Erich M.; Seland, Øyvind et al. (2019): Event-to-event intensification of the hydrologic cycle from 1.5 °C to a 2 °C warmer world. In *Sci Rep* 9 (1), p. 3483. DOI: 10.1038/s41598-019-39936-2.

Maher, N.; Matei, D.; Milinski, S.; Marotzke, J. (2018): ENSO Change in Climate Projections: Forced Response or Internal Variability? In *Geophys. Res. Lett.* 45 (20). DOI: 10.1029/2018GL079764.

Maher, Nicola; Lehner, Flavio; Marotzke, Jochem (2020): Quantifying the role of internal variability in the temperature we expect to observe in the coming decades. In *Environ. Res. Lett.* 15 (5), p. 54014. DOI: 10.1088/1748-9326/ab7d02.

Maher, Nicola; Milinski, Sebastian; Ludwig, Ralf (2021a): Large ensemble climate model simulations: introduction, overview, and future prospects for utilising multiple types of large ensemble. In *Earth Syst. Dynam.* 12 (2), pp. 401–418. DOI: 10.5194/esd-12-401-2021.

Maher, Nicola; Milinski, Sebastian; Suarez-Gutierrez, Laura; Botzet, Michael; Dobrynin, Mikhail; Kornblueh, Luis et al. (2019): The Max Planck Institute Grand Ensemble: Enabling the Exploration of Climate System Variability. In *J. Adv. Model. Earth Syst.* 11 (7), pp. 2050–2069. DOI: 10.1029/2019MS001639.

Maher, Nicola; Power, Scott B.; Marotzke, Jochem (2021b): More accurate quantification of model-to-model agreement in externally forced climatic responses over the coming century. In *Nature communications* 12 (1), p. 788. DOI: 10.1038/s41467-020-20635-w.

Marotzke, Jochem; Forster, Piers M. (2015): Forcing, feedback and internal variability in global temperature trends. In *Nature* 517 (7536), pp. 565–570. DOI: 10.1038/nature14117.

Martel, Jean-Luc; Brissette, François P.; Lucas-Picher, Philippe; Troin, Magali; Arsenault, Richard (2021): Climate Change and Rainfall Intensity–Duration–Frequency Curves: Overview of Science and Guidelines for Adaptation. In *J. Hydrol. Eng.* 26 (10), p. 3121001. DOI: 10.1061/(ASCE)HE.1943-5584.0002122.

Martel, Jean-Luc; Mailhot, Alain; Brissette, François (2020): Global and Regional Projected Changes in 100-yr Subdaily, Daily, and Multiday Precipitation Extremes Estimated from Three Large Ensembles of Climate Simulations. In *Journal of Climate* 33 (3), pp. 1089–1103. DOI: 10.1175/JCLI-D-18-0764.1.

McKenna, C. M.; Maycock, A. C. (2021): Sources of Uncertainty in Multimodel Large Ensemble Projections of the Winter North Atlantic Oscillation. In *Geophys Res Lett* 48 (14). DOI: 10.1029/2021GL093258.

McKinnon, Karen A.; Poppick, Andrew; Dunn-Sigouin, Etienne; Deser, Clara (2017): An "Observational Large Ensemble" to Compare Observed and Modeled Temperature Trend Uncertainty due to Internal Variability. In *J. Climate* 30 (19), pp. 7585–7598. DOI: 10.1175/JCLI-D-16-0905.1.

Mearns, Linda O.; Arritt, Ray; Biner, Sébastien; Bukovsky, Melissa S.; McGinnis, Seth; Sain, Stephan et al. (2012): The North American Regional Climate Change Assessment Program: Overview of Phase I Results. In *Bull. Amer. Meteor. Soc.* 93 (9), pp. 1337–1362. DOI: 10.1175/BAMS-D-11-00223.1.

Meinshausen, Malte; Smith, S. J.; Calvin, K.; Daniel, J. S.; Kainuma, M. L. T.; Lamarque, J-F. et al. (2011): The RCP greenhouse gas concentrations and their extensions from 1765 to 2300. In *Climatic Change* 109 (1-2), pp. 213–241. DOI: 10.1007/s10584-011-0156-z.

MeteoSwiss (2020): Federal Office of Meteorology and Climatology (MeteoSwiss): Hourly station observations of precipitation amount in mm. Federal Office of Meteorology and

Climatology (MeteoSwiss). Available online at https://gate.meteoswiss.ch/idaweb, checked on 7/20/2020.

Milinski, Sebastian; Maher, Nicola; Olonscheck, Dirk (2020): How large does a large ensemble need to be? In *Earth Syst. Dynam.* 11 (4), pp. 885–901. DOI: 10.5194/esd-11-885-2020.

Mittermeier, M.; Braun, M.; Hofstätter, M.; Wang, Y.; Ludwig, R. (2019): Detecting Climate Change Effects on Vb Cyclones in a 50-Member Single-Model Ensemble Using Machine Learning. In *Geophys. Res. Lett.* 46 (24), pp. 14653–14661. DOI: 10.1029/2019GL084969.

Mittermeier, M.; Weigert, M.; Rügamer, D.; Küchenhoff, H.; Ludwig, R. (2022): A deep learning based classification of atmospheric circulation types over Europe: projection of future changes in a CMIP6 large ensemble. In *Environ. Res. Lett.* 17 (8), p. 84021. DOI: 10.1088/1748-9326/ac8068.

Moss, Richard H.; Edmonds, Jae A.; Hibbard, Kathy A.; Manning, Martin R.; Rose, Steven K.; van Vuuren, Detlef P. et al. (2010): The next generation of scenarios for climate change research and assessment. In *Nature* 463 (7282), pp. 747–756. DOI: 10.1038/nature08823.

Myhre, G.; Alterskjær, K.; Stjern, C. W.; Hodnebrog, Ø.; Marelle, L.; Samset, B. H. et al. (2019): Frequency of extreme precipitation increases extensively with event rareness under global warming. In *Scientific reports* 9 (1), p. 16063. DOI: 10.1038/s41598-019-52277-4.

Nakicenovic, N. and Swart, R. (Ed.) (2000): Special Report on Emissions Scenarios. A Special Report of Working Group III of the Intergovernmental Panel on Climate Change. Intergovernmental Panel on Climate Change (IPCC). Cambridge, United Kingdom and New York, NY, USA: Cambridge University Press.

Nobre, G. Guimarães; Jongman, B.; Aerts, J.; Ward, P. J. (2017): The role of climate variability in extreme floods in Europe. In *Environ. Res. Lett.* 12 (8), p. 84012. DOI: 10.1088/1748-9326/aa7c22.

O'Gorman, Paul A.; Schneider, Tapio (2009): Scaling of Precipitation Extremes over a Wide Range of Climates Simulated with an Idealized GCM. In *J. Climate* 22 (21), pp. 5676–5685. DOI: 10.1175/2009JCLI2701.1.

Pendergrass, Angeline G.; Knutti, Reto; Lehner, Flavio; Deser, Clara; Sanderson, Benjamin M. (2017): Precipitation variability increases in a warmer climate. In *Sci Rep* 7 (1). DOI: 10.1038/s41598-017-17966-y.

Pfahl, S.; O'Gorman, P. A.; Fischer, E. M. (2017): Understanding the regional pattern of projected future changes in extreme precipitation. In *Nature Clim Change* 7 (6), pp. 423–427. DOI: 10.1038/nclimate3287.

Philip, Sjoukje Y.; Kew, Sarah F.; van Oldenborgh, Geert Jan; Anslow, Faron S.; Seneviratne, Sonia I.; Vautard, Robert et al. (2021): Rapid attribution analysis of the extraordinary heatwave on the Pacific Coast of the US and Canada June 2021.

Pichelli, Emanuela; Coppola, Erika; Sobolowski, Stefan; Ban, Nikolina; Giorgi, Filippo; Stocchi, Paolo et al. (2021): The first multi-model ensemble of regional climate simulations at kilometer-scale resolution part 2: historical and future simulations of precipitation. In *Clim Dyn* 56 (11-12), pp. 3581–3602. DOI: 10.1007/s00382-021-05657-4.

Pokorná, Lucie; Huth, Radan (2015): Climate impacts of the NAO are sensitive to how the NAO is defined. In *Theor Appl Climatol* 119 (3-4), pp. 639–652. DOI: 10.1007/s00704-014-1116-0.

Poschlod, Benjamin; Ludwig, Ralf (2021): Internal variability and temperature scaling of future sub-daily rainfall return levels over Europe. In *Environ. Res. Lett.* 16 (6), p. 64097. DOI: 10.1088/1748-9326/ac0849.

Prein, Andreas F.; Liu, Changhai; Ikeda, Kyoko; Trier, Stanley B.; Rasmussen, Roy M.; Holland, Greg J.; Clark, Martyn P. (2017): Increased rainfall volume from future convective storms in the US. In *Nature Clim Change* 7 (12), pp. 880–884. DOI: 10.1038/s41558-017-0007-7.

Rakovec, Oldrich; Samaniego, Luis; Hari, Vittal; Markonis, Yannis; Moravec, Vojtěch; Thober, Stephan et al. (2022): The 2018–2020 Multi-Year Drought Sets a New Benchmark in Europe. In *Earth's Future* 10 (3). DOI: 10.1029/2021EF002394.

Ritter, François; Berkelhammer, Max; Garcia-Eidell, Cynthia (2020): Distinct response of gross primary productivity in five terrestrial biomes to precipitation variability. In *Commun Earth Environ* 1 (1). DOI: 10.1038/s43247-020-00034-1.

Rodgers, K. B.; Lin, J.; Frölicher, T. L. (2015): Emergence of multiple ocean ecosystem drivers in a large ensemble suite with an Earth system model. In *Biogeosciences* 12 (11), pp. 3301–3320. DOI: 10.5194/bg-12-3301-2015.

Rowhani, Pedram; Lobell, David B.; Linderman, Marc; Ramankutty, Navin (2011): Climate variability and crop production in Tanzania. In *Agricultural and Forest Meteorology* 151 (4), pp. 449–460. DOI: 10.1016/j.agrformet.2010.12.002.

Rummukainen, Markku (2016): Added value in regional climate modeling. In *WIREs Clim Change* 7 (1), pp. 145–159. DOI: 10.1002/wcc.378.

Ruti, P. M.; Somot, S.; Giorgi, F.; Dubois, C.; Flaounas, E.; Obermann, A. et al. (2016): Med-CORDEX Initiative for Mediterranean Climate Studies. In *Bull. Amer. Meteor. Soc.* 97 (7), pp. 1187–1208. DOI: 10.1175/BAMS-D-14-00176.1.

Schlunegger, Sarah; Rodgers, Keith B.; Sarmiento, Jorge L.; Frölicher, Thomas L.; Dunne, John P.; Ishii, Masao; Slater, Richard (2019): Emergence of Anthropogenic Signals in the Ocean Carbon Cycle. In *Nature climate change* 9, pp. 719–725. DOI: 10.1038/s41558-019-0553-2.

Shepherd, Theodore G.; Boyd, Emily; Calel, Raphael A.; Chapman, Sandra C.; Dessai, Suraje; Dima-West, Ioana M. et al. (2018): Storylines: an alternative approach to representing uncertainty in physical aspects of climate change. In *Climatic Change* 151 (3), pp. 555–571. DOI: 10.1007/s10584-018-2317-9.

Sillmann, Jana; Shepherd, Theodore G.; van den Hurk, Bart; Hazeleger, Wilco; Martius, Olivia; Slingo, Julia; Zscheischler, Jakob (2021): Event-Based Storylines to Address Climate Risk. In *Earth's Future* 9 (2). DOI: 10.1029/2020EF001783.

Sillmann, Jana; Stjern, Camilla W.; Myhre, Gunnar; Samset, Bjørn H.; Hodnebrog, Øivind; Andrews, Timothy et al. (2019): Extreme wet and dry conditions affected differently by greenhouse gases and aerosols. In *npj Clim Atmos Sci* 2 (1). DOI: 10.1038/s41612-019-0079-3.

Sippel, Sebastian; Meinshausen, Nicolai; Merrifield, Anna; Lehner, Flavio; Pendergrass, Angeline G.; Fischer, Erich; Knutti, Reto (2019): Uncovering the Forced Climate Response from a Single Ensemble Member Using Statistical Learning. In *Journal of Climate* 32 (17), pp. 5677–5699. DOI: 10.1175/JCLI-D-18-0882.1.

Smoliak, Brian V.; Wallace, John M.; Lin, Pu; Fu, Qiang (2015): Dynamical Adjustment of the Northern Hemisphere Surface Air Temperature Field: Methodology and Application to Observations*. In *Journal of Climate* 28 (4), pp. 1613–1629. DOI: 10.1175/JCLI-D-14-00111.1.

Spinoni, Jonathan; Vogt, Jürgen V.; Naumann, Gustavo; Barbosa, Paulo; Dosio, Alessandro (2018): Will drought events become more frequent and severe in Europe? In *Int. J. Climatol* 38 (4), pp. 1718–1736. DOI: 10.1002/joc.5291.

Suarez-Gutierrez, Laura; Milinski, Sebastian; Maher, Nicola (2021): Exploiting large ensembles for a better yet simpler climate model evaluation. In *Clim Dyn* 57 (9-10), pp. 2557–2580. DOI: 10.1007/s00382-021-05821-w.

Sun, Lantao; Alexander, Michael; Deser, Clara (2018): Evolution of the Global Coupled Climate Response to Arctic Sea Ice Loss during 1990–2090 and Its Contribution to Climate Change. In *Journal of Climate* 31 (19), pp. 7823–7843. DOI: 10.1175/JCLI-D-18-0134.1.

Swain, Daniel L.; Langenbrunner, Baird; Neelin, J. David; Hall, Alex (2018): Increasing precipitation volatility in twenty-first-century California. In *Nature Clim Change* 8 (5), pp. 427–433. DOI: 10.1038/s41558-018-0140-y.

Tang, Tao; Shindell, Drew; Samset, Bjørn H.; Boucher, Olivié r; Forster, Piers M.; Hodnebrog, Øivind et al. (2018): Dynamical response of Mediterranean precipitation to greenhouse gases and aerosols. In *Atmos. Chem. Phys.* 18 (11), pp. 8439–8452. DOI: 10.5194/acp-18-8439-2018.

Taylor, Karl E.; Stouffer, Ronald J.; Meehl, Gerald A. (2012): An Overview of CMIP5 and the Experiment Design. In *Bull. Amer. Meteor. Soc.* 93 (4), pp. 485–498. DOI: 10.1175/BAMS-D-11-00094.1.

Tebaldi, Claudia; Dorheim, Kalyn; Wehner, Michael; Leung, Ruby (2021): Extreme metrics from large ensembles: investigating the effects of ensemble size on their estimates. In *Earth Syst. Dynam.* 12 (4), pp. 1427–1501. DOI: 10.5194/esd-12-1427-2021.

Thompson, David W. J.; Barnes, Elizabeth A.; Deser, Clara; Foust, William E.; Phillips, Adam S. (2015): Quantifying the Role of Internal Climate Variability in Future Climate Trends. In *J. Climate* 28 (16), pp. 6443–6456. DOI: 10.1175/JCLI-D-14-00830.1.

Torma, Csaba; Giorgi, Filippo; Coppola, Erika (2015): Added value of regional climate modeling over areas characterized by complex terrain-Precipitation over the Alps. In *J. Geophys. Res. Atmos.* 120 (9), pp. 3957–3972. DOI: 10.1002/2014JD022781.

United Nations Office for Disaster Risk Reduction (2021): GAR Special Report on Drought 2021. Geneva. Available online at https://www.undrr.org/media/49386/download, checked on 1/11/2023.

van der Wiel, K.; Wanders, N.; Selten, F. M.; Bierkens, M. F. P. (2019): Added Value of Large Ensemble Simulations for Assessing Extreme River Discharge in a 2 °C Warmer World. In *Geophys Res Lett* 46 (4), pp. 2093–2102. DOI: 10.1029/2019GL081967.

van der Wiel, Karin; Batelaan, Thomas J.; Wanders, Niko (2022): Large increases of multi-year droughts in north-western Europe in a warmer climate. In *Clim Dyn*. DOI: 10.1007/s00382-022-06373-3.

van der Wiel, Karin; Lenderink, Geert; Vries, Hylke de (2021): Physical storylines of future European drought events like 2018 based on ensemble climate modelling. In *Weather and Climate Extremes* 33, p. 100350. DOI: 10.1016/j.wace.2021.100350.

van Loon, Anne F. (2015): Hydrological drought explained. In *WIREs Water* 2 (4), pp. 359–392. DOI: 10.1002/wat2.1085.

van Vuuren, Detlef P.; Edmonds, Jae; Kainuma, Mikiko; Riahi, Keywan; Thomson, Allison; Hibbard, Kathy et al. (2011): The representative concentration pathways: an overview. In *Climatic Change* 109 (1-2), pp. 5–31. DOI: 10.1007/s10584-011-0148-z.

von Storch, Hans; Langenberg, Heike; Feser, Frauke (2000): A Spectral Nudging Technique for Dynamical Downscaling Purposes. In *Mon. Wea. Rev.* 128 (10), pp. 3664–3673. DOI: 10.1175/1520-0493(2000)128%3C3664:ASNTFD%3E2.0.CO;2.

von Trentini, F.; Leduc, M.; Ludwig, R. (2019): Assessing natural variability in RCM signals: comparison of a multi model EURO-CORDEX ensemble with a 50-member single model large ensemble. In *Clim Dyn* 53 (3-4), pp. 1963–1979. DOI: 10.1007/s00382-019-04755-8.

Vries, Hylke de; Lenderink, Geert; van der Wiel, Karin; van Meijgaard, Erik (2022): Quantifying the role of the large-scale circulation on European summer precipitation change. In *Clim Dyn* 59 (9-10), pp. 2871–2886. DOI: 10.1007/s00382-022-06250-z.

Wasko, Conrad; Sharma, Ashish; Westra, Seth (2016): Reduced spatial extent of extreme storms at higher temperatures. In *Geophys Res Lett* 43 (8), pp. 4026–4032. DOI: 10.1002/2016GL068509.

Westra, S.; Fowler, H. J.; Evans, J. P.; Alexander, L. V.; Berg, P.; Johnson, F. et al. (2014): Future changes to the intensity and frequency of short-duration extreme rainfall. In *Rev. Geophys.* 52 (3), pp. 522–555. DOI: 10.1002/2014RG000464.

Westra, Seth; Alexander, Lisa V.; Zwiers, Francis W. (2013): Global Increasing Trends in Annual Maximum Daily Precipitation. In *Journal of Climate* 26 (11), pp. 3904–3918. DOI: 10.1175/JCLI-D-12-00502.1.

Wiley (Ed.) (2021): Geophysical Research Letters. Available online at https://agupubs.onlinelibrary.wiley.com/journal/19448007, checked on 12/29/2021.

Wills, Robert C. J.; Battisti, David S.; Armour, Kyle C.; Schneider, Tapio; Deser, Clara (2020): Pattern Recognition Methods to Separate Forced Responses from Internal Variability in Climate Model Ensembles and Observations. In *Journal of Climate* 33 (20), pp. 8693–8719. DOI: 10.1175/JCLI-D-19-0855.1.

Wittenberg, Andrew T.; Rosati, Anthony; Delworth, Thomas L.; Vecchi, Gabriel A.; Zeng, Fanrong (2014): ENSO Modulation: Is It Decadally Predictable? In *J. Climate* 27 (7), pp. 2667–2681. DOI: 10.1175/JCLI-D-13-00577.1.

Wood, R. R.; Ludwig, R. (2020): Analyzing Internal Variability and Forced Response of Subdaily and Daily Extreme Precipitation Over Europe. In *Geophys. Res. Lett.* 47 (17). DOI: 10.1029/2020GL089300.

Wood, Raul R.; Lehner, Flavio; Pendergrass, Angeline G.; Schlunegger, Sarah (2021): Changes in precipitation variability across time scales in multiple global climate model large ensembles. In *Environ. Res. Lett.* 16 (8), p. 84022. DOI: 10.1088/1748-9326/ac10dd.

Woollings, T.; Franzke, C.; Hodson, D. L. R.; Dong, B.; Barnes, E. A.; Raible, C. C.; Pinto, J. G. (2015): Contrasting interannual and multidecadal NAO variability. In *Clim Dyn* 45 (1-2), pp. 539–556. DOI: 10.1007/s00382-014-2237-y.

Zappa, Giuseppe; Hawcroft, Matthew K.; Shaffrey, Len; Black, Emily; Brayshaw, David J. (2015): Extratropical cyclones and the projected decline of winter Mediterranean precipitation in the CMIP5 models. In *Clim Dyn* 45 (7-8), pp. 1727–1738. DOI: 10.1007/s00382-014-2426-8.

Zappa, Giuseppe; Shaffrey, Len C.; Hodges, Kevin I.; Sansom, Phil G.; Stephenson, David B. (2013): A Multimodel Assessment of Future Projections of North Atlantic and European Extratropical Cyclones in the CMIP5 Climate Models*. In *J. Climate* 26 (16), pp. 5846–5862. DOI: 10.1175/JCLI-D-12-00573.1.

Ziese, Markus; Rauthe-Schöch, Armin; Becker, Andreas; Finger, Peter; Meyer-Christoffer, Anja; Schneider, Udo (2018): GPCC Full Data Daily Version 2018 at 1.0°: Daily Land-Surface Precipitation from Rain-Gauges built on GTS-based and Historic Data.